# FLOW-THROUGH EVAPORATIVE SOLVENT REMOVAL AND APPLICATIONS WITH CHROMATOGRAPHY

A thesis submitted in fulfillment of the requirements for the degree of
Doctor of Philosophy

by

Elisenda Fornells Vernet
(BSc, MSc)

Australian Research Council Training Centre in Portable Analytical Separation Technologies (ASTech)
Australian Centre for Research on Separation Science (ACROSS)

School of Natural Sciences
University of Tasmania
August 2018

# DECLARATION

This thesis contains no material which has been accepted for a degree or diploma by the University or any other institution, except by way of background information and duly acknowledged in the thesis, and to the best of my knowledge and belief no material previously published or written by another person except where due acknowledgement is made in the text of the thesis, nor does the thesis contain any material that infringes copyright.

The publishers of the papers comprising Chapters 1 to 4 hold the copyright for that content, and access to the material should be sought from the respective journals. The remaining non-published content of the thesis may be made available for loan and limited copying and communication in accordance with the Copyright Act 1968.

Elisenda Fornells Vernet

August 2018

# ACKNOWLEDGMENTS

Firstly, I would like to express my sincere gratitude to my supervisor Prof. Michael Breadmore for agreeing to supervise me during my Ph.D studies. For his continuous support, guidance, and for sharing his immense knowledge. My sincere thanks also go to Dr. Robert Shellie and Prof. Emily Hilder for their input and support as part of my supervisory team, and for giving me the opportunity to travel across the world to do some exciting research in the first place. Besides, I would also like to thank Mr. Brett Barnett and Mr. Mike Bailey from our industry partner, Trajan Scientific and Medical, for their technical support and suggestions. Their knowledge has been essential.

I would like to acknowledge the ASTech center (Australian Research Council Training Centre for Portable Analytical Separation Technologies) for providing a scholarship, together with the University of Tasmania and Trajan. Also, the support received from the ACROSS center (Australian Centre for Research on Separation Science). Them all are diverse and multidisciplinary environments where ideas thrive.

I thank my ACROSS and ASTech labmates - those long gone and the newcomers - for the stimulating discussions, and for all the fun we have had in the last four years. The shared hardship has led to long lasting friendships. Also, to all those who shared with me my first steps in science and the first glance of research at the University of Barcelona.

Last but not the least, I need to acknowledge my beloved and unusual bunch of friends because they showed me how it feels when someone has your back. My sporting families too, which have provided much needed stress relieve. My parents and sister for always supporting me and my goals; any differently during my Ph.D 17.000Km away from them. Finally, thanks to Joan Marc for all of the above combined. The emotional support, advice, discussions, and the fun we have had in this adventure are invaluable. lil

*Life is full of mysteries but there are answers out there. And they won't be found by people sitting around looking serious and saying: "Isn't life mysterious?". Because throughout history every mystery ever solved has turned out to be not magic.*

*I am a tiny, insignificant, ignorant bit of carbon. I have one life and it is short and unimportant, but thanks to recent scientific advances I get to live twice as long as my great great great great uncles and aunts. Twice as long to live this life of mine. Twice as long to love this family of mine. Twice as many years of friends and wine.*

Tim Minchin – Storm

# AUTHORSHIP STATEMENT

The following people and institutions contributed to the publication of work undertaken as part of this thesis:

| | |
|---|---|
| **Elisenda Fornells Vernet** | ASTech, ACROSS, School of Natural Sciences, UTas (Candidate) |
| **Michael C. Breadmore** | ASTech, ACROSS, School of Natural Sciences, UTas (Supervisor) |
| **Emily F. Hilder** | ASTech, Future industries Institute, University of South Australia |
| **Robert A. Shellie** | ASTech, Trajan Scientific and Medical |
| **Mike Bailey** | ASTech, Trajan Scientific and Medical |
| **Brett Barnett** | Trajan Scientific and Medical |
| **Petr Smejkal** | ACROSS, School of Physical Sciences, UTas |

**Review,** Preconcentration by solvent removal: techniques and applications.
Located in chapter I. Candidate was the primary author (70%), while MCB (20%), EFH (5%), and RAS (5%) contributed to structure and presentation.

**Paper 1**, Membrane assisted and temperature controlled on-line evaporative concentration for microfluidics.
Located in chapter II. Candidate was the primary author (70%), BB and MB assisted with engineering and design (10%), while MCB (10%), EFH (5%), and RAS (5%) contributed to the idea realization and development.

**Paper 2**, Evaporative membrane modulation for comprehensive two-dimensional liquid chromatography.
Located in chapter III. Candidate was the primary author (65%), BB and MB assisted with engineering and design (10%), PS assisted with programing (5%) while MCB (10%), EFH (5%), and RAS (5%) contributed to the idea realization and development.

**Paper 3**, On-line solvent exchange system: Automation from extraction to analysis.

Located in chapter IV. Candidate was the primary author (65%), MCB (15%), RAS (10%) and EFH (10%) contributed to the idea realization and development.

We the undersigned agree with the above stated "proportion of the work undertaken" for each of the above published (or submitted) peer-reviewed manuscripts contributing to this thesis:

Prof. Michael C. Breadmore
Primary Supervisor
School of Natural Sciences
University of Tasmania
Date: 7/08/2018

Prof. Mark Hunt
Head of School
School of Natural Sciences
University of Tasmania
Date: 10/08/2018

# LIST OF PUBLICATIONS AND PRESENTATIONS

Publication list

**A review on preconcentration by solvent removal: techniques and applications**

Elisenda Fornells, Emily F. Hilder, Robert A. Shellie, Michael C. Breadmore

Submitted to a peer reviewed journal - July 2018

**On-line solvent exchange system: Automation from extraction to analysis**

Elisenda Fornells, Emily F. Hilder, Robert A. Shellie, Michael C. Breadmore

Submitted to a peer reviewed journal - July 2018

**Evaporative Membrane Modulation for Comprehensive Two-Dimensional Liquid Chromatography**

Elisenda Fornells, Brett Barnett, Mike Bailey, Emily F. Hilder, Robert A. Shellie, Michael C. Breadmore

January 2018 – *Analytica Chimica Acta, 1000 (2018) 303-309*

**Membrane assisted and temperature controlled on-line evaporative concentration for microfluidics**

Elisenda Fornells, Brett Barnett, Emily F. Hilder, Robert A. Shellie, Michael C. Breadmore

December 2016 - *Journal of Chromatography A, 1486 (2017) 110–116*

Patents

AU2017901898: Device and method for interfacing two separation techniques (filed 19 May, 2017)

PCT/AU2018/050485: Device and method for interfacing two separation techniques (filed 21 May, 2018)

Conference presentations

**Overview on membrane assisted on-line evaporative concentration for microfluidics**

Elisenda Fornells, Brett Barnett, Emily F. Hilder, Robert A. Shellie, Michael C. Breadmore

December 2015, 23th annual Royal Australian Chemical Institute Research and Development Topics Conference - (poster presentation)

**Membrane assisted on-line evaporative concentration**

Elisenda Fornells, Brett Barnett, Emily F. Hilder, Robert A. Shellie, Mike Bailey, Michael C Breadmore

December 2016, ACROSS 2nd International Symposium on Advances in Separation Science ASSAS$^2$ - (oral presentation)

**Membrane evaporative interface for LC×LC (multidimensional liquid chromatography)**

Elisenda Fornells, Brett Barnett, Emily F. Hilder, Robert A. Shellie, Michael C Breadmore

June 2017, 45th International Symposium on High Performance Liquid Phase Separations and Related Techniques (HPLC) - (oral and poster presentation)

**Evaporative Solvent Removal Interface for Comprehensive Multidimensional Liquid Chromatography**

Elisenda Fornells, Brett Barnett, Emily F. Hilder, Robert A. Shellie, Michael C Breadmore

December 2017, 25th annual Royal Australian Chemical Institute Research and Development Topics Conference - (oral presentation)

# ABSTRACT

This thesis describes the development of a device to address solvent issues in analysis techniques and improve automation. These include the removal of solvent for preconcentration or selective removal of organic solvent in mixtures to address solvent incompatibilities.

In chapter I, a review of preconcentration techniques and applications by solvent removal is presented. Preconcentration is typically the first part of analytical method development covering the need to improve detection sensitivity. This review gathers presented strategies to accomplish preconcentration by solvent removal. Evaporation and partitioning in an immiscible fluid has been reported in a variety of forms with good control of the interfaces and accurate results. A comprehensive comparison of different approaches is presented, as well as an indication on the research needs in this area. In addition, an overview on solvent incompatibility problems for instrumental coupling is provided, which can potentially be addressed by similar solvent removal techniques.

In chapter II, the development of a temperature controlled membrane evaporation concentrator for continuous flow conditions is described. An exponential relationship was observed between temperature and concentration factor and a theoretical model was described to better understand the performance of the concentrator. Caffeine was the analyte used to construct the model which was employed to predict the concentration performance of three target analytes at different conditions. Experimentally, a 30-fold concentration can be attained in less than 60 min whilst maintaining solute integrity under different sub-ambient pressure conditions and mild temperatures. While using the model it was determined that a 10-fold concentration (±0.5) can be performed at 56.72 ± 0.07°C and at a flow rate of 10 µL $min^{-1}$. Altogether, the model provides a better understanding of the

process and its applicability to analytical methods. This work demonstrates that it is possible to obtain high concentration factors with a continuously flowing fluid when temperature is precisely controlled and in times that are reasonable compared to existing evaporation concentration procedures

Chapter III describes a further development of the membrane evaporator as an evaporative membrane modulator (EMM) to address solvent incompatibilities in two-dimensional liquid chromatography. A feedback control mechanism was used to precisely control evaporation, adjusting temperature automatically in real time to address the need for high temperature precision described in Chapter II. In addition, the automated interface can keep evaporation constant regardless of the changing solvent content in the feed. It reduces the volume after $^{1}D$ elution by a pre-determined factor, regardless of the separation solvent gradient. This volume reduction ensures that the injection volume in the $^{2}D$ is appropriate for the second column, avoiding the detrimental effects of overloading. In addition, the fraction solvent composition is constant over the length of the separation increasing reproducibility of $^{2}D$ separations. The evaporative membrane modulator was demonstrated with a 10-fold reduction, reducing the fraction injection volume from 50 to 5 µL. A consequence of the EMM device is a reduction in the capacity of the first dimension, which is decreased by a factor of 2.4, but the peak width at half maximum was reduced by up to 22% in the second dimension. When band broadening is considered, the corrected peak capacity with the modulator was only 10% lower than that without the modulator, but with a gain in peak height of 2-3. Also a decrease in retention time between subsequent peak-slices reduced from 4 s to be negligible. Avoiding loss of performance in the second dimension when coupling two-dimensional liquid chromatography systems shows potential to facilitate peak identification and quantitation in more complex applications.

In chapter IV, the evaporation process across the membrane is fully characterized with water/solvent mixtures showing organic solvent removal

capabilities. The system allowed continuous methanol, ethanol and acetonitrile removal from samples containing up to 80% organic solvent. The use of the device is then demonstrated for on-line sample reconstitution after solvent extractions. Removal of organic solvent from sample extracts is required before analysis by RPLC to preserve chromatographic performance and allow for bigger injection volumes, boosting sensitivity. An automated on-line extraction evaporation procedure is integrated with HPLC analysis, applied to analysis of the antibiotic chloramphenicol in milk samples. Sample reconstitution and HPLC injection is performed in less than 10 min and can be executed simultaneously to HPLC analysis of the previous sample in a routine workflow, thus having minimal impact on the total sample analysis time when run in a sequence.

The developed device shows great potential to aid automation and address instrumental coupling issues arise from solvent incompatibilities. Advantages and further development options for this technology are discussed.

# TABLE OF CONTENTS

# PREFACE

Analytical chemistry focuses on the separation, identification and/or quantification of matter, either in one or combined steps. Samples or mixtures of analytes are transported by a carrier phase through the several stages of the analytical process such as preconcentration, clean-up, separation, and detection. The carrier phase is typically gas, liquid or supercritical fluid, but often it can be different for each of the above-mentioned stages. Even focusing on analysis in a liquid phase, ideal liquid properties (salt concentration, pH, solvent composition) are often different through the process. For instance, the presence of organic solvents may be essential for preconcentration but detrimental in the analytes separation or detection.

A relevant case is the implementation of clean-up and preconcentration extraction techniques that require the use of organic solvents, such as solid-phase extraction or liquid-liquid extraction. At the end of this process, the analytes will be dissolved in strong organic solvents. This poses a difficulty when proceeding analysis by liquid chromatography, since the analyte carrier is a strong organic solvent that can influence the interaction between analyte, stationary phase and mobile phase. Such effect of the sample solvent is detrimental for the separation performance [1]. Solvents immiscible with the mobile phase present even worse outcomes in terms of chromatographic performance and may damage the column. A common strategy to avoid such problems consists of evaporating the unwanted solvents and then reconstituting the sample in an appropriate compatible solvent [2].

So far, incompatibilities or detrimental effects of mobile phase composition have been illustrated between sample pre-treatment and separation. However, these issues can also be relevant in cases where more than one consecutive separation stage is used to analyse very complex samples that require a very large resolving power. Comprehensive two-dimensional liquid chromatography commonly involves the use of a switching valve with two identical sample loops.

These sample loops act as alternating collection and injection loops to systematically transfer segments of the first separation to the second one. When the first fraction mobile phase has higher elution strength than the second separation mobile phase, separation in the second dimension can be negatively affected [3]. Viscosity contrast also causes flow instabilities at the interface between the two fluids with different viscosities, with the fraction band undergoing a change in form as it enters the chromatography column. This phenomenon is known as viscous fingering and can also degrade separation performance [4]. These phenomena are also worsened since fraction volumes are usually higher than optimal sample injection volumes.

The aim of this PhD project was to develop innovative strategies to address solvent issues relevant to automation of multistep analysis procedures, focusing mainly on chromatographic techniques. Evaporation techniques and strategies were screened in chapter I to develop an adapted device for this purpose. The challenges detailed previously – coupling sample pre-treatment to liquid chromatography and interfacing two-dimensional liquid chromatography – were addressed using the developed evaporation device.

## REFERENCES


[1] J. Layne, T. Farcas, I. Rustamov, F. Ahmed, Volume-load capacity in fast-gradient liquid chromatography: Effect of sample solvent composition and injection volume on chromatographic performance, J. Chromatogr. A. 913 (2001) 233–242.

[2] S. Moldoveanu, V. David, Chapter 6 - Solvent Extraction, in: Mod. Sample Prep. Chromatogr., Elsevier, 2015: pp. 131–189.

[3] P. Jandera, T. Hájek, P. Česla, Effects of the gradient profile, sample volume and solvent on the separation in very fast gradients, with special attention to the second-dimension gradient in comprehensive two-dimensional liquid chromatography, J. Chromatogr. A. 1218 (2011) 1995–

2006.

[4] R.A. Shalliker, G. Guiochon, Solvent viscosity mismatch between the solute plug and the mobile phase: Considerations in the applications of two-dimensional HPLC, Analyst. 135 (2010) 222–229.

# I. PRECONCENTRATION BY SOLVENT REMOVAL: TECHNIQUES AND APPLICATIONS

# I. Preconcentration by Solvent Removal: Techniques and Applications

This chapter has been submitted to a peer reviewed journal as a review article. All efforts were made to keep the original features of this article except for minor changes. Layout, numbering, font size and style were modified in order to maintain a consistent formatting style of this thesis.


## Abstract

Preconcentration is the aspect of analytical method development covering the need to improve detection sensitivity. This review collects the advances in a diversity of approaches to achieve preconcentration by solvent removal. Evaporation and partitioning in an immiscible fluid have been reported in a variety of forms that demonstrate good control of the interfaces and accurate results. A comprehensive comparison of different strategies is presented here as well as the research needs in this area.


## 1. Introduction

Analytical chemistry is the branch of chemistry concerned with the identification and measurement of the constituents of a substance or of particular components within it, usually relying on selective detection and separation by chemical or instrumental means.

The need for sensitive techniques and low detection limits for low abundance analyte analysis has been recognised since the early times. The introduction of enrichment or preconcentration steps was considered the best approach to achieve the appropriate concentration for detection [1]. Since off-line techniques require handling of the sample between the enrichment and the

separation step, they are often complex, time consuming and not suitable for automated techniques (e.g. rotatory evaporation). Therefore, it is desirable to integrate every part of the analytical process from sample introduction to detection including sample preparation or preconcentration. On-line sample preparation procedures were introduced during the 1970s. The simplest approach in chromatography is to include a step in the gradient in which analytes are retained at the start of the chromatographic column before being separated with the eluent [1,2].

Miniaturization has more recently revolutionised analytical methodologies with a strong focus on integration [3]. Microfluidics emerged in the late 1980s as a multidisciplinary field for the design of miniaturized systems in which low volumes of fluids are processed to achieve multiplexing, automation, portability and high-throughput analysis with practical applications [4]. A primary goal for microfluidics is to develop technologies and methods that aim to replace traditional macroscale techniques exploiting the advantages of miniaturization including laminar flow, predictable hydrodynamics, and more efficient heat and mass transfer. However, working in small dimensions can further hinder practical applications when handling low-abundant analytes in complex samples. Therefore, large efforts are being put into the on-line incorporation of concentration stages as a necessary tool in the development of new integrated analysis procedures. These can offer solutions for macro and micro analysis without detriment to automation, portability and miniaturization.

A number of reviews gathering different strategies for preconcentration have been published [5–7]. Many techniques, however, are designed for particular applications and are not easily translatable to other systems. Concentration steps need to be regarded assessing potential integration in different and diverse methodologies and in comparison with other enrichment techniques. Generally, specific limitations apply to each approach and it is important to

choose an adequate procedure regarding the needs of each particular method.

For instance, an important part of concentration methods such as ion concentration polarization and isotachophoresis is the use of an electric field, as these are based on electrokinetic and electrophoretic principles - voltage is used to move and preconcentrate charged analytes in a specific region [8–10]. It follows that this approach is limited therefore to charged molecules. Others are based on surface-binding principles like solid-phase extraction (SPE), relying on analytes' affinity to the surface for it to be retained and concentrated prior to analysis [11]. Again, if there is no affinity with the surface, then this approach will not work for these molecules. These techniques discriminate in terms of analytes, separation procedures or detection methods to be integrated in.

An alternative, and potentially universal approach is solvent removal from the sample matrix, performing a reduction of volume but keeping all types of analytes in the solution. There are some classic and novel approaches that are worth considering using solvent removal either in static conditions – from a stationary and fixed volume – or dynamic conditions – from a flowing liquid. This review aims to address and compare different concentration techniques based on solvent removal. The coupling of these techniques to further analysis steps is also discussed to provide a comprehensive tool, enabling the user to choose the most appropriate method for their specific application.

Table 1. Summary of preconcentration techniques and performance indicative. CF: Concentration Factor

| | Interface / Membrane | Mode | Application | CF or evap. rate | time (s/min) | Year | Ref |
|---|---|---|---|---|---|---|---|
| Open evaporation | Levitating droplet | Dynamic – On-line | Amino-acids by CE | 166 | 3.5 min | 1998 | [12] |
| | Microcavity droplet evaporation | Static | Analysis by fast-scan cyclic voltammetry (FSCV) | 5 | few s | 2004 | [13] |
| | Droplet evaporation | Static | green fluorescent protein (EGFP) | n/a | n/a | 2012 | [16] |
| | Concentration at a reservoir meniscus | Dynamic – feed evaporation driven | fluorescent spheres / BSA | qualitative | n/a | 2002 | [17] |
| | | | | 20 pg.µm$^{-2}$.s$^{-1}$ | n/a | 2015 | [18] |
| | Open microchannel | Static | - | dryness | 21 s | 2014 | [19] |
| | Capillary wells | Static | fluorescent protein | 2 | 6.5 min | 2011 | [21] |
| | Paper based | Dynamic – feed evaporation driven | lipoarabinomannan (LAM) | 20 | 10 min | 2014 | [22] |
| | Thin porous substrate (chromatography paper) | Dynamic – feed evaporation driven | dyes | 100 | 180 min | 2017 | [23] |
| Enclosed evaporation | Micropillar array channel | Dynamic | Fluorescent dyes | 4 | 4 min | 2010 | [26] |
| | | Statyc | Fluorescent dyes / particles | 25 | 1 min | 2014 | [27] |
| | | Dynamic | Distillation | n/a | n/a | 2014 | [28] |
| | Annular G-L flow | Dynamic | Distillation | n/a | n/a | 2012 | [29] |
| | Microdroplets trapping | Static | Salts | 10 | - | 2012 | [30] |
| Flat membranes | PTFE | Dynamic | Electrolyte stream | 3 | 27 min | 2003 | [40] |
| | PTFE | Static | BSA | 1.8 mL.min$^{-1}$ | n/a | 2008 | [41] |
| | PTFE | Static | Bacteria | 100 | 15 min | 2010 | [42] |
| | PTFE | Static | Virus | 11.5 | 24 min | 2013 | [43] |
| | PTFE | Static | PET tracers | 10 | 19 min | 2014 | [44] |
| | PTFE | Dynamic, on-Line | Sample plugs | 27 | 60 min | 2016 | [46] |

| | | | | | | | |
|---|---|---|---|---|---|---|---|
| Tubular membranes | PP HF | Dynamic | Pharmaceuticals | 16.5-19 | 24 s | 2004 | [47] |
| | Nafion HF | | | 16.5 | | | |
| | Radiation grafted PTFE, COOH PP, Nafion, Nafion coated PP | Dynamic pre and post separation | Anions (Ion Chromatogrphy) | 6 | diverse | 2007 | [48] |
| | PP | Dynamic | Pharmaceuticals | ≤ 5.6 | - | 2011 | [49] |
| | CNIM PP | Dynamic | | 13-48 | - | 2011 | [50] |
| | PP HF, silicon nitride | Dynamic | Samples for NMR | 16 | - | 2016 | [51] |
| | | Dynamic post-separation and nebulisation | HPLC to ICP-MS hyphenation | n/a | n/a | 2005, 2006 | [52],[54] |
| | | | | | | 2015 | [53] |
| Porous materials | PDMS | | Osmotic pumps (salts) | n/a | n/a | 2005 | [57] |
| | PDMS | Dynamic nanofluidics | Fluorescent beads | 6500 | 55 min | 2009 | [58] |
| | Self-assembled particle membrane (SAPM) | Dynamic, off-line | Particles and cells | 100-120 | 120 min | 2016 | [59] |
| Shrinking droplets | Water / soybean oil | Dynamic | Solutes, Nanoparticles | to max. final concentration | 480 s | 2004 | [63] |
| | Water / soybean oil | Static | Glycerol | | 90-110 s | 2010 | [64] |
| | Octane / surfactant solution | Static | Selective droplet concentration | 500 | 30 min | 2015 | [69] |
| | Dimethyl carbonate / eluent | Dynamic | ESI/MS | 10 | 2 min | 2009 | [70] |

## 2. SOLVENT REMOVAL FOR PRECONCENTRATION

Solvent removal can be regarded as a route feasible for almost any biological or chemical application. The main ways to achieve volume reduction by solvent removal are discussed and classified in this section, exposing the advantages and limitations of each particular method. A schematic summary of the different strategies to achieve concentration by solvent removal is shown in Figure 1. Also, Table 1 provides a comprehensive classification of the current literature including applications.

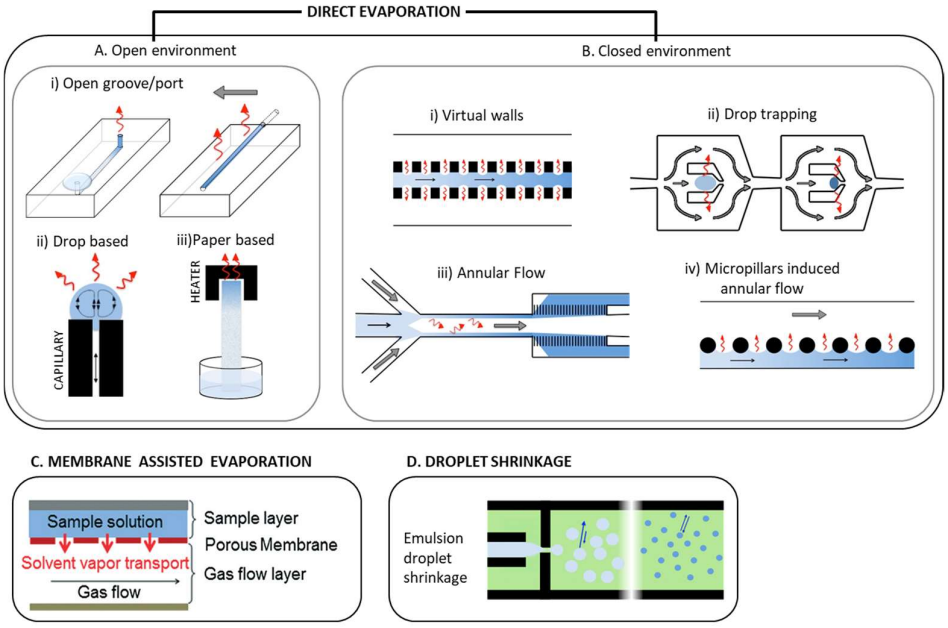


*Figure 1. Schematic summary of the different strategies to achieve concentration by solvent removal.*

### *2.1 DIRECT EVAPORATION*

Direct evaporation is referring to that occurring at a direct or non-mediated interface between the liquid and gaseous phase, ie, the gas and liquid phase are in intimate and direct contact.

*i. Ambient evaporation*

Ambient evaporation takes place in a non-confined chamber or space and is widely used in macrofluidics. A large number of variables influence the process which may not or cannot be regulated; such as humidity, air temperature and/or pressure to name a few. Sample enrichment by evaporation under gas flow is an established and routine procedure used to reduce large volumes of liquid. However, when very small sample volumes are required single drop evaporation is presented as an alternative. In order to control the drop volumes and evaporation process, the evaporation of a single levitating drop was reported in 1998. An ultrasonic frequency was used to levitate a drop while a liquid microdispenser ejected tuneable size microdroplets to join the levitated drop. The solvent was allowed to evaporate a total of 3.5 minutes to lower the limit of detection 166 times [12].

In a simpler way, droplets can be shrunk by evaporation on a surface. Microdroplets were dispensed into a cylindrical micro cavity, where they could be evaporated over a period of time [13]. A 5-fold enrichment was reported in just a few seconds. However, analyte loss due to dry ring stains as the droplet shrinks by evaporation is a disadvantage [14]. To overcome this limitation and achieve higher concentrations within the drop, the drying process has been extensively studied [15] and super-hydrophobic surfaces used to avoid staining [16]. Walker et. al. [17] presented one of the first approaches towards evaporation as a concentration technique in microfluidics. A chip was developed which consisted of two ports connected by a straight channel, where a water drop is placed on the inlet port once the channel is completely full of sample. This reservoir drop acts as a continuous supply by capillary force while evaporation occurs at the open collection port. A schematic representation of the device is shown in Figure 1A i) left. During this process, concentration was observed at the collection port via fluorescent detection of micro spheres. Later, a method using infrared (IR) radiation at the collection port to achieve enhanced evaporation rates was reported [18].

During the IR radiation an increase in the temperature of the meniscus interface was observed, until it reached a stable value and the temperature distribution became uniform. Evaporation rates became stable and were shown to linearly increase with increasing laser power, reaching around 20 $pg.\mu m^{-2}.s^{-1}$ when 30 nW was applied. Another open evaporation device consisted of a microchannel groove placed under perpendicular laminar dry air flow, shown in Figure 1A i) right [19]. The system was kept under constant temperature conditions (20°C) until the microchannel groove (150 x 80 µm width x depth) was completely dried by evaporation in 21 s. Shao et. al. adapted a drop mixing method in capillary wells [20] for concentration [21]. In this approach, a pendant drop is formed at the end of a capillary with air pressure and subsequently reintroduced. By doing so, mixing occurs inside the drop as represented in Figure 1A ii), increasing mass transfer and avoiding a concentration gradient between the air/drop interface and its centre. The time to achieve 2-fold concentration increase of fluorescent protein was calculated at different humidity conditions, the fastest being 6.5 minutes for 30% humidity. Fluorescence images obtained during droplet evaporation are shown in Figure 2A. A paper-based device was presented to concentrate analytes in biological fluids (Figure 1A iii)) [22]. The tip of a paper was heated while the opposite tip was still soaked into the target solution. Liquid travelled to the heated tip by capillary forces where the solvent was evaporated and the paper dried, which kept the sample moving. For optimized heating conditions, the heated tip held sample with a concentration factor of about 20 in 10 minutes, although this depended greatly on the sample matrix. This approach has certain limitations regarding the analytical techniques to be coupled with, but it is still a broad concentration technique for diverse soluble analytes that can separate them from a solid matrix. Also, chromatography paper was used as a substrate employing a fan to drive evaporation with increased air flow and avoid heating [23], resulting in a concentrated band as shown in Figure 2B. A model for capillary rise and concentration in the

presence of evaporation was presented and demonstrated to agree with experimental results showing 100-fold concentration in 3 h. Separation of concentrated dye bands was also obtained.

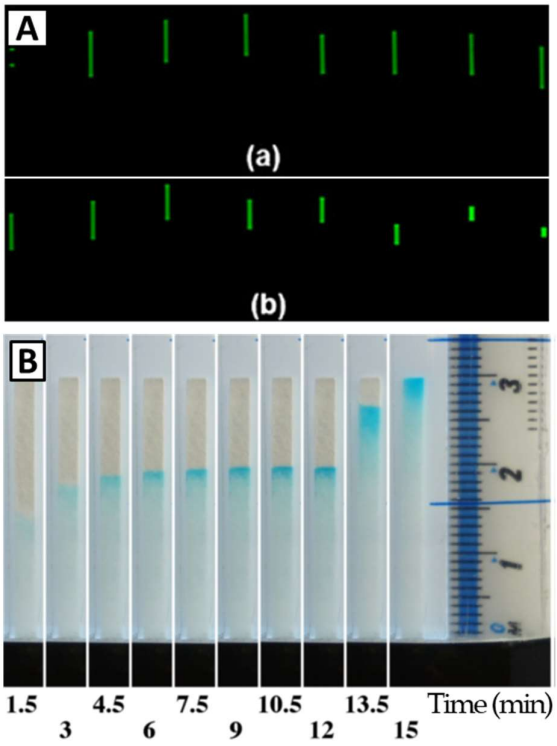


*Figure 2. A. Fluorescence images obtained in capillaries without (a) and with (b) the droplet mixing scheme. Reprinted from* [21] *with permission from Springer Nature. B. Images of a 30 mm long strip recorded during evaporation. After around 6 min the dye has reached the evaporation-dominated limit. At this point, a blue band of increasing strength provides evidence of concentration. After 12 min, the airflow is switched off and capillary action drives the concentrate to the tip of the. Reprinted from [23] with permission from AIP Publishing.*

*ii. Enclosed evaporation*

Other direct evaporation devices use closed microfluidic channels with different designs to provide a liquid/gas evaporation interface. These approaches generally provide a better control or monitoring of evaporation since the number of parameters to manipulate are limited. One early example is the use of virtual walls [24,25]. The device consists of a hydrophobic microchannel confined by a micropillar array connecting with air chambers [26]. A schematic of the device is shown in Figure 1B i). The traveling liquid does not fill the hydrophobic side creating a virtual channel as long as the pressure does not exceed a certain critical value. The evaporative concentration chip was used with electrokinetic flow where temperature increased due to Joule effect, causing evaporation of solvent and condensation inside the air chambers, effectively concentrating the sample as it travels. In a qualitative study, a 4-fold increase in fluorescent intensity was achieved within 4 min in the 3 cm channel. Later, a different heating system was implemented in a similar device by pre-heating sample before accessing the chip instead of taking advantage of the Joule effect, more appropriate for non-electrochemical analysis techniques [27]. Concentration of Rhodamine 6G was achieved at the micropillar array interface as shown in Figure 3A. The concentration factor increased exponentially with temperature, achieving 25 fold at 80°C in just one min. Micropillars have been used in a similar design with co-current gas-liquid flow for the purpose of distillation [28], where the liquid flow was confined by micropillars located perpendicular to one of the channel walls (Figure 1B iv).

Another method for organic solvent separation from water that could be adapted to sample enrichment by evaporation consists of the generation of annular flow. In a device shown in Figure 3B (simplified view in Figure 1B iii), three parallel microchannels are merged into one. The central channel has a gas stream while the two outer ones contain liquid. When channels are merged an annular gas-liquid stream is formed [29]. In the annular flow

regime the liquid phase contacts the channel walls while nitrogen flows through the centre of the channel, and it requires specific optimized flow rate and pressure conditions. This provides maximum gas-liquid interface achieving good evaporation rates, which are further enhanced by heating. After solvent removal, the gas and liquid flows are separated using a channel with side capillaries on the walls. The hydrophilic liquid phase enters the capillaries, while the gas stream remains in the wider main channel. In optimized conditions acetonitrile was reduced from 50% to fewer than 5%.

An alternative to virtual walls was presented by trapping and monitoring microdroplets in microchambers to subsequently shrink them with an air flow [30,31]. This device, shown in Figure 1B ii), consists of a series of microchambers each containing a single funnel-like trap microstructure. The target sample is pumped through the chambers leaving drops of captured liquid in the traps where the analyte will be concentrated. The sample can be recovered by reintroducing flow in the opposite direction. A 10 nM fluorescent solution was used to assess the efficiency showing that the droplet diameter shrunk 4.5 times (90-fold volumetric shrinkage), as shown in Figure 3C. Most of these approaches rely on the stability of the gas-liquid or immiscible liquid-liquid interface to provide consistent mass and energy transfer and therefore consistent results. Multiphase flows have been studied for decades [32] and its behaviour in microchannels are of interest to provide highly controlled processes [33]. In gas-liquid flow, the wetting properties of the fluid-wall are extremely important. They depend on properties of the fluid such as viscosity or surface tension, as well as the properties of the channel wettability and size. Also the velocity and pressure of liquid and gas is critical [34]. Even when structures such as micropillars are used to confine the liquid and preserve a stable interface, changes in liquid phase composition are disruptive. Concerning liquid–liquid flow, droplet formation processes are induced by the competition between viscous stresses and interfacial tension, where microfluidic structures play an important role. An external force can be

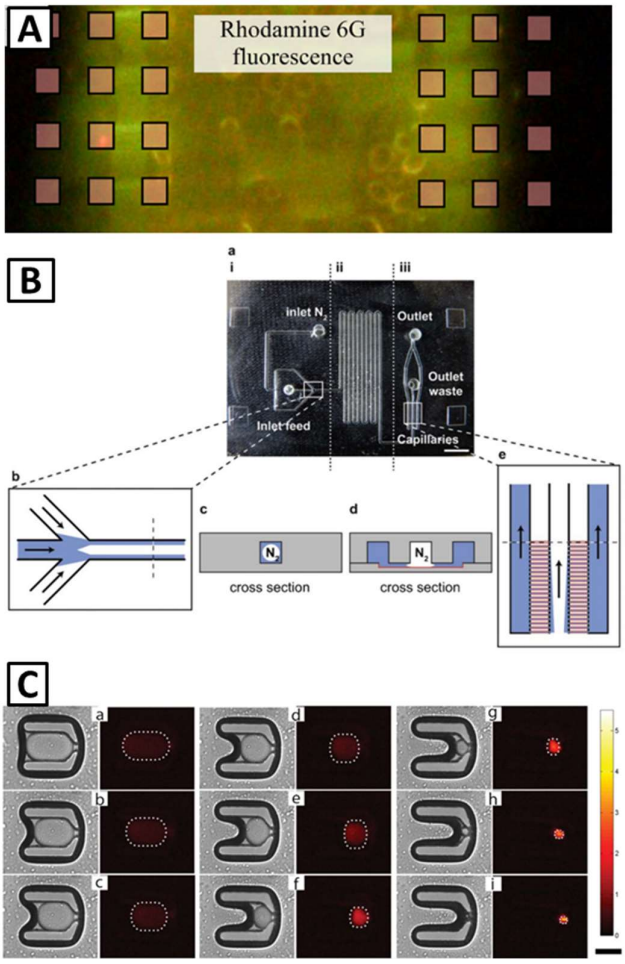


*Figure 3. A. Micropillar array virtual wall evaporation interface where Rhodamine 6G is concentrated. Reprinted from [27] with permission from AIP Publishing. B. Photograph (a) and schematic drawings (b–e) of the evaporation device. (a) The glass microdevice consists of three sections for (i) gas/liquid introduction, (ii) evaporation and (iii) gas–liquid phase separation. Schematic of the annular flow formation (b) and cross section (c). Schematic of phase separation (e) cross section (d). Reprinted from [29] with permission from Royal Society of Chemistry. C. Sequence from a to i: (left image of pair) bright field images of the progressive droplet shrinkage through evaporation (right image of pair) the respective fluorescence intensity measurements. Colour bar is in relative units and the scale bar is 50 mm. Reprinted from [30] with permission from Royal Society of Chemistry.*

applied to actively control droplet breakup. However, a change in any of the conditions may influence the droplets size, frequency or homogeneity [35]. Considering these potential difficulties in maintaining the interface, a different approach providing more confinement of the liquid phase may be desirable. That is especially true when the target solutions are diverse in nature and therefore conditions for a multiphase flow would have to be adjusted continuously.

### *2.2 MEMBRANE ASSISTED SOLVENT EVAPORATION*

An alternative to direct evaporation that can provide a more controlled interface is the introduction of a vapour permeable membrane as an evaporation interface. This membrane is not wetted and displays a barrier for the liquid phase, while the pores allow the gas phase to travel through it. The driving force of the process is given by a partial vapour pressure difference between both sides of the membrane, and is commonly enhanced by a temperature difference [36,37]. In addition, great effort has been put into improving the performance of gas-liquid membrane contactors. A lower drag over gas-liquid interface was achieved using different micro grooved membrane designs [38], while better contact between the target solution and the membrane was achieved by using different in-channel baffle arrangements for mixing [39].

#### *i. Flat membranes*

The first microfluidic evaporative concentrator was described in 2003 by Timmer et al. [40] containing a liquid flow channel separated from another parallel air channel by a hydrophobic membrane. These two channels were directly overlayed so the membrane acts as a common wall and the evaporation interface. It achieved around 3-fold concentration factor under continuous flow at 5 $\mu L.min^{-1}$ without heat and a counter-current nitrogen gas flow. In 2008 Sharma et al. [41] reported a design to concentrate bovine

serum albumin (BSA) from a large volume of water using a continuous-flow evaporator with millimeter-sized channels. Humidity of the air and temperature were controlled at all times, and the pressure of the airflow and extent of the vacuum in the air channel were studied. Water removal rates ranging from 0.6 $mL.min^{-1}$ to 1.8 $mL.min^{-1}$, for 18°C and 52°C, respectively, were obtained (13 $L.min^{-1}$ air flow and -6. 8 kPa vacuum pressure), although there was no concentration data presented.

Later, a similar concept was applied for various applications with slightly different configurations in their assembly. The sample was introduced in the membrane device and concentrated in static conditions before collection. Fluorescent stained bacteria were concentrated in a 100 µm x 700 µm (depth x width) channel, which slowly filled with air as the sample volume was reduced from 100 µL to 300 nL while preserving the original amount of bacteria [42]. Viruses were also concentrated in a similar device (1.7 mm x 100 µm, width x depth) [43]. Initially, 100 nm fluorescent beads were used to assess the concentration gradient during the process showing increased intensity with an 85% recovery. The overall length of the fluorescent region indicated movement of a highly concentrated meniscus towards the outlet as shown in Figure 4A – where the volume was reduced from 1 mL to 50 µL. However, a lower recovery of 50% was reported for virus RNA from both real and cultured samples with a concentration factor of 11.5 ± 3.3. More recently a similar approach has been applied to the production of positron emission tomography (PET) traces, which are injected for imaging in cancer diagnosis and research [44,45]. To easily concentrate diluted tracing liquid it was introduced in a 4.5 mm x 170 µm (width × depth) serpentine channel while gas flow and temperature were applied. Within 19 min, 90% of the channel volume was evaporated. The reported devices operating in static conditions achieved good concentration rates. However, they have large sample volume requirements, unknown concentration factors, sample loss or residue left in dry spots on the channels or membranes [42,44]. Recoveries under 85% were

reported. A device for on-line analyte concentration was developed where a sample plug in a liquid stream was concentrated before detection. Monitoring of concentration in the evaporation device using fluorescein is shown in Figure 4B.

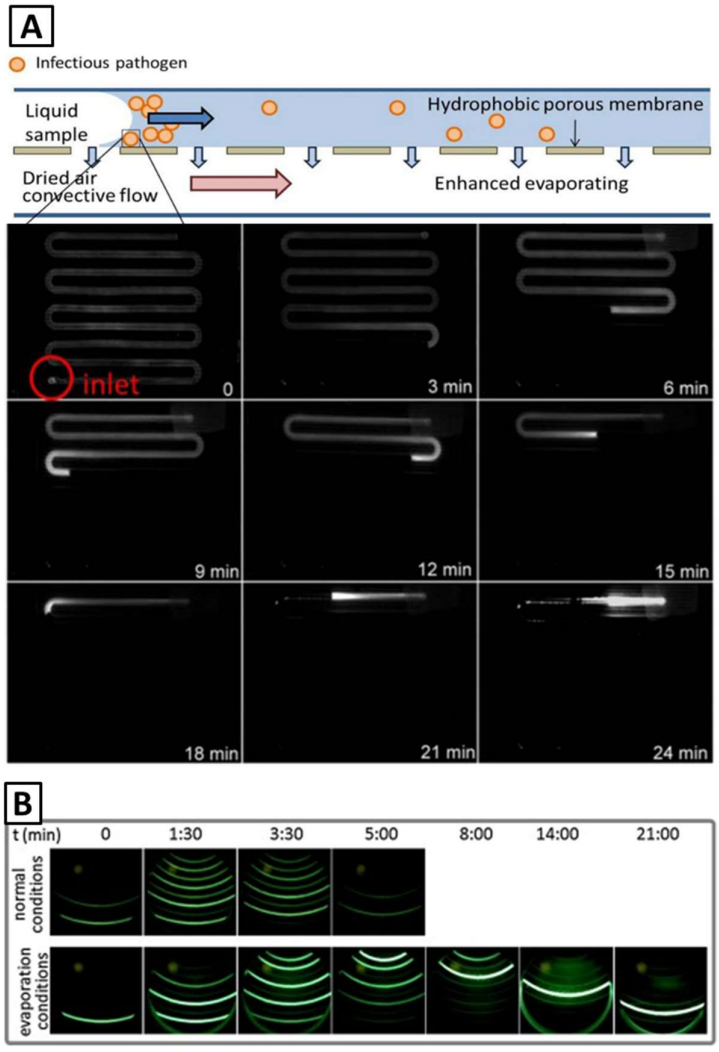


*Figure 4. A. Top: Schematic of the convective evaporation microfluidic device and representation of the meniscus dragging effect. Bottom: Concentration of fluorescent beads in the evaporator over time. Reprinted from [43]. B Captures of recorded fluorescein sample plug pathway in normal (room temperature, no vacuum) and evaporation conditions (45 °C, vacuum). Reprinted from [46] Copyright (2017), with permission from Elsevier.*

A model to describe the process was developed allowing for concentration factor prediction [46]. Therefore, for a given application with a target enrichment factor, the required experimental conditions could be calculated. Using optimal conditions, a 27-fold concentration factor was achieved in 60 min at less than 60 °C. However, precise temperature control is required for accurate and repeatable performance.

By using this approach for preconcentration, matrix components are concentrated along with target analytes. Therefore, it would be favourable for potential applications where broad scale concentration is desired to provide complete coverage of the sample. Complementary analysis steps may be insensitive to matrix components or include sample clean-up steps for complex samples. Since this is an on-line technique, it would provide significant benefits with regards to throughput, recovery and analysis integrity.

*ii. Tubular membranes*

The use of tubular membranes or porous hollow fibres as an alternative to flat membranes has been also reported. Tubular membranes are advantageous since they present evaporation in all directions achieving a more uniform process. In 2004 [47] a membrane concentrator was developed where target solution was pumped, before analysis, through membrane hollow fibres sealed in a 50 cm casing. Two variants were studied, one using siloxane coated hydrophobic polypropylene (PP) fibres for non-polar solvents, and another using a Nafion hollow fibre for polar solvents. In both cases several temperatures and flow rates were used, as well as a counter-current nitrogen at several gas pressures. All these parameters were found to have an impact on solvent removal and were optimised. At 55 degrees, enrichment factors were 16.5-19 and a maximum recovery of 81% was achieved for the target analytes from hexane solutions, while only 5.7-7 from methanol solutions with lower recoveries. In 2007 a comprehensive study was carried out

evaluating evaporative performance of four main tubular membranes including cation exchange and porous materials, used in four configurations [48]. These were located after anion chromatography separation and before detection, so that cation exchange membranes operated in the required alkaline media. Only in this condition pervaporation occurred, and evaporation rates were greater than those observed for porous membranes. Concentration factors as high as 16.5 were reported while analyte loss was considered to be due to a combination of volatility and $pK_a$ of the analytes, for example in the case of carbonate. When the evaporators were located before separation, and therefore before suppression, other cations were captured by the membrane and pervaporation decreased over time. Thus, the membrane needed to be regenerated periodically or an additional suppressor could be used before concentration, highlighting the benefits and drawbacks of ionic membranes compared to porous membranes. The unavoidable deterioration of resolution due to dispersion within the evaporation path was acknowledged. Later, an automated system for the preconcentration of pharmaceutical compounds before high performance liquid chromatography (HPLC) separations was developed [49]. Polypropylene tubular membranes were used in an in-house module and all relevant parameters optimised. Enrichment factors of up to 5.6 were reported with less than 5% deviation. In order to improve this concentration performance carbon nanotube immobilised membranes (CNIMs) were later used [50]. The increase in preconcentration compared to plain membranes was analyte dependent between 65 and 164%. Recently, a microfluidic evaporative in-line sample concentrator was developed, using either polypropylene porous hollow fibre or silicon nitride membrane [51]. Under optimised conditions, the hollow fibre evaporator showed a maximum 16-fold concentration factor at flow rate lower than 10 $\mu L.min^{-1}$, with high precision required for repeatability. A theoretical model was also developed but did not match experimental data, due to the complexity of the membrane evaporation phenomenon.

Intuitively, detection sensitivity can be enhanced via solvent removal, however, when solvents act as an interference for certain detection or interfacing techniques, the benefits of solvent removal are greater than preconcentration. One of those cases is detection by Inductively Coupled Plasma – Mass Spectrometry (ICP-MS) after HPLC separations with solvent and solvent gradients, which greatly influence signal intensity. Commercial membrane desolvation units have been used after nebulisation and prior ICP-MS detection showing reduced signal suppression during solvent gradients. However, large variations in sensitivity were observed for different species and LODs were not improved [52,53], while linearity was compromised [54].

*iii. Porous materials*

Advantage may be taken of the porosity of polymeric materials for microfluidics. Various applications with porous materials, thus having porous walls, involving gas transport have been reported [55,56]. The concept of membrane assisted evaporation is presented in Figure 1C. Water vapour movement was observed [57] from a salt solution to outside the channel through a 2.3 µm thin wall of a polyimide channel 500 µm high. A water transport rate of 3 µm $s^{-1}$ was calculated and the observed phenomenon was suggested for concentration applications. Later, an evaporation device was used in a bioanalysis procedure using a 20-30µm PDMS layer acting as a membrane between a liquid and air channels [58]. The 100 µm x 12 µm (width x depth) flow channel was connected to a sample reservoir at the inlet, while an actuation valve at the other end was used to interrupt the flux and prevent it from entering the detection chamber. Dry nitrogen was passed through the evaporation channel to enhance solvent removal, which enabled more sample introduction from the reservoir and accumulation of analyte at the dead end. This operation procedure avoided the above-mentioned issue involving dry channels due to volume reduction. The effect of temperature and gas pressure were studied achieving evaporation rates as high as 120 $nL.min^{-1}$ at 80°C and 25 PSI. Recently, sample enrichment was performed via

evaporation through a self-assembled particle membrane (SAPMembrane) [59]. The device consists of triangular microchamber arrays connecting a sample channel on one of the triangle vertex and the gas channel at the opposite triangle side. At this side, a low-level section was filled with 1 µm particles via self-assembly from a particle suspension, acting as a membrane for evaporation with a theoretical pore size of around 0.4 µm. Sample solution was drawn from the channel into the triangular chamber via evaporation-driven capillary forces while particles/cells were concentrated adjacent to the SAPMembrane. Concentration factors ranged from 100 to 120 for microparticles within 2 h and approximately 30 for bacterial cells within 1 h.

### *2.3 Shrinkage of emulsion droplets*

Droplet based microfluidics are based on micrometer sized droplets dispersed in an immiscible continuous phase; systems that have all the advantage of microfluidics plus higher interface surface. All kinds of processes can be achieved within single droplets providing tools for multi-step operations and coupling of concentration steps to total analysis systems [60]. Techniques for droplet generation are numerous and provide diverse droplet properties such as uniformity, size and stability, which can be adjusted for each application requirements [61]. One of the potential applications of these dispersions is concentration of dissolved species or particles within individual microdroplets, relying on slow dissolution of the droplet solvent into the continuous phase while the solutes are enclosed within the droplet, as suggested in Figure 1D. [62] This concentrating effect will only work for solutes that do not dissolve in or react with the continuous phase. An early approach for concentration by shrinking water-in-oil droplets was described for particles and solutes using soybean oil as a continuous phase [63]. For water droplets that did not contain any solutes, the droplet continued to shrink until it was completely dissolved into the organic phase. But for

droplets with solutes the size initially decreased with time until it had reached its final size. The shrinking process was monitored using microscopy as shown in Figure 4A.

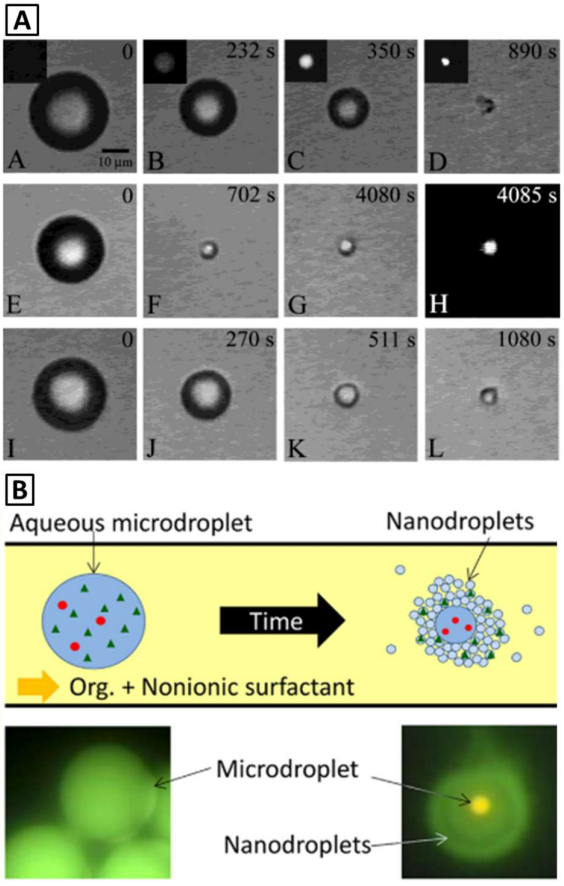


*Figure 5. A Sequence of micrographs showing the concentration of aqueous microdroplets in soybean oil containing (A-D) Fluorescent polystyrene nanoparticles (E-H) dye-labelled carbonic andydrase. (H) shows the fluorescence image of the concentrated dye-tagged protein. (I-L) sodium chloride. Reprinted from [63], Copyright (2004) with permission from American Chemical Society. B. Selective concentration of a microdroplet's contents by spontaneous emulsification. Reprinted from* [64] *Copyright (2015) with permission from American Chemical Society.*

The decrease in droplet volume was found to be linearly proportional to the increase in fluorescence intensity of fluorescent dye containing droplets. In a more simple approach, 2 µL drops of water-in-oil emulsions were manually placed on a bulk heater protected by a hydrophobic coverslip to concentrate cryoprotectant [65]. The solution was maintained at 35°C and the size of the water droplet monitored while it shrunk. It was suggested that droplets follow a common pattern of shrinkage and a concentration profile reaching a final maximum concentration. The emulsion was prepared manually instead of in a microfluidics platform resulting in inconsistent droplet sizes. However, the concentration underwent thermodynamic investigation [66] in agreement with the previous observations.

Dynamics of aqueous microdroplets shrinkage were analysed in other studies [67–69] as it is believed that by understanding the kinetics and the factors that affect droplet shrinkage, it should be possible to control precisely the concentrations of dissolved species within individual droplets. Furthermore, a selective concentration method was reported, where fluorescent dyes were concentrated up to 500 times by shrinking water droplets in an octane surfactant solution [64]. It is a selective method since properties such as the size and hydrophobicity of the microdroplet contents determined whether analytes either stayed in the microdroplet or partitioned into nanodroplets, formed by spontaneous emulsification. Fluorescence microscopy images of the initial and final stages in the emulsification process can be observed in Figure 5B. Hydrophilic and larger molecules tended to be concentrated rather than partitioned into nanodroplets. This behaviour broadens the applicability of shrinking water-in-oil droplets. The shrinking droplet technique has also been used as an interfacing procedure, between a separation technique and detection by ESI/MS. Ji et al. [70] reported a concentration interface that was capable of enriching online separated peptides 10 times within the microdroplet before their detection by ESI-MS/MS. However, lower concentration rates were achieved at lower organic solvent composition

being 4-5 times the fluorescence signal increase under 50% acetonitrile. This presents a problem for analysis of gradient separations.

## 3. Conclusions and Future Perspectives

Applications where solvent removal is the most appropriate preconcentration strategy are numerous and focus on chemical and biological issues. This review presents a variety of strategies that have been used for the purpose, and the great amount of technologies that have been developed to achieve integrated solvent removal for preconcentration. All the techniques show different advantages or drawbacks in terms of ability to integrate, attainable concentration factor, time required or accuracy. Table 1 summarizes the characteristics of the presented technologies as well as the applications they were used for. However, it is important to highlight that results generally show performance depending on certain analyte properties, such as hydrophilicity or boiling point. Also, the matrix or solvent composition has a remarkable impact on reproducibility and viability of these preconcentration strategies, so this information is specified too. In addition, we have provided our point of view regarding the feasibility to integrate each concentration strategy in a broader analytical process.

Although the reported techniques offer very good results for certain specific applications, they tend to be very susceptible to changes in conditions such as humidity or temperature in the surrounding area, which can lower accuracy. This configuration with an open gas/liquid interface also has a greater risk of sample contamination by foreign compounds. On the other hand, they may be advantageous since the sample solvent composition is not crucial to maintain a stable gas/liquid interface, requiring only further optimisation to cater for different evaporation rates. It does however determine evaporation time and performance. In terms of integration, they often offer the possibility

of in situ detection but usually require manual steps if sample recovery for further analysis is desired.

The main advantage of enclosed evaporation compared to ambient evaporation is the possibility to integrate the procedure in an analytical process with automatic sample collection. Also advantageous is the ability to better control the properties of the gas phase and limit sample contamination due to the environment. However, contamination can be introduced by the materials used. A clear disadvantage is the vulnerability of the gas-liquid interface to changes in conditions, as it can be easily disrupted by changes in solvent composition or viscosity, as well as gas pressure.

Membrane assisted evaporation offers higher stability of the interface to changes in conditions such as pressure or velocity, and even changes in solvent composition may be tolerated. However, when the presence of organic solvents surpasses a critical point, polymeric membrane pores are wetted and the interface is disrupted. Micropatterned membranes can also become permeable at lower viscosities while efficiency of ion exchange membranes is highly pH dependant. All membranes are susceptible to solvent damage so materials used need to be watched carefully. As an additional advantage, the evaporation of certain volatile compounds can be reduced by controlling pore size, thickness and material.

Nevertheless, analytes may interact and bind to membrane materials and therefore are lost in the process. Small particles tend to block the pores and reduce evaporation efficiency; although in most cases membranes can be easily replaced, they should be preferentially used to concentrate solutes and not particles to avoid blockage as well as analyte loss. Contamination from foreign sources is reduced due to the membrane barrier, but contamination from within the system such as leakage of membrane materials can occur.

Tubular membranes present higher surface area to volume ratio, therefore offer higher efficiency than flat membrane devices. Both are easy to integrate

in longer processes. The use of porous materials within a microchip is obviously beneficial for total integration; however, frequent replacement of the membrane is not possible and so the lifetime of the device is limited.

Shrinkage of emulsion drops is an excellent option for droplet based systems; however, integration is difficult for non-droplet systems. Moreover, it can provide sample clean-up benefits due to partitioning of unwanted analytes into the dispersion medium [75], which can also be detrimental if concentration of all analytes is required. Regarding sample solvent composition needs to be surveyed to be avoid miscibility of dispersed and dispersion media.

For example, ambient evaporation techniques are difficult to integrate but can be ideal for dry residue handling. Membrane assisted evaporation needs careful planning to avoid loss of volatile analytes, as well as those that could be affine to the membrane material.

In conclusion, the interface where solvent transfer occurs is usually stable in a range of conditions only, so changing them can be catastrophic. The presence of organic solvents generally increases concentration speed, but it also changes the interface properties deterring its stability. It is therefore difficult to point out a technique that could become standard for all cases.

Future perspectives. To allow for extensive application of solvent removal as a concentration technique in complex systems, the gas/liquid interface needs to be stable under a very broad range of conditions and not vulnerable to small fluctuations to avoid constant optimisation. Membrane assisted evaporation can provide for aqueous or low organic solvent content samples. However, further development regarding solvent resistance is of paramount importance to its success. Ampyphobic membrane coatings [71,72] can provide such properties. Furthermore, novel microfabrication techniques can lead to a new generation of gas-liquid contactors where the barrier for the liquid phase is an amphiphobic nanostructure - functionalised silicon

nanowires [73]. Point-of-care devices using very selective analysis and detection procedures generally do not require collection of the concentrate. Thus, ambient evaporation techniques are more suitable since they offer easy implementation regardless of the solvent composition and high efficiency.

## ACKNOWLEDGEMENTS

This research was conducted by the ARC Training Centre for Portable Analytical Separation Technologies (IC140100022). MCB is the recipient of an ARC Future Fellowship. E. Fornells is the recipient of an ARC CHDR scholarship and a University of Tasmania tuition fee scholarship.

## REFERENCES

[1] H.P.M. Van Vliet, T.C. Bootsmann, R.W. Frei, U.A.T. Brinkman, On-line trace enrichment in high-performance liquid chromatography using a pre-column, J. Chromatogr. A. 185 (1979) 483–495.

[2] C.E. Werkhoven-Goewie, U.A.T. Brinkman, R.W. Frei, Trace enrichment of polar compounds on chemically bonded and carbonaceous sorbents and application to chlorophenol, Anal. Chem. 53 (1981) 2072–2080.

[3] P.A. Auroux, D. Iossifidis, D.R. Reyes, A. Manz, Micro total analysis systems. 2. Analytical standard operations and applications, Anal. Chem. 74 (2002) 2637–2652.

[4] L.R. Volpatti, A.K. Yetisen, Commercialization of microfluidic devices., Trends Biotechnol. 32 (2014) 347–50.

[5] K. Sueyoshi, F. Kitagawa, K. Otsuka, Recent progress of online sample preconcentration techniques in microchip electrophoresis, J. Sep. Sci. 31 (2008) 2650–2666.

[6] C.C. Lin, J.L. Hsu, G.B. Lee, Sample preconcentration in microfluidic devices, Microfluid. Nanofluidics. 10 (2011) 481–511.

[7] S. Song, A.K. Singh, On-chip sample preconcentration for integrated microfluidic analysis, Anal. Bioanal. Chem. 384 (2006) 41–43.

[8] D.S. Stegehuis, H. Irthu, U.R. Tjaden, J. Van Der Greef, Isotachophoresis as an on-line concentration pretreatment technique in capillary electrophoresis, J. Chromatogr. A. 538 (1991) 393–402.

[9] A. Wainright, S.J. Williams, G. Ciambrone, Q. Xue, J. Wei, D. Harris, Sample pre-concentration by isotachophoresis in microfluidic devices, J. Chromatogr. A. 979 (2002) 69–80.

[10] T. Rosenfeld, M. Bercovici, 1000-fold sample focusing on paper-based microfluidic devices., Lab Chip. 14 (2014) 4465–74.

[11] J.D. Ramsey, G.E. Collins, Integrated microfluidic device for solid-phase extraction coupled to micellar electrokinetic chromatography separation., Anal. Chem. 77 (2005) 6664–70.

[12] M. Petersson, J. Nilsson, L. Wallman, T. Laurell, J. Johansson, S. Nilsson, Sample enrichment in a single levitated droplet for capillary electrophoresis, in: J. Chromatogr. B Biomed. Appl., 1998: pp. 39–46.

[13] S. Neugebauer, S.R. Evans, Z.P. Aguilar, M. Mosbach, I. Fritsch, W. Schuhmann, Analysis in Ultrasmall Volumes: Microdispensing of Picoliter Droplets and Analysis without Protection from Evaporation, Anal. Chem. 76 (2004) 458–463.

[14] R.D. Deegan, O. Bakajin, T.F. Dupont, G. Huber, S.R. Nagel, T.A. Witten, Capillary flow as the cause of ring stains from dried liquid drops, Nature. 389 (1997) 827–829.

[15] S. Dash, S. V. Garimella, Droplet evaporation on heated hydrophobic

and superhydrophobic surfaces, Phys. Rev. E - Stat. Nonlinear, Soft Matter Phys. 89 (2014) 042402.

[16] F. Shao, T.W. Ng, O.W. Liew, J. Fu, T. Sridhar, Evaporative preconcentration and cryopreservation of fluorescent analytes using superhydrophobic surfaces, Soft Matter. 8 (2012) 3563.

[17] G.M. Walker, D.J. Beebe, An evaporation-based microfluidic sample concentration method., Lab Chip. 2 (2002) 57–61.

[18] Q. Xu, R. Chen, H. Wang, X. Zhu, Q. Liao, X. He, IR laser induced meniscus evaporation from a microchannel, Chem. Eng. Sci. 130 (2015) 31–40.

[19] S. Kachel, Y. Zhou, P. Scharfer, C. Vrančić, W. Petrich, W. Schabel, Evaporation from open microchannel grooves., Lab Chip. 14 (2014) 771–8.

[20] J.K.K. Lye, T.W. Ng, A. Neild, O.W. Liew, A capacity for mixing in capillary wells for microplates., Anal. Biochem. 410 (2011) 152–4.

[21] F. Shao, T.W. Ng, J.K.K. Lye, O.W. Liew, Evaporative preconcentration of fluorescent protein samples in capillary based microplates, J. Fluoresc. 21 (2011) 1835–1839.

[22] S.Y. Wong, M. Cabodi, J. Rolland, C.M. Klapperich, Evaporative Concentration on a Paper-Based Device to Concentrate Analytes in a Biological Fluid, Anal. Chem. 86 (2014) 11981–11985.

[23] R. Syms, Rapid evaporation-driven chemical pre-concentration and separation on paper, Biomicrofluidics. 11 (2017) 044116.

[24] W. Xu, H. Xue, M. Bachman, G.P. Li, Virtual walls in microchannels, Annu. Int. Conf. IEEE Eng. Med. Biol. - Proc. (2006) 2840–2843.

[25] B. Zhao, J.S. Moore, D.J. Beebe, Surface-directed liquid flow inside

microchannels., Science. 291 (2001) 1023–6.

[26] W. Xu, L.L. Wu, G.P. Li, M. Bachman, A Vapor Based Microfluidic Sample Concentrator, in: 14th Int. Conf. Miniaturized Syst. Chem. Life Sci., 2010.

[27] J.-W. Choi, S.M. Hosseini Hashemi, D. Erickson, D. Psaltis, A micropillar array for sample concentration via in-plane evaporation, Biomicrofluidics. 8 (2014) 044108.

[28] A. Constantinou, F. Ghiotto, K.F. Lam, A. Gavriilidis, Stripping of acetone from water with microfabricated and membrane gas–liquid contactors, Analyst. 139 (2014) 266–272.

[29] B.Z. Cvetković, O. Lade, L. Marra, V. Arima, R. Rinaldi, P.S. Dittrich, Nitrogen supported solvent evaporation using continuous-flow microfluidics, RSC Adv. 2 (2012) 11117.

[30] X. Casadevall i Solvas, V. Turek, T. Prodromakis, J.B. Edel, Microfluidic evaporator for on-chip sample concentration, Lab Chip. 12 (2012) 4049.

[31] A. Huebner, D. Bratton, G. Whyte, M. Yang, A.J. Demello, C. Abell, F. Hollfelder, Static microdroplet arrays: a microfluidic device for droplet trapping, incubation and release for enzymatic and cell-based assays., Lab Chip. 9 (2009) 692–8.

[32] H. Bruce Stewart, B. Wendroff, Two-phase flow: Models and methods, J. Comput. Phys. 56 (1984) 363–409.

[33] C.N. Baroud, H. Willaime, Multiphase flows in microfluidics, Comptes Rendus Phys. 5 (2004) 547–555.

[34] C.X. Zhao, A.P.J. Middelberg, Two-phase microfluidic flows, Chem. Eng. Sci. 66 (2011) 1394–1411.

[35] A. Günther, K.F. Jensen, Multiphase microfluidics: from flow

characteristics to chemical and materials synthesis, Lab Chip. 6 (2006) 1487–1503.

[36] E. Drioli, V. Calabro, Y. Wu, Microporous membranes in membrane distillation, Pure Appl. Chem. 58 (1986).

[37] A. Alkhudhiri, N. Darwish, N. Hilal, Membrane distillation: A comprehensive review, Desalination. 287 (2012) 2–18.

[38] J.M. Jani, M. Wessling, R.G.H. Lammertink, A microgrooved membrane based gas-liquid contactor, Microfluid. Nanofluidics. 13 (2012) 499–509.

[39] A. Lautenschleger, E.Y. Kenig, A. Voigt, K. Sundmacher, Model-based analysis of a gas/vapor-liquid microchannel membrane contactor, AIChE J. 61 (2015) 2240–2256.

[40] B.H. Timmer, K.M. van Delft, W. Olthuis, P. Bergveld, A. van den Berg, Micro-evaporation electrolyte concentrator, Sensors Actuators B. 91 (2003) 342–346.

[41] N.R. Sharma, A. Lukyanov, R.L. Bardell, L. Seifried, M. Shen, Development of an evaporation-based microfluidic sample concentrator, in: W. Wang, C. Vauchier (Eds.), Microfluid. BioMEMS, Med. Microsystems VI, 2008: p. 68860R.

[42] J.Y. Zhang, J. Do, W.R. Premasiri, L.D. Ziegler, C.M. Klapperich, Rapid point-of-care concentration of bacteria in a disposable microfluidic device using meniscus dragging effect., Lab Chip. 10 (2010) 3265–3270.

[43] J. Zhang, M. Mahalanabis, L. Liu, J. Chang, N. Pollock, C. Klapperich, A Disposable Microfluidic Virus Concentration Device Based on Evaporation and Interfacial Tension, Diagnostics. 3 (2013) 155–169.

[44] W.-Y. Tseng, R.M. van Dam, Compact microfluidic device for rapid

concentration of PET tracers., Lab Chip. 14 (2014) 2293–302.

[45] P.H. Chao, J. Collins, J.P. Argus, W.-Y. Tseng, J.T. Lee, R. Michael van Dam, Automatic concentration and reformulation of PET tracers via microfluidic membrane distillation, Lab Chip. 17 (2017) 1802–1816.

[46] E. Fornells, B. Barnett, M. Bailey, R.A. Shellie, E.F. Hilder, M.C. Breadmore, Membrane assisted and temperature controlled on-line evaporative concentration for microfluidics, J. Chromatogr. A. 1486 (2017) 110–116.

[47] E.J. Bishop, S. Mitra, Hollow fiber membrane concentrator for on-line preconcentration, J. Chromatogr. A. 1046 (2004) 11–17.

[48] M. Takeuchi, P.K. Dasgupta, J. V. Dyke, K. Srinivasan, Postcolumn Concentration in Liquid Chromatography. On-Line Eluent Evaporation and Analyte Postconcentration in Ion Chromatography, Anal. Chem. 79 (2007) 5690–5697.

[49] K. Gethard, S. Mitra, Membrane distillation as an online concentration technique: application to the determination of pharmaceutical residues in natural waters., Anal. Bioanal. Chem. 400 (2011) 571–5.

[50] K. Gethard, S. Mitra, Carbon nanotube enhanced membrane distillation for online preconcentration of trace pharmaceuticals in polar solvents., Analyst. 136 (2011) 2643–8.

[51] H. Zhang, R.M. Tiggelaar, S. Schlautmann, J. Bart, H. Gardeniers, In-line sample concentration by evaporation through porous hollow fibers and micromachined membranes embedded in microfluidic devices, Electrophoresis. 37 (2016) 463–471.

[52] L. Bendahl, B. Gammelgaard, Sample introduction systems for reversed phase LC-ICP-MS of selenium using large amounts of methanol—comparison of systems based on membrane desolvation, a spray

chamber and direct injection, J. Anal. At. Spectrom. 20 (2005) 410–416.

[53] L.H. Møller, C.S. Jensen, T.T.T.N. Nguyen, S. Stürup, B. Gammelgaard, Evaluation of a membrane desolvator for LC-ICP-MS analysis of selenium and platinum species for application to peptides and proteins, J. Anal. At. Spectrom. 30 (2015) 277–284.

[54] K. Kahen, K. Jorabchi, A. Montaser, Desolvation-induced non-linearity in the analysis of bromine using an ultrasonic nebulizer with membrane desolvation and inductively coupled plasma mass spectrometry, J. Anal. At. Spectrom. 21 (2006) 588.

[55] J. de Jong, B. Ankoné, R.G.H. Lammertink, M. Wessling, New replication technique for the fabrication of thin polymeric microfluidic devices with tunable porosity., Lab Chip. 5 (2005) 1240–1247.

[56] J. de Jong, M.J. Geerken, R.G.H. Lammertink, M. Wessling, Porous Microfluidic Devices – Fabrication and Applications, Chem. Eng. Technol. 30 (2007) 309–315.

[57] J.C.T. Eijkel, J.G. Bomer, A. Van Den Berg, Osmosis and pervaporation in polyimide submicron microfluidic channel structures, Appl. Phys. Lett. 87 (2005) 85–88.

[58] C.M. Puleo, T.-H. Wang, Microfluidic means of achieving attomolar detection limits with molecular beacon probes., Lab Chip. 9 (2009) 1065–1072.

[59] J. Lee, M. Kim, J. Park, T. Kim, Self-assembled particle membranes for in situ concentration and chemostat-like cultivation of microorganisms on a chip, Lab Chip. 16 (2016) 1072–1080.

[60] M. Leman, F. Abouakil, A.D. Griffiths, P. Tabeling, Droplet-based microfluidics at the femtolitre scale, Lab Chip. 15 (2015) 753–765.

[61] P. Zhu, L. Wang, Passive and active droplet generation with microfluidics: a review, Lab Chip. 17 (2017) 34–75.

[62] F. Eslami, J. a W. Elliott, Stability analysis of microdrops during concentrating processes, J. Phys. Chem. B. 118 (2014) 3630–3641.

[63] M. He, C. Sun, D.T. Chiu, Concentrating Solutes and Nanoparticles within Individual Aqueous Microdroplets, Anal. Chem. 76 (2004) 1222–1227.

[64] M. Fukuyama, A. Hibara, Microfluidic Selective Concentration of Microdroplet Contents by Spontaneous Emulsification, Anal. Chem. 87 (2015) 3562–3565.

[65] A. Bajpayee, J.F. Edd, A. Chang, M. Toner, Concentration of Glycerol in Aqueous Microdroplets by Selective Removal of Water, Anal. Chem. 82 (2010) 1288–1291.

[66] F. Eslami, J.A.W. Elliott, Design of Microdrop Concentrating Processes, J. Phys. Chem. B. 117 (2013) 2205–2214.

[67] F. Eslami, J. a W. Elliott, Design of microdrop concentrating processes, J. Phys. Chem. B. 117 (2013) 2205–2214.

[68] G.D.M. Jeffries, J.S. Kuo, D.T. Chiu, Dynamic Modulation of Chemical Concentration in an Aqueous Droplet, Angew. Chemie Int. Ed. 46 (2007) 1326–1328.

[69] A.Q. Shen, D. Wang, P.T. Spicer, Kinetics of colloidal templating using emulsion drop consolidation, Langmuir. 23 (2007) 12821–12826.

[70] J. Ji, L. Nie, Y. Li, P. Yang, B. Liu, Simultaneous Online Enrichment and Identification of Trace Species Based on Microfluidic Droplets, Anal. Chem. 85 (2013) 9617–9622.

[71] S. Lin, S. Nejati, C. Boo, Y. Hu, C.O. Osuji, M. Elimelech, Omniphobic

Membrane for Robust Membrane Distillation, Environ. Sci. Technol. Lett. 1 (2014) 443–447.

[72] M. Rezaei, D.M. Warsinger, J.H. Lienhard V, W.M. Samhaber, Wetting prevention in membrane distillation through superhydrophobicity and recharging an air layer on the membrane surface, J. Memb. Sci. 530 (2017) 42–52.

[73] A.K. Singh, D.H. Ko, N.K. Vishwakarma, S. Jang, K.I. Min, D.P. Kim, Micro-total envelope system with silicon nanowire separator for safe carcinogenic chemistry, Nat. Commun. 7 (2016) 10741.

# II. MEMBRANE ASSISTED AND TEMPERATURE CONTROLLED ON-LINE EVAPORATIVE CONCENTRATION

This chapter has been published as a research article in *Journal of Chromatography A* except for the appendix. All efforts were made to keep the original features of this article except for minor changes. Layout, numbering, font size and style were modified in order to maintain a consistent formatting style of this thesis.

## GRAPHICAL ABSTRACT

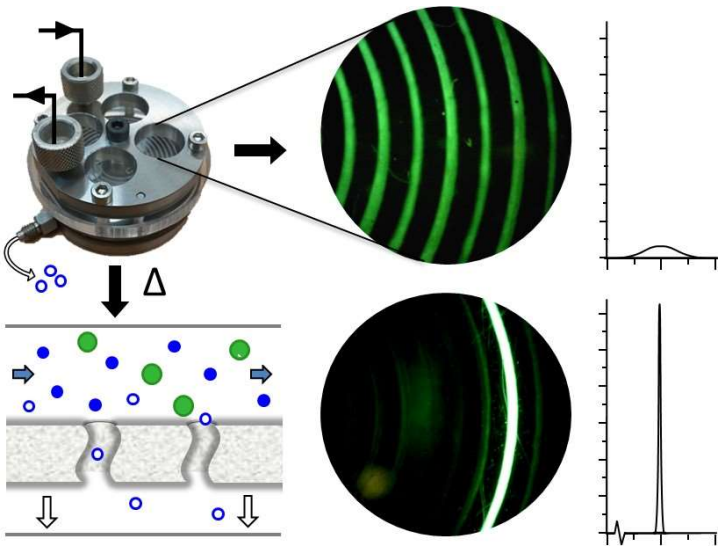


## ABSTRACT

A membrane evaporation concentrator for continuous flow conditions is introduced. The membrane evaporation concentrator provides nearly 30-fold concentration in less than 60 min whilst maintaining solute integrity under different sub-ambient pressure conditions and mild temperatures. To better understand the performance of the concentrator, a theoretical model was developed using caffeine as a model analyte and used to predict the concentration performance of three target analytes at different conditions.

An exponential relationship exists between temperature and concentration factor. By using the model it was determined that a 10-fold concentration (±0.5) can be performed at 56.72 ± 0.07°C and at a flow rate of 10 µL $min^{-1}$. Altogether, the model provides a better understanding of the process and ease of application in a wide variety of analytical methods. This work demonstrates that it is possible to obtain high concentrations with a continuously flowing fluid when temperature is precisely controlled and in times that are reasonable compared to existing evaporation concentration procedures

## 1. INTRODUCTION

Integrated and automated microfluidic systems have generated much interest due to their useful capabilities. Small quantities of samples and reagents, potential high resolution separations, low cost, short analysis time or small device footprint are seen as some of the advantages of a miniaturized platform [1]. To date, research efforts have mainly focused on proof-of-concept demonstration of different chemical processes that could be integrated in a micro total analysis system (µTAS). More recent focus has been on applying microfluidic systems to the resolution of problems [2]. Notwithstanding the myriad of benefits, poor analysis performance can be faced when handling low-abundance analytes in the characteristic small sample volumes posing a significant practical limitation [3]. Incorporation of concentration stages in micro-scale analytics is therefore necessary in the development of new analysis procedures [4] so that sample size can be kept small but analytes are well enough represented.

Preconcentration techniques can be classified into several categories based on their principle of action. The first involves adsorption onto a substrate, such as solid-phase extraction (SPE) and solid-phase micro-extraction (SPME), which exploit hydrophobic, electrostatic, or affinity interactions between analytes and a surface. To this end the microchannel surface may be modified

or coated to provide the extraction phase. Alternatively, the channel may be packed with particles [5–7] or filled with a monolith [8–11], fibrous polymeric materials [12,13] or other more specific molecularly imprinted phases [14]. Adsorbed analytes are released using a change in composition of the solution. The second approach is extraction into an immiscible liquid phase, liquid-liquid extraction (LLE), which is another popular technique where the analytes in aqueous solution are enriched within an organic solvent by phase transfer. LLE has been implemented on chip using centrifugal forces [15] and droplet-based microfluidics [16,17] but generally requires a back-extraction or solvent-evaporation and reconstitution in an aqueous solvent for subsequent analysis. The third frequently used approach exploits electrokinetic and sometimes hydrodynamic phenomena [4], including field-amplified stacking (FAS), isotachophoresis (ITP), and sweeping [18]. These all require the use of an electric field and are generally coupled exclusively with electrophoretic analysis. Fourth, is the use of nanoporous membranes that concentrate analytes by a size-exclusion mechanism. This approach is generally focused on macromolecules such as proteins [19,20]. However, if the pore size is small enough and the membrane is hydrophobic it can be used as an interface for evaporative concentration. In this technique also called membrane assisted evaporation, a hydrophobic membrane is used as a barrier for the liquid but water vapor in the liquid channel passes freely through the membrane, reducing the amount of solvent relative to solutes [21]. The driving force is from a partial vapor pressure difference between the different sides of the membrane, which is enhanced at elevated temperatures [22].

Extraction methods can provide extremely high concentration factors of over a thousand-fold while also providing clean-up as the targets are removed from the sample matrix. However, the use of organic solvent for elution is generally unavoidable. This can pose limitations when trying to integrate the preconcentration step into a complete analysis system, since organic solvent may hinder separation and/or detection capabilities. Furthermore, special

care and optimization is required for each particular group of analytes. When evaporation is used for concentration, volatile analytes are also at risk of being lost. However, when a membrane is used as an evaporation interface, loss of volatile compounds can be minimized by controlling the membrane's pore size. This makes membrane assisted evaporation a very attractive approach as there is no restriction in the nature of the targeted analytes that can be concentrated and it can be applied generally to any kind of analyte. This includes particles, biological material such as cells or viruses, soluble ions and non-ionizable compounds. It is worth mentioning that membrane assisted evaporation is not a clean-up method. Therefore, without complementary purification, analytes as well as matrix components are concentrated in complex samples.

Membrane assisted evaporation has been extensively used for water treatment as an alternative to reverse osmosis [22,23], and other industrial processes [24,25]. It is potentially advantageous in a microfluidic device because evaporation of small quantities of fluids can be extremely rapid. The first microfluidic evaporative concentrator was described in 2003 by Timmer et al. [26] and achieved around 3-fold concentration factor under continuous flow at 5 µL $min^{-1}$ without heat. In 2008 Sharma et al. [27] reported a design to concentrate bovine serum albumin from a large volume of water using a continuous-flow evaporator with millimeter-sized channels. Later, a similar concept was applied to bacteria [28] and virus [29] particles in a microfluidic serpentine channel in static conditions. The large channel slowly filled with air as the sample volume was reduced from hundreds of microliters down to microliters in 15 min yielding over 12-fold concentration. A similar device was recently introduced as a method to produce concentrated labeled biologically active molecule suspensions as tracers for positron emission tomography [30,31].

While the suggested devices operated in static conditions achieved good concentration rates, they faced large sample volume requirements, unknown

concentration factors, sample loss or residue left in the channels and membranes [28,31]. As such, these procedures do not always lend themselves to viable routine application. The device reported by Timmer et al. showed online concentration in a small sized channel [26] holding 135 µL, and used a counter-current nitrogen gas flow across the membrane. The influence of $N_2$ gas velocity and analyte flow rate was considered while temperature was not studied. A 3-fold concentration effect was demonstrated at room temperature. More recently, Zhang et al. [32] studied two microfluidic evaporative in-line sample concentrators using a polypropylene porous hollow fiber and a silicon nitride membrane. The evaporators were evaluated at different input flow rates with varied $N_2$ flow rates in the gas chamber. The hollow fiber evaporator showed a maximum 16-fold concentration factor at flow rate lower than 10 µL.min$^{-1}$. The authors indicated that high precision was required for this to be repeatable. A theoretical model was also developed but did not match experimental data, highlighting the high degree of complexity involved in the membrane evaporation phenomenon.

In this study we present a custom designed membrane evaporative concentrator where vacuum is applied over the membrane and mild temperatures are used to enhance evaporation to concentrate a continuously flowing sample. The device shows exponential concentration factors at increasing temperature and is capable of achieving >10 fold concentration factor at under 60°C within 40 min. Performance at different flow rates has been studied and a model developed in order to predict the behaviour. The established equation can be used to set experimental conditions to achieve a desired final concentration.

## 2. Materials and Methods

### *2.1 System overview*

The system used for the evaporative concentration experiments consisted of an HPLC pump (LC-20AD Shimadzu, Kyoto, Japan) connected to a Low Dispersion injection valve Model 8125 from Rheodyne (Rohnert Park, CA, USA) equipped with a 25 µL sample loop connected to the evaporative concentration device. This device was placed on a heating plate and temperature was controlled with a digital thermometer to within ±1°C. To perform concentration, a small vacuum pump (model 1420VP BLDC, Gardner Denver Thomas, Fürstenfeldbruck, Germany) was connected to the gas side of the concentration module. The liquid outlet was connected to a UV detector SPD-20A (Shimadzu) to monitor the process. Both the HPLC pump and the UV detector were connected to a LC-20AD Shimadzu controller and operated with LabSolutions software (Shimadzu).

The evaporative concentrator was manufactured using a $CO_2$ laser (VLS4.60 Laser Platform, Laser & Sign Technology, NSW, Australia) for polymethyl metacrylate (PMMA) cutting and engraving. A metal cutting laser purchased form Rofin-LASAG (Gwatt, Switzerland) was used for shaping and cutting metallic parts.

Sterlitech PTFE 0.2 µm pore size membrane disc filters were purchased from Sterlitech Corp (Kent, WA, USA). MilliQ water and HPLC grade methanol from Merck (Darmstadt, Germany) were used to prepare both samples and carrying solutions. Solutions of 4 and 2 mg $L^{-1}$ fluorescein (Aldrich) and caffeine (Sigma-Aldrich), respectively, were used as analytes.

### *2.2 CONCENTRATION DEVICE ASSEMBLY*

The evaporative concentration module was assembled using 5 screws and a metallic case that provides sealing within the channels. The upper metallic case (Fig. 1a) has four large holes for visualization of the layers underneath, and inlet and outlet screw fittings to connect to ancillary instrumentation. Just under the case (Fig. 1b) is a 2 mm thick PMMA disc with a laser engraved channel on the bottom surface. The engraved surface is, once assembled, in

contact with a hydrophobic membrane (Fig. 1, red line) providing an evaporation interface. On the other side of the interface, an airflow channel (Fig. 1d) cut on a metallic disc perfectly overlays the liquid flow channel path above, creating air-liquid contact through the membrane. The air-flow channel is 300 µm wide cut with the metal cutting laser, and placed on the bottom metallic case (Fig. 1e). This metallic case has a 0.5 mm deep cavity and an outlet hole where the vacuum pump is connected. Therefore, it acts both as support and as vacuum cavity, linking the airflow channel and the vacuum pump. A 2 mm rubber gasket is placed between the air channel layer and the metal base with vacuum cavity to provide sealing.

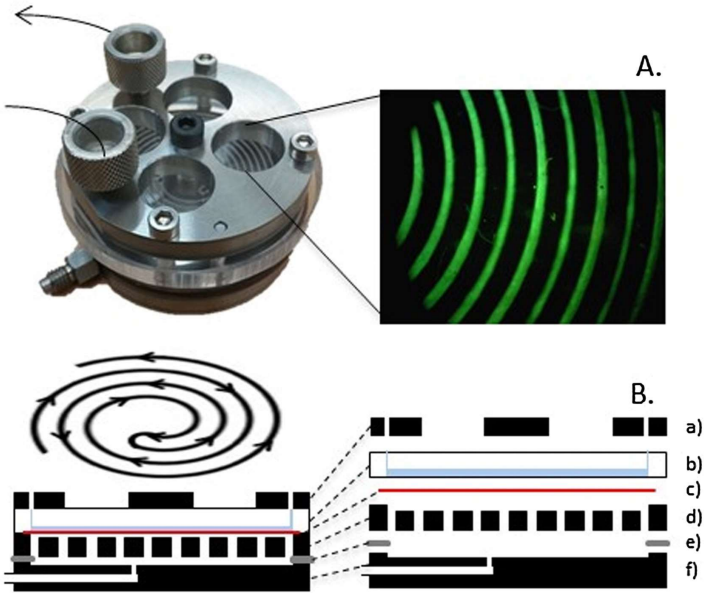


*Figure 1. A. Device picture and viewing platform capture. B. Scheme of the concentration device module assembly and flowpath. a) Upper case and viewing platform. b) Liquid flow channel. c) Membrane. d) Airflow channel. e) Gasket. f) Bottom case including vacuum cavity and outlet*

### *2.3 EXPERIMENTAL PROCEDURE*

The concentration performance of the device was assessed both qualitatively and quantitatively. Initially, 4 mg.L$^{-1}$ fluorescein solution was injected and the fluorescence measured at various points in the fluidic channels with a USB fluorescence microscope (Dino-Lite AM4115T digital microscope, Torrance, CA, USA). A control experiment at room temperature and without vacuum was compared with experiments performed at different temperatures with application of vacuum. Each data point for a particular dataset (flow rate) was obtained not consecutively and at different dates in random order. This allowed a representative amount of experimental variability in the data. The membrane was replaced periodically every few days. Concentration factors (c.f.) were calculated from Flow Injection Analysis (FIA) set-up using plain solvent or solvent mixture as carrier, and recording UV absorbance at 276 nm with a HPLC UV detector. Peak heights of caffeine with temperature and vacuum ($h_1$) were normalized to results from the control experiment ($h_o$) according to Eq. 1.

(1) $$c.f. = \frac{\chi}{\chi_o} = \frac{h_i}{h_o}$$

## 3. RESULTS AND DISCUSSION

The principle of the developed device is explained in Fig. 2, which shows the analyte concentrating along a flowing channel as well as the water vapor transport across the membrane pores.

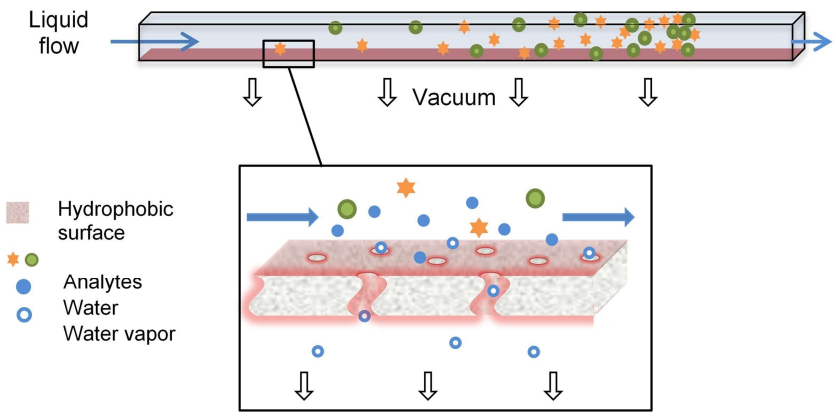


*Figure 2. Analyte concentration by evaporation along a flowing channel and principle of membrane evaporative concentration.*

### *3.1 Channel characterization and optimization*

The liquid flow channel was engraved on an acrylic disc 3 mm thick using a $CO_2$ laser, and several parameters were assessed to obtain an optimal channel shape and size. During the optimization process, the channels were assessed and characterized in a number of ways. First, a solution of fluorescein was injected into the evaporative concentration module. The fluid path was imaged through the viewing platform to evaluate sealing and channel roughness. A profile of the channel was also obtained with a Wyko NT9100 optical interferometry profiler (Veeco Instruments Inc., Plainview, NY, USA) and average channel width and depth were measured. Peak shape of a caffeine test probe at several flow rates was also assessed providing information of fluidic flow through the channels and microscope captions of the channel cross section were taken. This data for two designs is shown for comparison in Fig. 3. From the data in Fig. 3 better peak shape for caffeine was obtained using the shallower microchannel, fabricated by using an unfocused $CO_2$ laser [33], setting the laser focus point at 5 mm above from the polymeric surface.

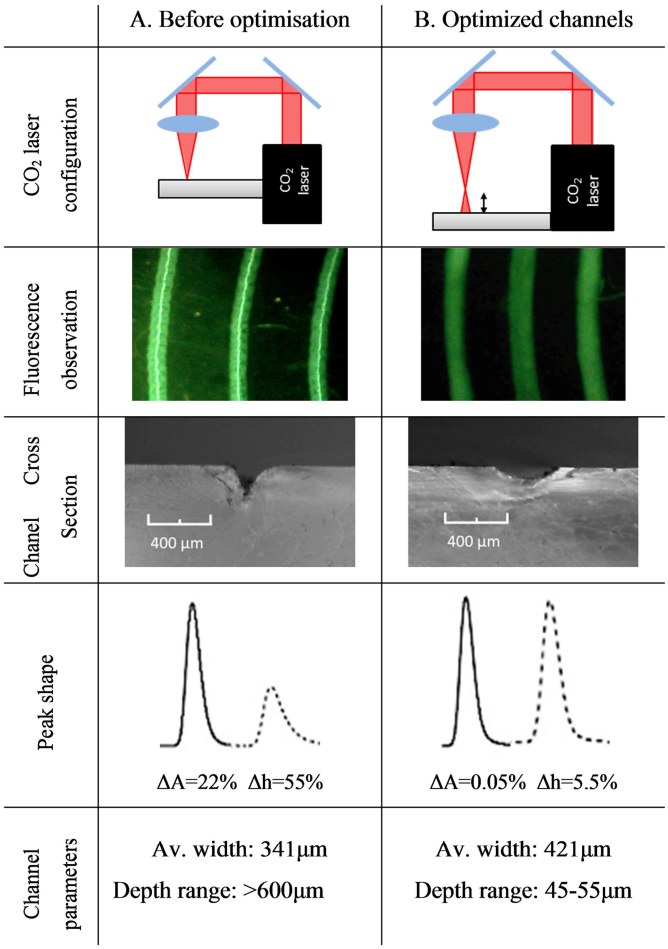


*Figure 3. Comparison between channels before (A) and after (B) optimization using a set of techniques. Scheme of focused and unfocused laser configurations. Fluorescein flow observation. Channel cross sections. Peak shape comparison without (solid line) and with (dashed line) on-line concentration device. Channel parameters measured with an optical profiler.*

### *3.2 PERFORMANCE ASSESSMENT*

To qualitatively assess the concentration process, videos of fluorescein passing through the channel under different conditions were compared, with images from the control (no temperature and vacuum) and evaporation (vacuum and 45 °C) videos shown in Fig. 4 and available as Electronic Supplementary Information at the publishers' database. The consequences of

evaporation of the solvent can be clearly seen by the increased intensity of the fluorescein plug, which also became smaller and brighter with time. Also, the residence time was longer, over 20 min compared to 5 min, evidence that there was a reduction in output flow due to evaporation of the solvent given that the input flow rate was 10 μL $min^{-1}$ for both. Quantitative measurement of the enrichment factor was obtained by replacing fluorescein with caffeine and monitoring the peak area with UV detection. Increasing the power to the vacuum pump, and therefore the extent of vacuum did not improve the concentration performance. Conversely, feed flow rate and temperature were found to have a strong influence on the concentration performance of the device and will be discussed separately.

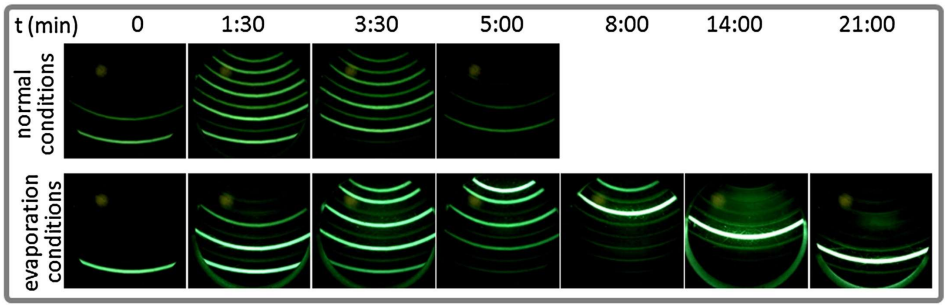


*Figure 4. Captures of recorded fluorescein sample plug (25 μL, 4 mg L-1) pathway in normal (room temperature, no vacuum) and evaporation conditions (45 °C, vacuum). Both experiments were performed at an input flow rate of 10 μL min-1. (Video available at doi.org/10.1016/j.chroma.2016.12.003)*

### *3.2.1 Temperature*

A 2 mg $L^{-1}$ sample of caffeine in water was injected at increasing temperatures at a flow rate of 10 μL $min^{-1}$. Concentration factors were calculated and plotted against temperature as shown in Fig. 5. It can be seen that there is an

exponential increase, with higher enrichment factors achieved at higher temperatures.

This data indicates that high (> 10) concentration factors can be achieved at a very narrow fringe of higher temperature, but precise temperature control is crucial to obtain predictable and controlled concentration. In the set-up used here, temperature measurements were performed with a precision of ±1°C. This caused significant fluctuation in evaporation rate along the fluid pathway, and therefore, similar but different concentration factors were recorded at the same measured temperature. This phenomenon is believed to be the main source of error in the current device.

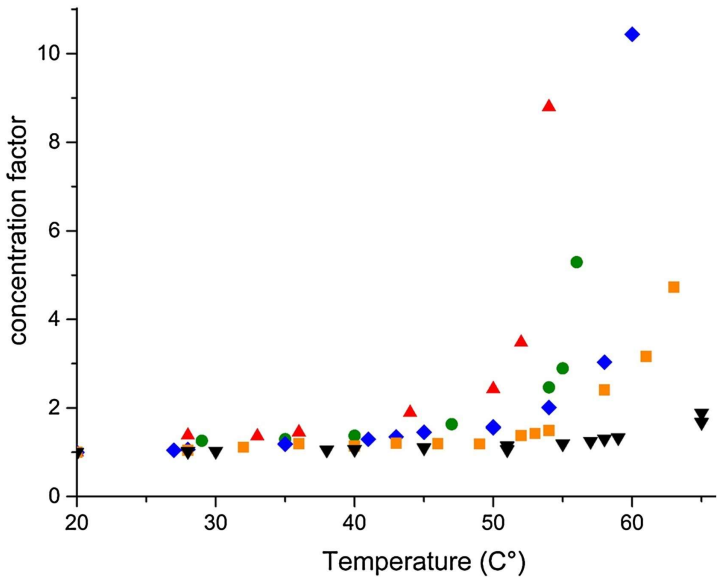


*Figure. 5. Concentration factor vs. temperature plot at different flow rates: (▲) 8, (●) 10, (◆) 15, (■) 20 and (▼) 50µL min-1. Exponential increase on concentration is achieved at increasing temperatures.*

### *3.2.2 Feed flow rate*

The performance of the evaporative concentrator was examined by varying the temperature at different flow rates. As anticipated, the results in Fig. 5 show that the exponential increase occurs at lower temperatures with decreasing flow rate, with less heating needed at the lower flow rates to achieve the highest concentration factors. This is due to a higher residence time of the sample in the device as well as better interaction with the membrane at lower flow rates. These results are in good agreement with previous studies [26,32] and reinforces the need for high flow rate precision.

## *3.3 MODELLING*

As stated above, temperature drives the concentration performance at a given pressure difference (vacuum). However, the temperature must be precisely set and controlled in order to repeatedly achieve the desired concentration factor. It is therefore desirable to know in advance what settings are required. Here, we provide a model to predict the concentration factor at any given temperature and flow rate. While the model is specific to this particular design, it is anticipated that the same procedure can be followed for any other designs.

### *3.3.1 Model development*

As reported earlier, the concentration factor (*c.f.*) is defined as final analyte concentration or molar fraction divided by initial. In terms of solvent, it is defined as total solvent mass $M'$ (remaining and removed by evaporation) divided by final solvent mass $M$. Even though there is a temperature gradient, a constant density of 1 g $L^{-1}$ is assumed as the variation in the density of water over the studied temperature range 280-340 °K (7-67 °C) is around 2% only, and is negligible between 1 and 10 bar [34]. Therefore, $c.f.$ can be expressed as total volume $V'$ divided by actual channel volume $V$ (Eq. 2). Total volume

is the addition of channel volume and the volume of water removed by evaporation.

(2) $$c.f. = \frac{\chi}{\chi_o} = \frac{M'}{M} \simeq \frac{V'}{V}$$

The total volume depends on the residence time $t$ (min), as well as evaporation rate $\dot{m}$ (mm$^3$ min$^{-1}$) expressed here as volume of liquid evaporated each minute (Eq. 3).

(3) $$V' = V + V_{evap} = V + \dot{m}\, t$$

Using Eq. 3, Eq. 2 can be transformed in to Eq. 4, which has two unknown terms, $t$ and $\dot{m}$.

(4) $$c.f. = \frac{V + \dot{m}t}{V} = 1 + \frac{\dot{m}t}{V}$$

In an online setup, the residence time $t$ is dependent on the set flow rate ($U$ in µL min$^{-1}$) and evaporation rate, as evaporation causes flow reduction. Without evaporation, the residence time is represented by $V/U$. However, in this system, as there is flow reduction along the channel $\frac{\partial U}{\partial x} < 0$, flow is considered as an average of $U_{x_i}$ so $\overline{U}_{x_i} = U - U_{evap}$. Therefore, Eq. 5 can be used to calculate residence time

(5) $$t = \frac{V}{U - U_{evap}} = \frac{V}{U - \dot{m}}$$

When using Eq. 5 to replace the $t$ term in Eq. 4, an expression is obtained to define concentration factor using only known experimental parameters and unknown evaporation rate $\dot{m}$. Finally, rearranging that expression yields equation 6 to predict concentration factor in any flow and temperature conditions:

(6) $$c.f. = \frac{U}{U - \dot{m}}$$

In order to use Eq. 6 for prediction, a value must be assigned to $\dot{m}$. Evaporation rate is a complex parameter. It varies according to changes in experimental conditions, however, it is defined by a number of phase coefficients and physical properties, together with the system specifications including membrane properties [35,36]. The use of such complex theoretical approaches in previous modeling attempts was suggested as the discrepancy between theoretical and experimental data [32]. The interface design plays a great role too; as it defines the channel volume, membrane surface area or flow regime amongst others. In this study, to avoid error associated with calculation of the parameter, it was estimated using a subset of the experimental data obtained earlier. The data shown in Fig. 5 was divided in two sets, a training set to allow empirical determination of the variable $\dot{m}$ at known experimental temperatures, and a test set for evaluation of the equation. The data was sorted in such a manner that both sets had data in similar experimental conditions. Eq. 5 was used to calculate evaporation rate for the training set and plotted in a $\dot{m}$ vs. $1000/T$ graphic and the data was then fitted to a polynomial equation (Fig. 6A). The equation was used to retrieve predicted evaporation rates for a range of temperatures.

Concentration factors were then calculated in the temperature range using predicted evaporation rates. Predicted concentration factors using the experimental training data set at different flow rates were plotted together with the experimental test data set and found to be in agreement, therefore supporting the goodness of the prediction (supplementary information Fig. S1). Fitting accuracy at the highest studied flow rate of 50 µL $min^{-1}$ cannot be assessed at high c.f. due to lack of data at temperatures over 65 °C that would damage the PMMA channel plate. However, it is still plotted as a prediction, so there is greater uncertainty around this prediction than with the others. However, given the good agreement with the other conditions, it is sufficient to serve as a guide to the temperature required to achieve these c.f. at this flow rate.

Subsequently, the models prediction ability regarding analytes not involved in the model development was assessed. Three diverse analytes (chlorthiazide, 4-hydroxybenzaldehide and benzylamine) were used to perform further concentration experiments at 10 and 20 µL min-1. Data was plotted (data points Fig. 6B) in comparison with expected behaviour from the model (solid lines Fig. 6B) predicted using caffeine concentration data. Again, good agreement is shown between experimental and predicted data, indicating that the model is valid for a variety of thermally stable analytes, therefore not intrinsic to each molecule.

### *3.3.2 Application of the model*

By using the model, experimental conditions can be set according to the analysis needs. For example, by fixing the desired concentration factor at a particular flow rate, it is possible to calculate the temperature required to achieve it by iteration using Eq. 7 – a combination of Eq. 6 and the polynomial fitting. To do this, an initial input $T$ value was introduced and least-squares

regression used to minimize the difference between the calculated $c.f.$ and the desired concentration factor.

(7) $$c.f. = \frac{U}{U - 38.49\left(\frac{1000}{T}\right)^4 + 502.3\left(\frac{1000}{T}\right)^3 - 2457.3\left(\frac{1000}{T}\right)^2 + 5341.2\left(\frac{1000}{T}\right) + 4352.53}$$

Temperatures required to achieve different concentration factors at two different flow rates are shown in Table 1, together with the acceptable deviations on the set temperature ($\sigma_T$) required to obtain the desired c.f. with 2 and 5% RSD (relative standard deviation), respectively. Positive $\sigma^+{}_T$ and negative $\sigma^-{}_T$ deviations are slightly different due to the exponential nature of the curve requiring smaller changes in temperature to cause the same effect in concentration factor at increasing temperatures.

Information in Table 1 shows that different flow rates provide different temperature ranges over which the desired concentration can be achieved, with higher c.f. needing higher temperatures as discussed earlier. More significantly, the acceptable deviation in the temperature required to achieve a precise and repeatable c.f. decreases, in other words, the higher the c.f. required, the tighter the temperature needs to be controlled. The required precision of the temperature settings to achieve 10-fold concentration rates is under 0.1 °C at the studied flow rates, demonstrating that the ability to set temperature precisely is essential to obtain known concentration factors

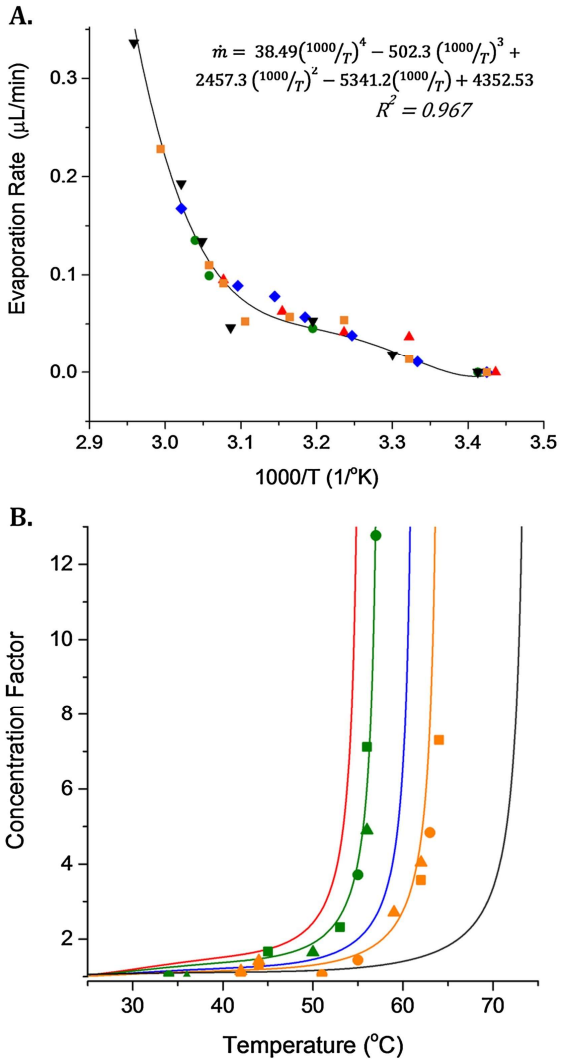


*Figure 6. A. Evaporation rate (ṁ) dependence on Temperature (1000/T). Different series correspond to data acquired at different flow rates: (▲) 8, (●) 10, (◆) 15, (■) 20 and (▼) 50µL min-1. Evaporation rate data points were calculated from experimental and fitted to a polynomial curve (solid line). The fitting equation and coefficient of determination R2 are shown. B. Predicted behavior (solid lines) and experimental data (data points). Prediction regarding caffeine concentration factor at increasing temperatures and at the following flow rates 8 (red), 10 (green), 15 (blue), 20 (orange) and 50µL min-1 (black). Experimental data obtained at 10 (green points) and 20 (orange points) µL min-1 for three molecules other than caffeine: (▲/▲)4-hydroxybenzaldehyde, (●/●) chlorthiazide, (■/■) benzylamine.*

Table 1. Calculated temperatures and required precision for the desired concentration factors at set flows.

| Flow ($\mu L\ min^{-1}$) | c.f. | T (°C) | 2% RSD(c.f.) | | 5% RSD(c.f.) | |
|---|---|---|---|---|---|---|
| | | | $\sigma^{+}{}_{T}$ | $\sigma^{-}{}_{T}$ | $\sigma^{+}{}_{T}$ | $\sigma^{-}{}_{T}$ |
| 10 | 2 | 50.69 | 0.2 | 0.2 | 0.5 | 0.6 |
| | 5 | 55.59 | 0.05 | 0.05 | 0.1 | 0.1 |
| | 8 | 56.45 | 0.03 | 0.03 | 0.06 | 0.07 |
| | 10 | 56.72 | 0.02 | 0.02 | 0.05 | 0.07 |
| 50 | 2 | 66.61 | 0.2 | 0.2 | 0.5 | 0.6 |
| | 5 | 71.72 | 0.06 | 0.06 | 0.1 | 0.2 |
| | 8 | 72.76 | 0.03 | 0.03 | 0.08 | 0.09 |
| | 10 | 73.09 | 0.03 | 0.03 | 0.06 | 0.07 |

RSD: relative standard deviation; c.f.: concentration factor; T: temperature; $\sigma^{+}{}_{T}$ , $\sigma^{-}{}_{T}$ : positive and negative temperature standard deviations respectively

## 4. CONCLUSIONS

A device for on-line analyte concentration using membrane assisted evaporation for microfluidic analysis was developed. The device performance was studied under different experimental conditions changing parameters such as temperature and airflow configuration. In addition, the process was described by a model allowing for concentration factor prediction. Using optimal conditions, a 27-fold concentration factor was achieved in 60 minutes at less than 60°C. Precise temperature control (at least ± 0.05) is required for repeatable performance.

By using this approach for preconcentration, matrix components are concentrated along with target analytes. Therefore, it would be favorable for potential applications where broad scale concentration is desired to provide

complete coverage of the sample. Complementary analysis steps may be insensitive to matrix components or include sample clean-up steps for complex samples. Since this is an on-line technique, it would provide significant benefits with regards to throughput, recovery and analysis integrity.

## ACKNOWLEDGEMENTS

This research was conducted by the ARC Training Centre for Portable Analytical Separation Technologies (IC140100022). MCB the recipient of an ARC Future Fellowship (FT130100101). E. Fornells is a recipient of an ARC post-graduate scholarship in ASTech, University of Tasmania. ACROSS and ASTech at University of Tasmania as well as Trajan Scientific and Medical provided access to facilities.

# APPENDIX: INVESTIGATING SOLVENT MIXTURES

It is anticipated that different solvent compositions will result in different enhancement factors. In order to examine this effect, 25 µL of 2 ppm caffeine solutions with different methanol composition were injected at increasing temperatures at a flow rate of 10 µL/min. The feed solution contained the same organic composition as the sample in each case (0, 20, 40, 60 and 80%). Methanol was chosen as it is one of the most common organic solvents used in analytical chemistry, and a maximum amount of 80% was set to ensure wetting of the PTFE hydrophobic membrane was avoided. Results in Figure 7 showed a non-exponential concentration enhancement with temperature. However, two sequential stages can be observed.

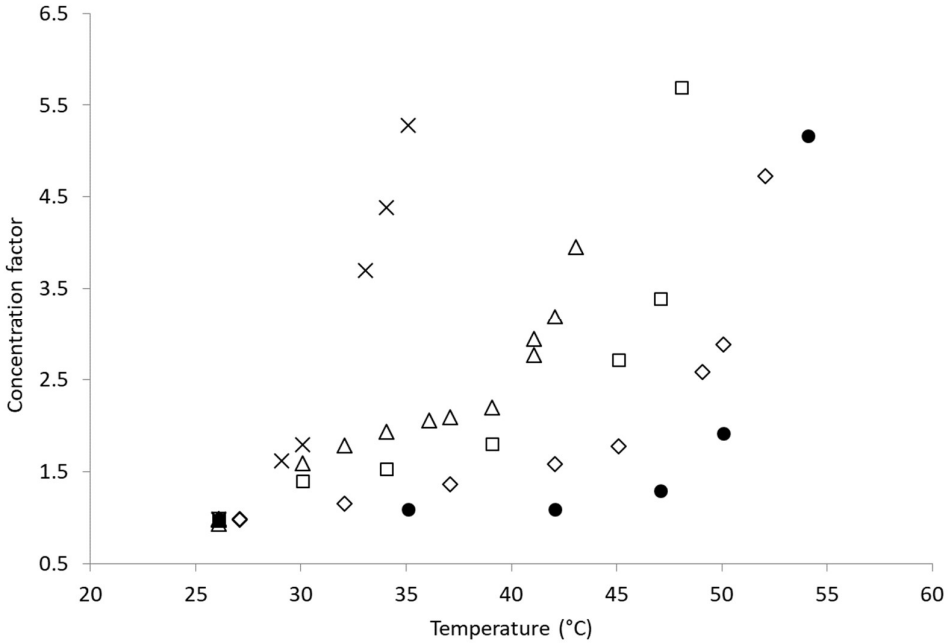


*Figure 7. Concentration factor vs. temperature plot of 2ppm caffeine samples in water (•), and different methanol compositions: 20% ◇, 40% □, 60% △, 80% ×. The curve shows two stages due to the different boiling points of methanol and water.*

A first small increase in concentration was observed followed by a higher increase. At higher organic solvent contents the first stage increase was bigger, while the second stage increase happened at lower temperatures. This is believed to be due to a majority of methanol evaporation at lower temperatures and simultaneous methanol and water evaporation at higher temperature.

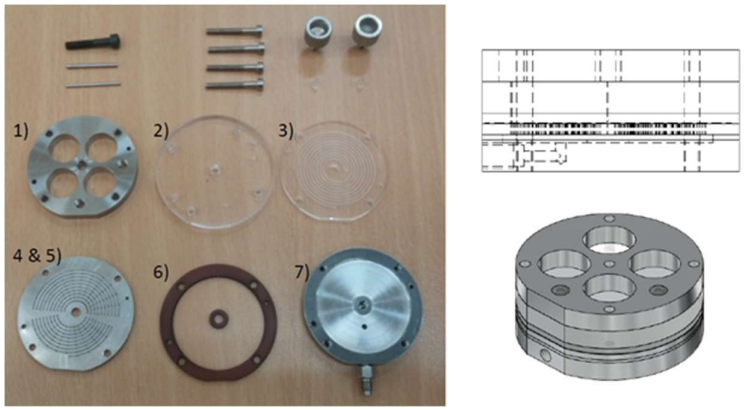


*Figure 8. Additional information of device parts and assembly. Left: Device parts. Top) aligning pins and screws. a) upper case, 2) PMMA viewing platform, 3) PMMA channel disc 4) laser cut gas channel disc 5) connection disc between gas chamber and channel 6) gasket 7) gas chamber and outlet. Top right: side schematic view of the assembled device. Bottom left: ensembled prototype design.*

## REFERENCES


[1] A. Manz, D.J. Harrison, E.M.J. Verpoorte, J.C. Fettinger, A. Paulus, H. Lüdi, H.M. Widmer, Planar chips technology for miniaturization and integration of separation techniques into monitoring systems. Capillary electrophoresis on a chip, J. Chromatogr. A. 593 (1992) 253–258.

[2] G.M. Whitesides, The origins and the future of microfluidics., Nature. 442 (2006) 368–73.

[3] K. Sueyoshi, F. Kitagawa, K. Otsuka, Recent progress of online sample preconcentration techniques in microchip electrophoresis, J. Sep. Sci. 31 (2008) 2650–2666.

[4] C.C. Lin, J.L. Hsu, G.B. Lee, Sample preconcentration in microfluidic devices, Microfluid. Nanofluidics. 10 (2011) 481–511.

[5] J.P. Kutter, S.C. Jacobson, J.M. Ramsey, Solid phase extraction on microfluidic devices, J. Microcolumn Sep. 12 (2000) 93–97.

[6] M.C. Breadmore, K.A. Wolfe, I.G. Arcibal, W.K. Leung, D. Dickson, B.C. Giordano, M.E. Power, J.P. Ferrance, S.H. Feldman, P.M. Norris, J.P. Landers, Microchip-based purification of DNA from biological samples, Anal. Chem. 75 (2003) 1880–1886.

[7] A.B. Jemere, R.D. Oleschuk, F. Ouchen, F. Fajuyigbe, D.J. Harrison, An integrated solid-phase extraction system for sub-picomolar detection, Electrophoresis. 23 (2002) 3537–3544.

[8] H. Zhai, J. Li, Z. Chen, Z. Su, Z. Liu, X. Yu, A glass/PDMS electrophoresis microchip embedded with molecular imprinting SPE monolith for contactless conductivity detection, Microchem. J. 114 (2014) 223–228.

[9] J.D. Ramsey, G.E. Collins, Integrated microfluidic device for solid-phase extraction coupled to micellar electrokinetic chromatography separation., Anal. Chem. 77 (2005) 6664–70.

[10] K.N. Battle, J.M. Jackson, M. a Witek, M.L. Hupert, S. a Hunsucker, P.M. Armistead, S. a Soper, Solid-phase extraction and purification of membrane proteins using a UV-modified PMMA microfluidic bioaffinity μSPE device., Analyst. 139 (2014) 1355–63.

[11] H. Yang, J.M. Mudrik, M.J. Jebrail, A.R. Wheeler, A digital microfluidic method for in situ formation of porous polymer monoliths with application to solid-phase extraction, Anal. Chem. 83 (2011) 3824–3830.

[12] Y. Saito, K. Jinno, On-line coupling of miniaturized solid-phase extraction and microcolumn liquid-phase separations, Anal. Bioanal. Chem. 373 (2002) 325–331.

[13] K. Jinno, M. Ogawa, I. Ueta, Y. Saito, Miniaturized sample preparation using a fiber-packed capillary as the medium, TrAC - Trends Anal. Chem. 26 (2007) 27–35.

[14] F. Qiao, H. Sun, H. Yan, K.H. Row, Molecularly Imprinted Polymers for Solid Phase Extraction, Chromatographia. 64 (2006) 625–634.

[15] M.J. Madou, L.J. Lee, S. Daunert, S. Lai, C.-H. Shih, Design and Fabrication of CD-like Micro¯uidic Platforms for Diagnostics: Micro¯uidic Functions, Biomed. Microdevices. 33 (2001) 245–254.

[16] J.M. Kokosa, Recent trends in using single-drop microextraction and related techniques in green analytical methods, TrAC Trends Anal. Chem. 71 (2015) 194–204.

[17] H. Chen, Q. Fang, X.-F. Yin, Z.-L. Fang, Microfluidic chip-based liquid-liquid extraction and preconcentration using a subnanoliter-droplet trapping technique., Lab Chip. 5 (2005) 719–725.

[18] B.C. Giordano, D.S. Burgi, S.J. Hart, A. Terray, On-line sample pre-concentration in microfluidic devices: A review, Anal. Chim. Acta. 718 (2012) 11–24.

[19] S. Song, A.K. Singh, B.J. Kirby, Electrophoretic concentration of proteins at laser-patterned nanoporous membranes in microchips, Anal. Chem. 76 (2004) 4589–4592.

[20] R.S. Foote, J. Khandurina, S.C. Jacobson, J.M. Ramsey, Preconcentration of Proteins on Microfluidic Devices Using Porous Silica Membranes, Anal. Chem. 77 (2005) 57–63.

[21] S. Song, A.K. Singh, On-chip sample preconcentration for integrated microfluidic analysis, Anal. Bioanal. Chem. 384 (2006) 41–43.

[22] A. Alkhudhiri, N. Darwish, N. Hilal, Membrane distillation: A comprehensive review, Desalination. 287 (2012) 2–18.

[23] S. Roy, M. Bhadra, S. Mitra, Enhanced desalination via functionalized carbon nanotube immobilized membrane in direct contact membrane distillation, Sep. Purif. Technol. 136 (2014) 58–65.

[24] M. Purwasasmita, D. Kurnia, F.C. Mandias, Khoiruddin, I.G. Wenten, Beer Dealcoholization Using Non-Porous Membrane Distillation, Food Bioprod. Process. 94 (2015) 180–186.

[25] S. Nii, Membrane evaporators, J. Memb. Sci. 201 (2002) 149–159.

[26] B.H. Timmer, K.M. van Delft, W. Olthuis, P. Bergveld, A. van den Berg, Micro-evaporation electrolyte concentrator, Sensors Actuators B. 91 (2003) 342–346.

[27] N.R. Sharma, A. Lukyanov, R.L. Bardell, L. Seifried, M. Shen, Development of an evaporation-based microfluidic sample concentrator, in: W. Wang, C. Vauchier (Eds.), Microfluid. BioMEMS, Med. Microsystems VI, 2008: p. 68860R.

[28] J.Y. Zhang, J. Do, W.R. Premasiri, L.D. Ziegler, C.M. Klapperich, Rapid point-of-care concentration of bacteria in a disposable microfluidic

device using meniscus dragging effect., Lab Chip. 10 (2010) 3265–3270.

[29] J. Zhang, M. Mahalanabis, L. Liu, J. Chang, N. Pollock, C. Klapperich, A Disposable Microfluidic Virus Concentration Device Based on Evaporation and Interfacial Tension, Diagnostics. 3 (2013) 155–169.

[30] M.E. Phelps, Positron emission tomography provides molecular imaging of biological processes., Proc. Natl. Acad. Sci. U. S. A. 97 (2000) 9226–9233.

[31] W.-Y. Tseng, R.M. van Dam, Compact microfluidic device for rapid concentration of PET tracers., Lab Chip. 14 (2014) 2293–302.

[32] H. Zhang, R.M. Tiggelaar, S. Schlautmann, J. Bart, H. Gardeniers, In-line sample concentration by evaporation through porous hollow fibers and micromachined membranes embedded in microfluidic devices, Electrophoresis. 37 (2016) 463–471.

[33] T.F. Hong, W.J. Ju, M.C. Wu, C.H. Tai, C.H. Tsai, L.M. Fu, Rapid prototyping of PMMA microfluidic chips utilizing a CO2 laser, Microfluid. Nanofluidics. 9 (2010) 1125–1133.

[34] W.M. Haynes, ed., CRC Handbook of Chemistry and Physics, 94th ed., *CRC Press*, 2016.

[35] S. Kachel, Y. Zhou, P. Scharfer, C. Vrančić, W. Petrich, W. Schabel, Evaporation from open microchannel grooves., Lab Chip. 14 (2014) 771–8.

[36] G.M. Walker, D.J. Beebe, An evaporation-based microfluidic sample concentration method., Lab Chip. 2 (2002) 57–61.

# III. Evaporative membrane modulation for comprehensive two-dimensional liquid chromatography

This chapter has been published as a research article in *Analytica Chimica Acta* except for the appendix. All efforts were made to keep the original features of this article except for minor changes. Layout, numbering, font size and style were modified in order to maintain a consistent formatting style of this thesis.

## Graphical abstract

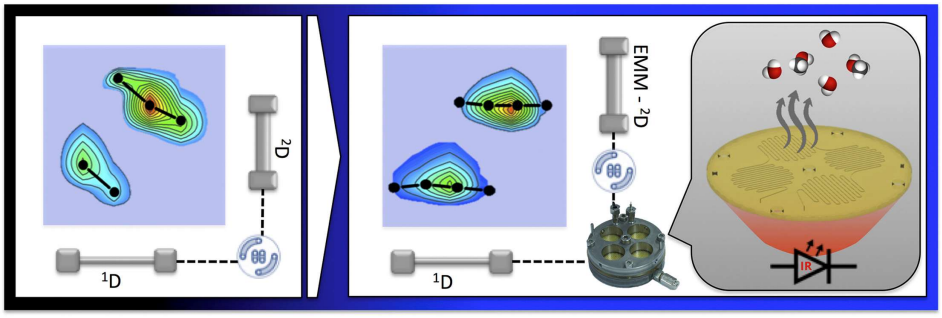


## Abstract

An evaporative membrane modulator was developed, built and evaluated to avoid loss of performance in the second dimension when coupling two-dimensional liquid chromatography systems. The automated interface reduces the volume after $^{1}$D elution on-line by a pre-determined factor, regardless of the separation gradient. This volume reduction ensures that the injection volume in the $^{2}$D is appropriate for the second column, avoiding the detrimental effects of overloading. In addition, the fraction solvent composition is constant over the length of the separation increasing reproducibility of $^{2}$D separations. The evaporative membrane modulator was demonstrated with a 10-fold reduction, reducing the injection volume from 50 to 5 µL. A consequence of the EMM device is a reduction in the capacity of

the first dimension, which is decreased by a factor of 2.4, but the peak width at half maximum was reduced by up to 22% in the second dimension. When band broadening is considered, the corrected peak capacity with the modulator was only 10% lower than that without the modulator, but with a gain in peak height of 2-3, and a decrease in retention time between subsequent peak-slices reduced from 4s to be negligible. This improves peak shape and shows potential to facilitate peak identification and quantitation in more complex applications.

## 1. INTRODUCTION

Successful separation of complex biological and environmental samples often requires very high peak capacity, and cannot be achieved in a reasonable time using one-dimensional separation approaches. Peak capacity ($n_C$) is related to resolution, and approximates the maximum number of peaks that can be separated under given chromatography conditions [1]. Multi-dimensional separation approaches often provide more effective separation of multicomponent samples that exceed the peak capacity of single dimension systems.

Comprehensive two-dimensional liquid chromatography (LC×LC) commonly involves the use of a switching valve with two identical sample loops. These sample loops act as alternating collection and injection loops to systematically transfer segments of the first-dimension ($^1$D) separation column effluent to the second-dimension ($^2$D) separation column. This methodology is referred to as passive modulation. Passive modulation has a number of limitations. First, each solute band eluted from $^1$D should be sampled at least three times by $^2$D to avoid remixing of separated solutes (undersampling), and reduced two-dimensional resolution [2]. Second, to minimise band broadening and band distortion, the smallest possible volume should be injected onto the second dimension column. Third, if the $^1$D mobile phase has higher elution

strength than the $^{2}$D mobile phase the above stated effects are worsened [3–5]. Fourth, the large number of fast and large pressure pulses when the interface valve switches can affect the second dimension column lifetime [6]. Fifth, dilution of the analytes occurs through collection and transfer of consecutive fractions, hindering detection of low abundance analytes or forcing the user to overload the $^{1}$D column [7]. As a result of all these issues, method development is often complex. Selection of chromatographic columns and separation conditions is crucial. Micro/nano flow rates and narrow columns in $^{1}$D, and larger-bore columns for $^{2}$D are often used in an attempt to fulfil all the mentioned requirements [8,9].

Active modulation can alleviate some of complications associated with passive modulation by modifying the volume, concentration, and/or solvent of $^{1}$D segments before they are introduced into the $^{2}$D column. Ideal active modulation is achieved when the volume of collected segments is sufficiently reduced without analyte loss such that the $^{2}$D band broadening is not significant [10,11]. The most common active modulation approach in LC×LC is stationary-phase-assisted modulation where analytes are focused by being trapped in a packed loop interface and subsequently released [10]. However, the efficiency may slowly decrease during analysis due to lack of trap column re-equilibration in-between each $^{1}$D segment. Retention mismatch between trap and separation columns and solvent systems must be avoided and further optimisation might be required [12].

The use of counter gradients added to the $^{1}$D effluent can be used to maintain a constant solvent composition and lower the solvent strength [13] to produce more reproducible baselines and separations. However, further dilution then occurs in addition to the intrinsic dilution of multidimensional LC separations. Post-$^{1}$D flow splitting reduces the volume of the $^{1}$D segments as well as the amount of organic solvent that may disrupt the $^{2}$D separation [14] but the mass of low-abundance analytes is reduced further making them difficult to detect.

Thermal modulation is the main active modulation approach used to practice comprehensive two-dimensional gas chromatography, and it has also been employed in LC×LC. Here, analytes are retained on a highly retentive porous graphitic carbon packed column positioned between the $^{1}$D and $^{2}$D columns, then remobilised applying temperature ramps [15,16]. Temperature has also been used for peak focusing before detection in a number of forms [17,18], while a combination of solid-phase and thermal peak focusing was recently studied demonstrating great potential[19].

In-loop direct evaporation was introduced aiming to address solvent mismatch and loss of sensitivity for heart-cutting [20,21] and LC×LC [22]. The system featured heated collection loops connected to vacuum. The interface achieved solvent evaporation as fast as the collection time, keeping the solutes in a few microliters solution that was then transferred to the second dimension column. The recovery of analytes strongly depended on their boiling point, varying from 15 to over 100%. Although some peak broadening was visible due to the vacuum-loop interface, the results showed an enhancement in chromatographic performance for solvent strength mismatch systems. The approach for LC×LC demonstrated remarkable improvement on baseline in the second dimension and increased retention for weakly retained analytes, but it also showed recoveries under 60% even for non-volatile analytes.

A combination of stationary phase assisted and evaporation assisted modulation mechanisms was recently used to exchange solvents effectively coupling normal and reversed phase separations [23]. However, featuring two sets of loop enrichment units, the elution and regeneration times limited the separation speed.

In this work, we utilise evaporation through a porous hydrophobic membrane as an alternative to direct loop evaporation with substantially higher evaporation control. In membrane evaporation systems, the solvent is removed by evaporation through a gas permeable hydrophobic membrane

[24–30]. To implement an on-line evaporative concentrator as a modulator in LC×LC it is necessary to precisely control temperature to ensure constant evaporation rate and therefore maintain constant flow rate despite the changing amounts of organic solvent. This was addressed by monitoring the $^{1}$D outlet flow rate, using an interactive feedback control mechanism run by a microcontroller to adjust the intensity of a heating element such that the output flow matched the desired flow rate. The feedback control mechanism implemented was the extensively used PID, or proportional-integral-derivative control [31]. Controlling then the evaporation rate automatically, we developed and built an on-line evaporative membrane modulator that allows successful coupling of LC×LC. The benefits of this evaporative interfacing are demonstrated with the separation of phenolic acids.

## 2. EXPERIMENTAL

### *2.1 MATERIALS*

Analytical Reagent grade gallic acid, 4-hydroxybenzoic acid, syringic acid, vanillic acid, and 98% formic acid were purchased from Sigma-Aldrich (St Louis MO, USA). Solutions were prepared in Milli-Q water from a Milli-Q Plus Ultrapure Water System (Millipore, Bedford, MA, USA). Acetic acid 100% (Merck KGaA, Darmstad, Germany) and ammonia solution 28% (Univar, Seven Hills NSW Australia) were used to prepare pH 4.3 ammonium acetate solution. HPLC grade methanol (VWS Chemicals, Fontenay-sous-Bois, France) and HPLC grade acetonitrile (ACN) (Unichrom, Taren Point, NSW, Australia) were used for mobile phase preparation.

### *2.2 EVAPORATION MODULE*

The evaporation module consists of a polytetrafluoroethylene (PTFE) hydrophobic membrane sandwiched between a liquid and a gas channel. The

membrane was constructed from unlaminated hydrophobic PTFE membrane filters with 0.2 µm pore size (Sterlitech Corp. Kent, WA, USA)

A liquid channel was engraved in a 1.5 mm thick polyetherimide (PEI) disc using a Computerized Numerical Control (CNC) drill. PEI rod was purchased from Quadrant Plastics (Lenzburg, Switzerland) and cut into discs for machining. The channel was 220 ± 12 µm wide and 216 ± 18 µm deep with a total length of 741.7 mm. Once the channels were machined on the PEI disc surface, the discs were polished using aluminium oxide particles and vapour polished with dichloromethane to increase transparency.

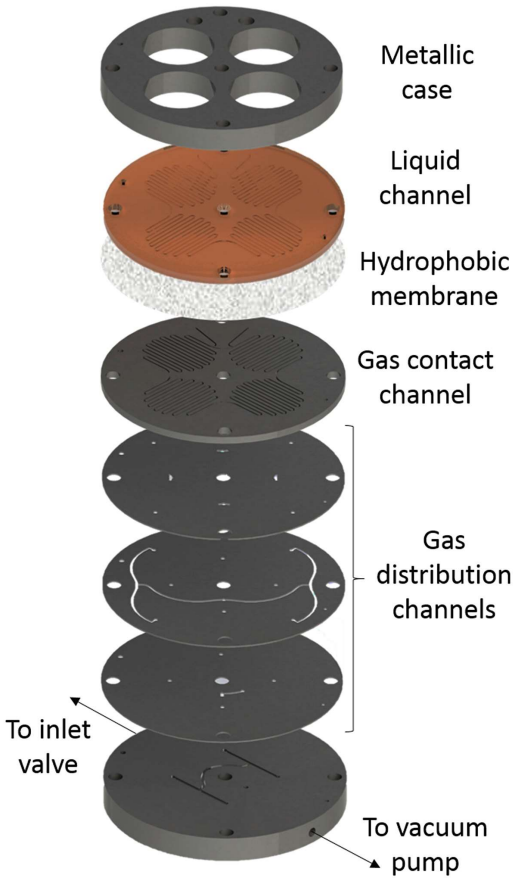


*Figure 1. Exploded view of the membrane evaporation device*

The 250 µm wide air channel was laser cut into a 250 µm thick stainless steel disc and diffusion bonded to further discs to construct the gas inlet and outlet. The channels were sealed using a bottom and top metallic case held together with 4 screws sandwiching the discs and membrane in between. An exploded view of the device is presented in Figure 1. The top metallic surface has inlet and outlet fittings as well as four large holes positioned directly over the liquid channel. These holes were designed to fit four infrared LEDs used as heat source for evaporation of the liquid. Pulsed infrared light emitting diodes (LEDs) at a wavelength of 3000 nm were purchased from Helioworks Inc (Santa Rosa, CA, USA). The LEDs provide two heating mechanisms both as a heat source that slowly heats the module, and direct heating of the water in the liquid channel by the 3000 nm infrared radiation that travels across the PEI disc providing very fast response.

The outlet of the gas/vacuum channel is connected to a miniature vacuum pump (model 1420VP BLDC, Gardner Denver Thomas; Fürstenfeldbruck, Germany) powered at constant voltage while the gas inlet can be regulated using an adjustable graded valve to provide reduced pressure and a sweeping air-flow. The optimum aperture was determined by applying constant heating at a flow rate of 20 µL $min^{-1}$ with a closed inlet valve and subsequently opening the screw inlet valve at 0.1, 0.2 or 0.5 intervals for around a minute. The flow rate was monitored after the evaporation device and the aperture that achieved maximum flow reduction was set as optimum.

An n-channel MOSFET (metal-oxide-semiconductor field-effect transistor containing excess of free electrons) (ON Semiconductor, Phoenix, AZ, USA), Arduino UNO microcontroller board, and bench top power supply (Tenma, Washington Township, OH, USA) were used to control the LEDs. A calorimetric flowmeter (Elvesys, Paris, France) with a measuring range 0-7 µL $min^{-1}$ and accuracy of 5% over 0.4 µL $min^{-1}$ was used for flowrate measurements.

### *2.3 Evaporative Membrane Modulator Operation*

A schematic diagram of the modulator and its position and control for LC×LC is shown in Figure 2. The evaporation module is connected in-line between the $^{1}$D separation column and the fraction collection valve. Fractions are collected in a loop (orange in Figure 2) with the outlet of this loop connected to the flow meter. Since temperature based flow meters are sensitive to solvent and solute composition in the stream, a water reservoir coil was placed at the inlet of the flow meter so that only water flows through the meter during measurement. The flow rate was measured for the PID feedback loop, which regulated the power supply to a series of 4 IR LEDs. To power the LEDs, an external current limited power supply was used which was regulated by the microcontroller through an n-MOSFET. When the valve is switched after collection, the loop contents are injected into the $^{2}$D separation column. UV detection was performed after $^{2}$D separation.

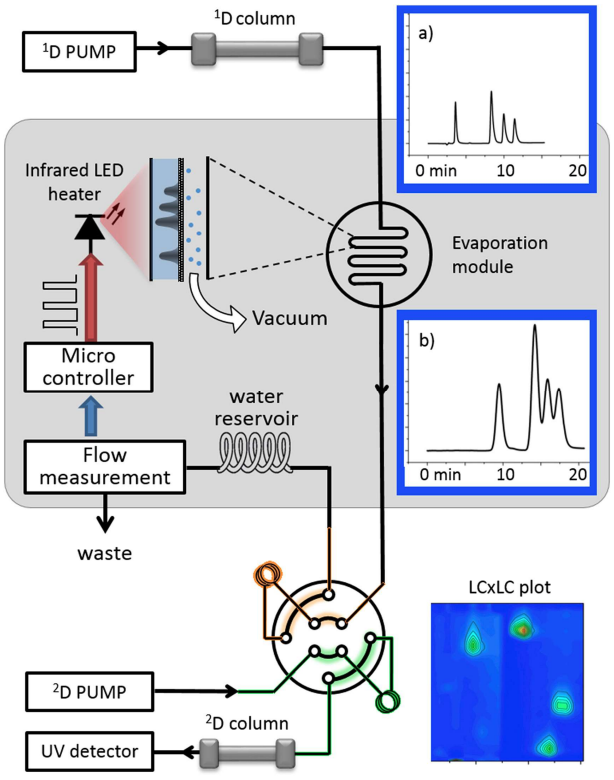


*Figure 2. Diagram of the LC×LC system with an evaporative interface. Chromatogram before (a) and after (b) evaporation.*

### *2.4 CHROMATOGRAPHIC SYSTEMS*

A 1290 Infinity 2D-LC instrument (Agilent Technologies, Santa Clara, CA, United States) featuring two binary pumps, a 4-port duo switching valve for LC×LC interfacing and a UV detector was used for all analyses. The instrument was controlled by OpenLab software (Agilent Technologies).

$^{1}$D separation was performed using a Zorbax Eclipse Plus C18 2.1 × 50 mm and 1.8 µm sized particles (Agilent Technologies). The mobile phase used was 0.1% formic acid in water (A) and methanol (B) at a flow rate of 50 µL min$^{-1}$. Methanol content was increased from 10-30% in 22 min.

$^{2}$D separation was performed using a Chromolith Performance $NH_2$ 4.6 × 10 mm (Merck KGaA, Darmstadt, Germany) in reverse-phase mode. The mobile phase used was 20 mM ammonium acetate pH 4.3 in water (A) and ACN (B), at a flow rate of 4 mL min$^{-1}$. $^{2}$D separations were 0.80 min long with a 0.01 min equilibration time. UV detection was performed at 254 nm. The gradients in $^{2}$D separations increased from 13 to 16% ACN in the 0.8 min separation time for the first 7 min. After that, 0.8 min gradients were 6 to 8% ACN from minute 7 until 6 to 10% ACN at 16 min. Whenever the evaporative interface was used, the $^{2}$D separations were delayed by 5.5 min.

A mixture of standards was used as trial sample in the chromatographic separations containing gallic, 4-hydroxybenzoic, syringic and vanillic acids. This emulates a sample of interest in the separation of phenolic and flavone antioxidants resolved in an LC×LC system [32].

One-dimensional HPLC separations were performed and the chromatograms recorded either before or after the evaporative interface for comparison, referred as $^{1}$D and $^{1}D^{EEM}$, respectively. Three sets of triplicate analyses were acquired on different days for both conditions. LC×LC separations were performed in triplicate on different days with both a switching valve dual-loop interface and the evaporative membrane modulator. In the first case 50 µL loops were used to collect 48 µL fractions. When using the evaporative

interface, initial 50 µL $min^{-1}$ input flow rate was reduced to 5.00 µL $min^{-1}$, evaporating 90% of the mobile phase. In this case, 5 uL loops were used to collect 4.8 µL fractions.

## 3. RESULTS AND DISCUSSION

On-line evaporative membrane concentration benefits from the use of a closed interface to preserve the integrity of the target solution: preventing contamination and minimizing loss of analytes. It can be carried out at mild temperatures to avoid degradation and has been proven to be reproducible for diverse analytes [33]. In this work, the concept of evaporative concentration was adapted to LC×LC interfacing since solvent removal and analyte concentration is considered beneficial for active modulation. The online concentration device was complemented with an interactive feedback control mechanism to obtain an Evaporative Membrane Modulation (EMM) device. The device was optimized and subsequently assessed in LC and LC×LC separations.

### *3.1 DEVELOPMENT AND TUNING OF THE EVAPORATIVE INTERFACE*

To optimize the effectiveness of the evaporative interface and PID control system, flow measurements together with voltage output for the infrared LED were monitored. PID parameters were then optimized to provide minimum fluctuation in the output flow. The gas inlet valve was also adjusted at an optimum aperture to achieve maximum evaporation with minimal temperature required. The optimum aperture was that which achieved the minimum flow rate as shown in Figure 3, determined to be 2.8 turns. Over the optimal aperture, the flow rate increased sharply up to the initial evaporation performance and remained constant even with a fully open valve. Hence, the gas channel configuration featuring an air flow at a pressure lower than

atmospheric showed better removal of the solvent vapors in the gas channel, and therefore lower heating needed.

To ensure correct function of the EMM, measured flow and LED voltage applied during LC×LC separations were recorded, shown in Figure 4A-B, along with the $^{1}$D gradient performed (Figure 4C). It can be seen from Figure 4A that the output flow rate was constant over the entire $^{1}$D gradient and overlaid almost perfectly with the set flow rate of 5 µL min$^{-1}$ (Figure 4A red). The heating voltage (Figure 4B) decreased when the amount of organic solvent in the mobile phase increased and returned to initial voltage when the mobile phase returned to starting conditions. Regular pulses in both the flow rate measurements and LED voltage were recorded due to the pressure pulses originating in the switching valve once $^{2}$D separations are started. However, considering the fast response of the feedback loop, the voltage and flow rapidly returned to the set point and has minimal impact in the performance of the evaporating interface.

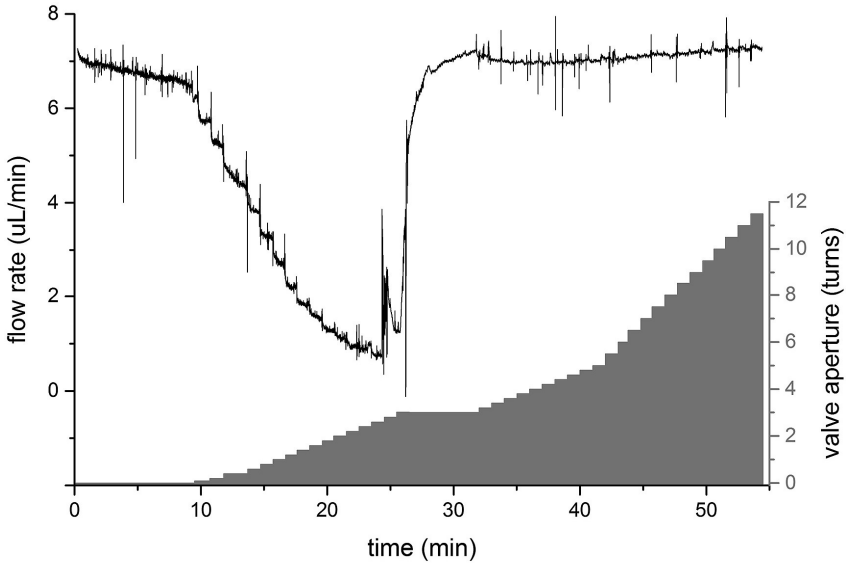


*Figure 3. Flow rate monitoring at increasing aperture of the gas inlet valve under constant heating.*

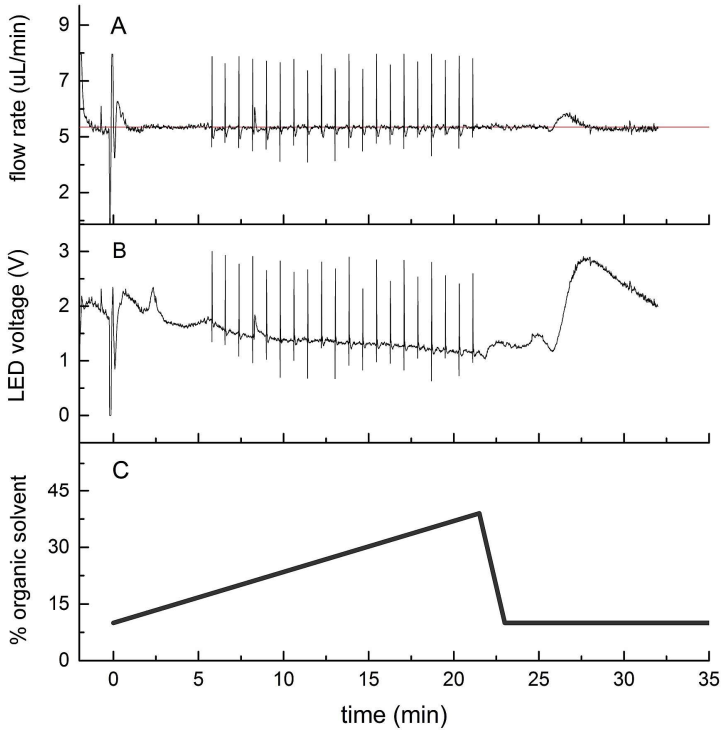


*Figure 4. Evaporative interface monitoring of a given experiment. (A) Flow measurements (black) and set point (red), (B) voltage applied to the heating elements and (C) 1D gradient.*

### *3.2 $^{1}D^{EMM}$ - EVALUATION BEFORE $^{2}D$ SEPARATION*

Figure 2 a) and b) show chromatograms of the separation of gallic, 4-hydroxybenzoic, syringic and vanillic acids, in the same time and absorbance scale. An average delay of around 5.5 min in peaks detection was observed when the evaporative interface was used. Retention time in between replicates performed on the same day show a very low relative standard deviations (RSD) of up to 0.85% with EMM, only just over the 0.72% without the modulator. Regarding the RSD for 9 replicates - carried out in sets of 3 in 3 different days – varied between 1.9-4.2%, again over 0.99% without the modulator. This increased variability is due to the principle of calorimetric flow sensing that detects the thermal profile due to fluid flow around a heater.

Therefore, proper thermal flow sensor response is dependent upon a constant fluid temperature and a minimal inaccuracy due to temperature drift is observed. To avoid it, the temperature can simply be controlled in the flow measurement station [34].

Analytes were quantified in triplicate before and after the evaporative interface. Peak height increase was found to be significantly higher for all analytes (2.5-2.7 fold), achieving though a lower increase for gallic acid (1.7 fold). To compare the peak areas with and without modulator, the time scale was converted to volume by multiplying by the flow rates of 5 and 50 uL $min^{-1}$, respectively. Recoveries were then calculated to be between 77 and 96%. Peak symmetry was greatly improved from 1.66 ± 0.06 to 1.16 ± 0.01. Peak widths measured in µL were used to assign the volume of the analyte band. Peak volume decreased around 4 times, except for gallic acid which was only reduced by 2.6. Ideally, with a 100% recovery and no longitudinal diffusion, when reducing flow rate by a factor of 10 the peak band volume should decrease by a factor of 10 and the peak height increase by 10. The results show that the observed enhancement with the evaporative modulator is noticeably lower, most likely due to the fluid in the evaporator spending considerable time at elevated temperatures, which increases longitudinal diffusion. This results in a decreased peak capacity in the first dimension from 13.6 to 5.7. We believe that heating and evaporation occurring at opposite sides of a square 200 µm channel strongly contribute to the longitudinal diffusion and may cause some turbulence. Alternative channel geometries are to be considered in order to minimize this phenomenon to preserve the separation resolution of the $^{1}$D separation, and therefore fully exploit the increased peak capacity of LC×LC.

### *3.3 INTERFACE EVALUATION IN $LC^{EMM}$×LC*

LC×LC separations were performed using the model mixture, with and without the EMM (Figure 5). The evaporation module allowed each $^{1}$D peak to be sampled between 3-4 times in the second dimension in contrast to the switching valve approach where each $^{1}$D peak was only sampled 2-3 times. This improves quantification capabilities since the $^{1}$D peak is better represented in the 2D plot, while sensitivity is not impaired because analyte mass is preserved (i.e. $^{1}$D flow splitting is avoided). To assess other improvements, the separation widths of peaks in the second dimension were compared with and without the evaporative modulator.

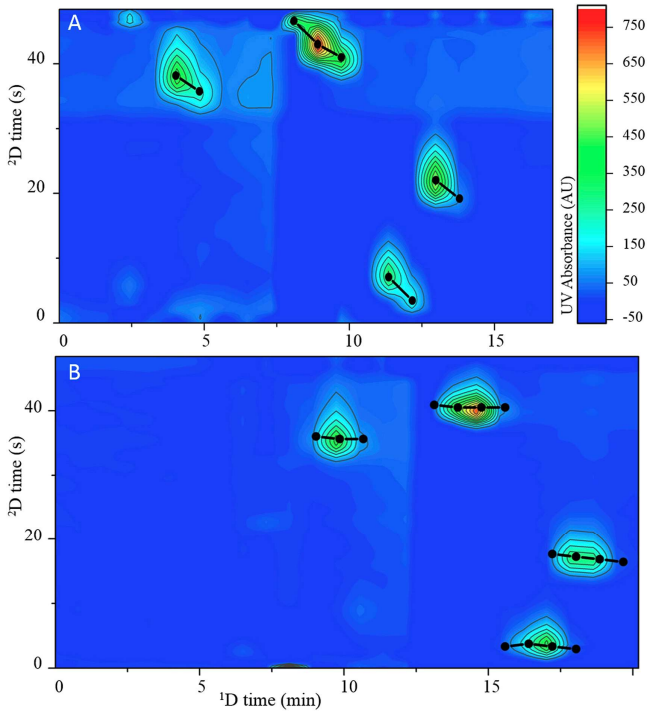


*Figure 5. LC×LC 2D plot chromatograms of normal (A) and evaporative (B) interfacing and cross-peak shape study.*

Single dimension peak capacity ($^{i}n_C$) was calculated using Equation 1, while theoretical and effective LC×LC peak capacity ($n_{C,2D}$ and $n^{*}_{C,2D}$ respectively) were calculated using Equations 2-3 [35]. The use of the correction factor <β> has been extensively studied [36,37] in order to take into account the

undersampling. The extensively described [38,39] coverage factor ($f_{coverage}$) can be used in Equation 3 when considering the orthogonality of the separation.

(1) $$ {}^{i}n_C = 1 + \frac{t_{R,last} - t_{R,first}}{\bar{W}} $$

(2) $$ n_{C,2D} = {}^{1}n_C \times {}^{2}n_C $$

(3) $$ n^{*}{}_{C,2D} = \frac{{}^{1}n_C \times {}^{2}n_C}{<\beta>} \times f_{coverage} $$

Widths of the two biggest peak fractions were recorded in triplicate, and the average $^2$D peak width was found to be reduced between 6-22% at half maximum (PWHM) and 2-25% at w10%. Consequently, $^2n_C$ is enhanced by 10%. All individual values for various chromatographic parameters are shown in Table 1 for comparison. The theoretical peak capacity $n_{C,2D}$ both with and without the evaporative modulator was calculated and was higher without, 91 compared to 43 with the EMM. However, when the peak broadening factor <β> is considered to take into account undersampling, corrected peak capacities ($n^*_{C,2D}$) are comparable, being 35 and 32, respectively. Although the effect of diffusion in the interface on peak capacity of the first dimension ($^1n_C$) is substantial, the comparable correct peak capacity suggests that this effect is compensated in the 2D system by an increase in the $^2$D peak capacity and better sampling of the $^1$D peaks. In this study $f_{coverage}$=1 is considered for the purpose of comparison between LC×LC and $LC^{EEM}$×LC separations.

Table 1. Individual chromatographic parameters of each individual analyte in passive and active modulation

| | LC×LC - passive modulation | | | | $LC^{EEM}$×LC - active modulation | | | |
|---|---|---|---|---|---|---|---|---|
| acids | gallic | 4-hydroxy benzoic | syringic | vanillic | gallic | 4-hydroxy benzoic | syringic | vanillic |
| Fraction volume (µL) | 48 | | | | 4.8 | | | |
| Collection loops volume (µL) | 50 | | | | 5 | | | |
| $^1$D peak symmetry | 1.580 ±0.084 | 1.692 ±0.017 | 1.681 ±0.013 | 1.688 ±0.021 | 1.15 ±0.01 | 1.168 ±0.003 | 1.170 ±0.004 | 1.146 ±0.005 |
| $^1$D peak height | 181.7 ±5.2% | 226.1 ±2.0% | 124.8 ±1.9% | 103.2 ±1.8% | 309 ±11.3% | 572 ±9.4% | 326 ±8.8% | 281 ±7.0% |
| $^1D^{EEM}$ peak height increase | - | - | - | - | 1.70 | 2.53 | 2.61 | 2.72 |
| $^1$D peak area (µL AU) | 139459 ±2.0% | 259028 ±1.2% | 148979 ±0.9% | 122740 ±1.8% | 89851 ±10.7% | 168952 ±8.1% | 102359 ±7.2% | 98601 ±7.1% |
| $^1D^{EEM}$ recoveries (%) | - | - | - | - | 77.3 | 78.3 | 82.5 | 96.4 |
| $^1$D peak width (min) | 0.414 ±0.036 | 0.656 ±0.012 | 0.696 ±0.013 | 0.6889 ±0.0051 | 1.5865 ±0.0065 | 1.6000 ±0.0000 | 1.697 ±0.010 | 1.7978 ±0.0039 |
| $^1$D peak width 4σ (µL) | 20.7 ± 1.8 | 32.78 ±0.59 | 34.78 ±0.67 | 34.44 ±0.25 | 7.933 ±0.032 | 8.000 ±0.0000 | 8.489 ±0.051 | 8.989 ±0.019 |
| $^1D^{EEM}$ peak volume reduction | - | - | - | - | 2.61 ±0.23 | 4.10 ±0.07 | 4.10 ±0.10 | 3.83 ±0.02 |
| $^2$D peak base width (min) | 0.1138 ±0.0052 | 0.0880 ±0.0035 | 0.1019 ±0.0132 | 0.1127 ±0.0046 | 0.1068 ±0.0073 | 0.081 ±0.014 | 0.079 ±0.010 | 0.100 ±0.015 |
| $^2$D peak width decrease (%) | - | - | - | - | 6.1 | 8.4 | 22.7 | 11.6 |
| $n_{C,1}$ | 13.6 | | | | 5.7 | | | |
| $n_{C,2}$ | 6.6 | | | | 7.5 | | | |
| $n_{C,2D}$ | 90.8 | | | | 42.7 | | | |
| $n^*_{C,2D}$ | 34.7 | | | | 31.9 | | | |

In addition, when using the evaporative interface there were remarkably less peak-slice to peak-slice retention $^{2}$D time differences. Using common switching valve modulation the retention time in the second dimension decreased by 3-4 s with each slice, while using EMM this decrease was reduced by 10 times to 0.4 s. This phenomenon can be observed in the cross-peak shape study in Figure 5 where the experimental $^{2}$D retention times were plotted overlaying the 2D peaks. Such achievement highlights a key benefit of solvent removal preserving the 2D separation performance. In an LC×LC system, it is a remarkable advantage for peak identification of complex samples where some analytes may be partially co-eluted.

## 4. Conclusions

Evaporative Membrane Modulation (EMM) was implemented in an LC×LC system by monitoring the $^{1}$D outlet flow rate and automatically adjusting the heating intensity to keep evaporation constant.

Even though there is a loss of peak capacity in the first dimension, the introduction of the evaporative interface preserves peak capacity of the LC×LC separation, while improving peak identification by eliminating the interference of $^{1}$D solvent in the $^{2}$D separation system. This provides a wider choice of chromatographic conditions and stationary phases that would otherwise be unsuitable.

The evaporator allows for wider columns to be used in the first dimension, as well as larger flow, allowing more independent optimization of subsequent separation systems, easing method development of high orthogonality LC×LC. Also, faster separations are to be expected.

EMM is a significant development in fraction transfer technology; the second dimension analysis is improved and incompatibilities attenuated. However, fundamental work on overcoming diffusion and minimising broadening in the

interface is required in order to harness the full resolving capability of LC×LC separations.

## ACKNOWLEDGMENTS

This research was conducted by the ARC Training Centre for Portable Analytical Separation Technologies (IC140100022). MCB is the recipient of an ARC Future Fellowship. E. Fornells is a recipient of an ARC post-graduate scholarship in ASTech, University of Tasmania.

# APPENDIX A: ADDITIONAL SYSTEM INFORMATION

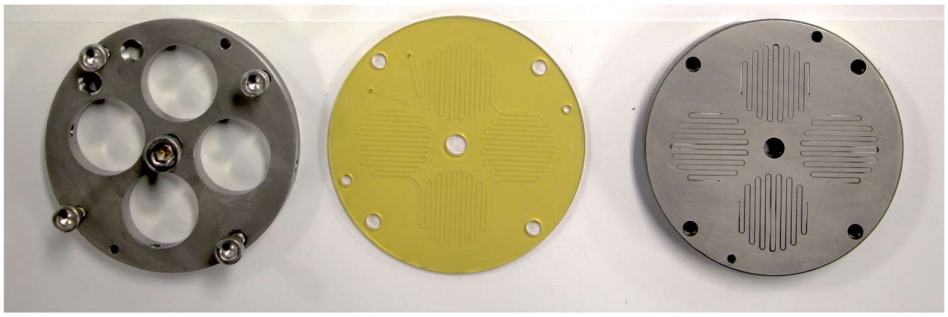

*Figure 6. Parts of the evaporative device used. Left to right: Tope case, PEI liquid channel disc, gas channel diffusion bonded to gas distribution, inlet and outlet.*

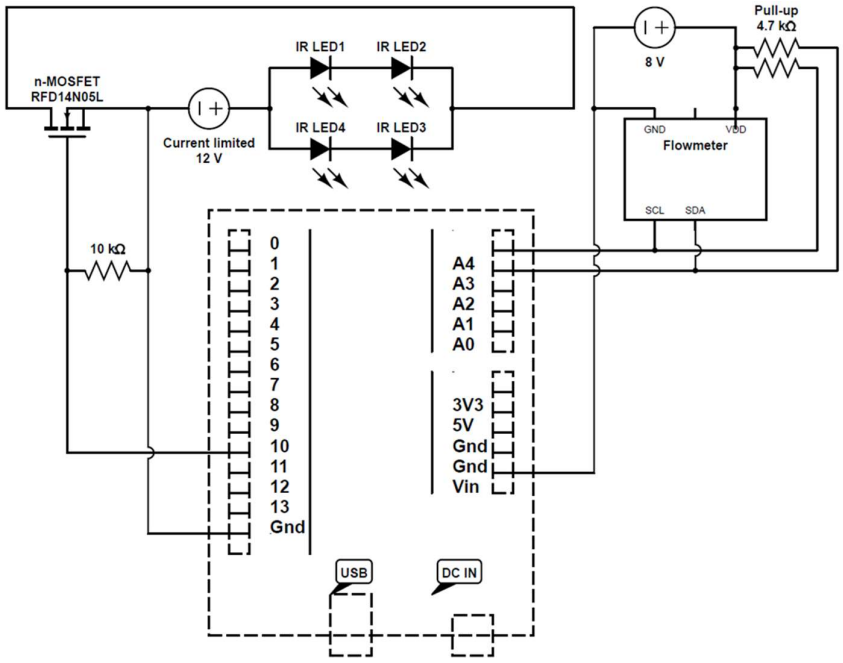


*Figure 7. Diagram of the circuit used to perform PID control on the evaporative device.*

# APPENDIX B: ADDRESSING BAND BROADENING

## *ALIQUOT MERGING*

### *Materials and Methods*

Band broadening was assessed after an HPLC gradient separation. A separation of 6 pharmaceuticals and by-products (sulfamerazine, sulfamethazine, sulfamethizole, sulfamethoxine, furosemide and prednisolone analytical grade, Sigma-Aldrich) was achieved in a Zorbax EclipsePlus $C_{18}$ 50 x 2.1 mm, 1.8µm column (Agilent Technologies) performing a solvent gradient at 40 µL $min^{-1}$. Initial mobile phase was 90% 10mM ammonium acetate pH 5.55 and 10% acetonitrile, increasing up to 50% acetonitrile in 14 min.

Band broadening due to channel geometry, not the evaporation process, was evaluated comparing the chromatogram acquired before and after entering the evaporative device (referred to as off-line and 0% respectively) Besides, different evaporation conditions were also compared to 0%.

In addition, an approach to minimise band broadening was tested. A switching valve was used as shown in Figure 8 to intercalate aliquots of the eluted separation (chromatogram fractions - yellow) within solvent aliquots (volume between fractions - blue). When these aliquots merged during their path through the evaporation device, the chromatogram was reconstituted before detection and band broadening was reduced.

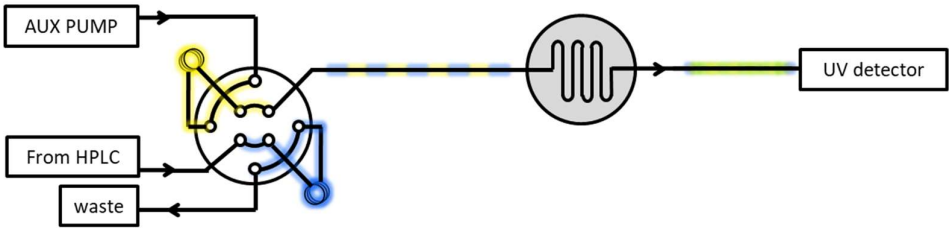


*Figure 8. Experimental set-up to intercalate solvent (blue) and elution (yellow) aliquots.*

The aliquot volumes and their ratio was defined by the valve switching or collection time ($t_{collection}$), the loop size (17.3 µL), and the flow rate of both the separation (40 µL $min^{-1}$) and the auxiliary pump ($U_{aux}$). This approach was tested at 60 and 80 % evaporation, and conditions tested were: 120, 140 and 160 µL $min^{-1}$ for the auxiliary flow; 0.25 and 0.17 min for collection time.

*Results*

Figure 9 B shows chromatograms acquired before (off-line, dashed line) and after the evaporative device at 0% (black, solid line), 60% (blue) and 80% (red) evaporation. This comparison showed that peak height was halved after its path through the device in non-evaporation conditions. When evaporation was regulated, peak height increased because of the preconcentration effect but band broadening caused peaks to merge. As expected, broadening increased at increasing evaporation percentages. Chromatograms in Figure 9 A were obtained using the valve system at different auxiliary flowrates and collection times.

The effects of intercalated aliquots were evaluated in different conditions, proving that separation can be preserved to a level comparable to 0% evaporation in optimized conditions. The volume ratios $V_{fraction}$:$V_{between\ fractions}$ ($V_f$:$V_{bf}$) for each set of conditions tested are summarized in Table 2. The best ratio was found to be 1:3 since no further improvement was observed at lower ratios. At higher ratios (1:4), distortion of the peak shape occurs as the aliquots are not fully merged. The extreme example of such distortion is that which occurs when using the valve system at 0% evaporation, shown in the top chromatogram in Figure 9.

Table 2. Volume ratios as a function of tested conditions.

| $U_{aux}$ | $t_{collection}$ | $V_{loop}$ | $V_{fraction}$ | $V_{between\ fractions}$ | Ratio ($V_f$ : $V_{bf}$) |
|---|---|---|---|---|---|
| 160 | 0.25 | 17.3 | 10 | 30 | 1 : 4.0 |
| 140 | 0.25 | 17.3 | 10 | 25 | 1 : 3.5 |
| 120 | 0.25 | 17.3 | 10 | 20 | 1 : 3.0 |
| 160 | 0.17 | 17.3 | 6.8 | 20.4 | 1 : 4.0 |
| 140 | 0.17 | 17.3 | 6.8 | 17 | 1 : 3.5 |
| 120 | 0.17 | 17.3 | 6.8 | 13.6 | 1 : 3.0 |

Shorter collection times provide smaller fractions with the same ratio, improving merging further. Collection times lower than 0.17 min (10.2 s) may be preferable but such lower valve switching time increases instability in the evaporation regulation due to pressure pulses. In addition, conditions set are limited by the flow meter reading range and the evaporation capability of the device. For example, at $U_{aux}$ 160 µL $min^{-1}$, 80% evaporation leads to very hot temperatures at the top of the working range.

Despite preconcentration was not achieved due to dilution, this strategy can reduce dramatically the band broadening arising from the evaporation process and potentially preserve separation. It is therefore an encouraging step towards the viability of evaporative devices in separation science. In addition, it was demonstrated that diffusion and band broadening due to the device design itself was notable. To minimize it, it is important to consider alternative channel geometries. Several channel geometries were explored and are commented in the following section.

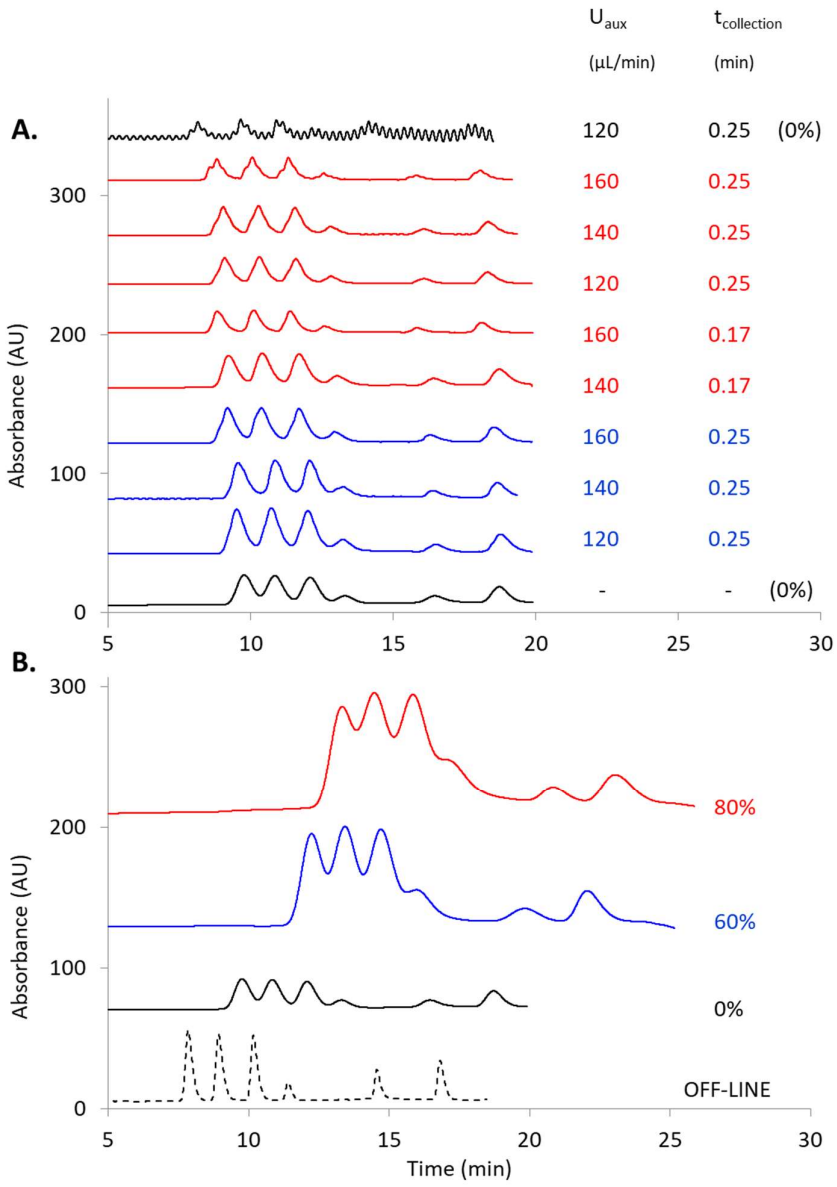


*Figure 9. A. Chromatograms acquired at different conditions using the using the switching valve system in Figure 7 and B. using the stand-alone evaporation device. Blue and red lines correspond to 60 and 80% evaporation, respectively. Black solid lines were acquired at 0% evaporation while the dashed line was the chromatogram at the columns exit.*

*COMPUTATIONAL FLUID DYNAMICS STUDY: INFLUENCE OF CHANNEL GEOMETRY*

In an attempt to understand the causes of band broadening in the microfluidic channel, three different channel geometries were studied by Computational Fluid Dynamics (CFD) using COMSOL 4.3 software. The first design was a straight channel matching the experimental cross section size of 200×200 µm, as well as its total length (70 mm). Two additional serpentine designs with 16 turns also matching the total length of the experimental channel were also constructed. The cross section of the channel was also 200×200 µm for both serpentine designs, however one of them featured tapered turns sized 200 µm deep and 100 µm wide. Comparison between tapered and not tapered serpentine geometry is shown in Figure 10.

In all cases, the upper channel wall was defined as a water-leaking channel and the leaking rate adjusted so that flow rate would decrease as desired. Two sets of simulations were performed for each design featuring no leakage and a 10 times flow reduction (90% evaporation), respectively. Elution sample bands obtained in different simulated conditions and geometries are shown in Figure 10.

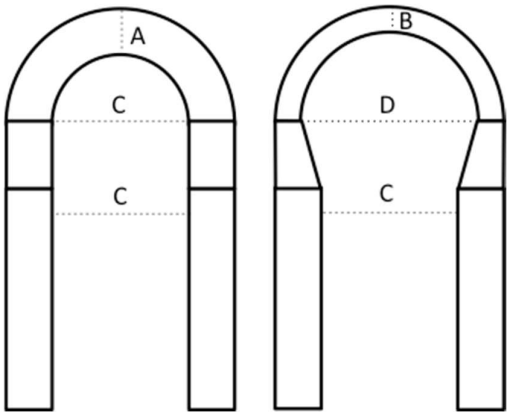


*Figure 10. Scheme of the serpentine channel geometries studied by CFD. A = 200 µm, B = 100 µm, C = 600 µm, D = 700 µm*

Compared to the sample band at the inlet (black, plateau shaped), elution bands were Gaussian shaped. Intensity of the peak was halved when there was no evaporation occurring, in accordance with the expected band broadening in experimental results. When flow rate was reduced 10 times by evaporation, peak intensity increased by around a factor of 5 instead of 10-fold, also as expected. In both evaporative and non-evaporative conditions, a straight channel and a serpentine channel (200x200 µm in size) had similar elution time. In contrast, the serpentine with tapered turns showed earlier elution due to smaller volume, while peak intensity was only slightly higher than that of a regular serpentine. Decreased concentration factor was observed for both serpentine geometries compared to straight channel, however small.

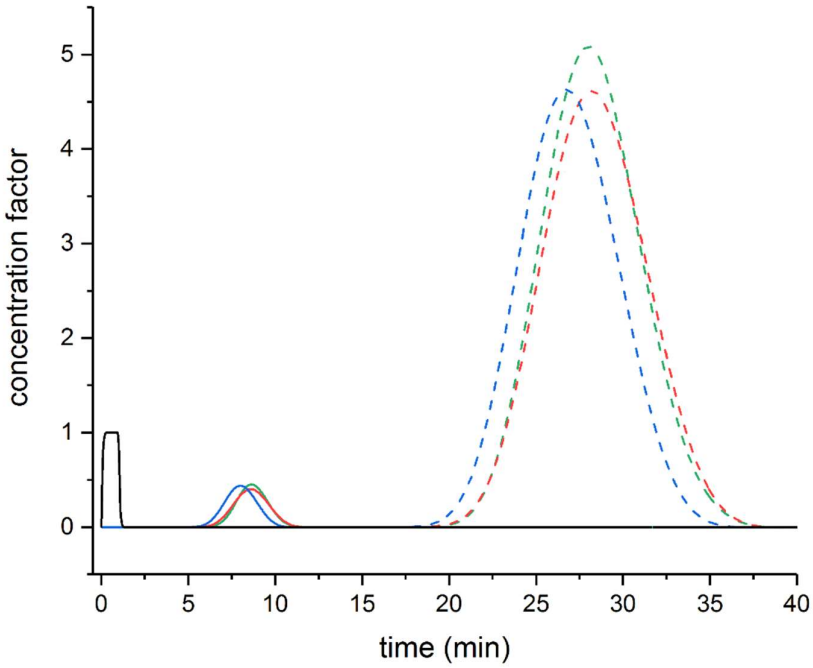


*Figure 11. Simulated elution bands in a straight channel (green), serpentine (red) and tapered serpentine (blue). Solid lines show simulations without evaporation and dashed lines show 90% evaporation.*

Therefore, these results suggested that serpentine turns were not the main source of band broadening. Dispersion was similarly high for the three geometries in the relatively big, square-shaped microfluidic channel. Such large band broadening during evaporation could be caused by the cross-sectional velocity gradient due to evaporation occurring in one side only. This in turn caused a concentration gradient in all geometries, as shown in Figure 12.

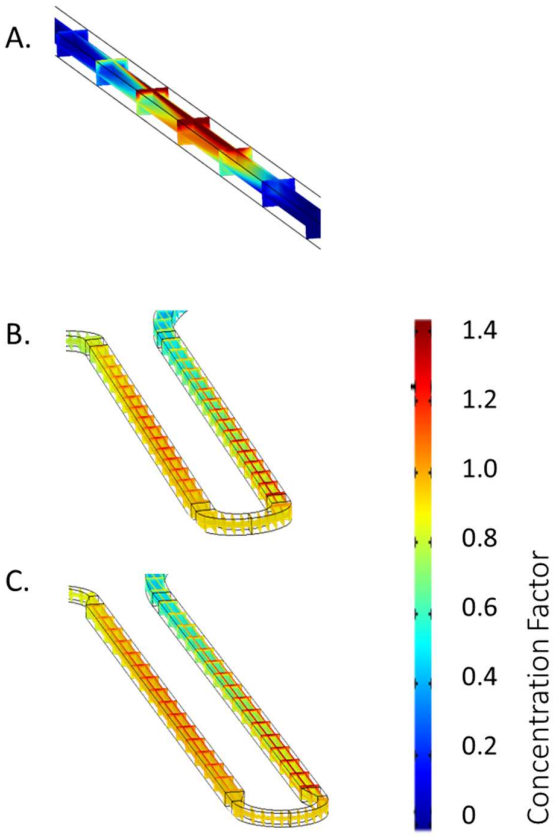


*Figure 12. Concentration tracked along different channel geometries showing higher concentrations the closer to the leaking wall (acting as evaporative membrane).*

Focused heating at the center of the serpentine may be an additional source of band broadening, creating fast temperature gradients along the channel. For a better understanding of these phenomena, a model including heating would be beneficial.

## REFERENCES

[1] J.C. Giddings, Maximum number of components resolvable by gel filtration and other elution chromatographic methods, Anal. Chem. 39 (1967) 1027–1028.

[2] R.E. Murphy, M.R. Schure, J.P. Foley, Effect of Sampling Rate on Resolution in Comprehensive Two-Dimensional Liquid Chromatography, 70 (1998) 1585–1594.

[3] P. Jandera, T. Hájek, P. Česla, Effects of the gradient profile, sample volume and solvent on the separation in very fast gradients, with special attention to the second-dimension gradient in comprehensive two-dimensional liquid chromatography, J. Chromatogr. A. 1218 (2011) 1995–2006.

[4] P. Jandera, Column selectivity for two-dimensional liquid chromatography, J. Sep. Sci. 29 (2006) 1763–1783.

[5] X. Li, P.W. Carr, Effects of first dimension eluent composition in two-dimensional liquid chromatography, J. Chromatogr. A. 1218 (2011) 2214–2221.

[6] E.S. Talus, K.E. Witt, D.R. Stoll, Effect of pressure pulses at the interface valve on the stability of second dimension columns in online comprehensive two-dimensional liquid chromatography, J. Chromatogr. A. 1378 (2015) 50–57.

[7] K. Horváth, J.N. Fairchild, G. Guiochon, Detection issues in two-dimensional on-line chromatography, J. Chromatogr. A. 1216 (2009) 7785–7792.

[8] H. Malerod, E. Lundanes, T. Greibrokk, Recent advances in on-line multidimensional liquid chromatography, Anal. Methods. 2 (2010) 110–122.

[9] P.J. Schoenmakers, G. Vivó-Truyols, W.M.C. Decrop, A protocol for designing comprehensive two-dimensional liquid chromatography separation systems, J. Chromatogr. A. 1120 (2006) 282–290.

[10] R.J. Vonk, A.F.G. Gargano, E. Davydova, H.L. Dekker, S. Eeltink, L.J. de Koning, P.J. Schoenmakers, Comprehensive Two-Dimensional Liquid Chromatography with Stationary-Phase-Assisted Modulation Coupled to High-Resolution Mass Spectrometry Applied to Proteome Analysis of Saccharomyces cerevisiae, Anal. Chem. 87 (2015) 5387–5394.

[11] P. Česla, J. Křenková, Fraction transfer process in on-line comprehensive two-dimensional liquid-phase separations, J. Sep. Sci. 40 (2017) 109–123.

[12] A.F.G. Gargano, M. Duffin, P. Navarro, P.J. Schoenmakers, Reducing Dilution and Analysis Time in Online Comprehensive Two-Dimensional Liquid Chromatography by Active Modulation, Anal. Chem. 88 (2016) 1785–1793.

[13] P.G. Stevenson, D.N. Bassanese, X.A. Conlan, N.W. Barnett, Improving peak shapes with counter gradients in two-dimensional high performance liquid chromatography., J. Chromatogr. A. 1337 (2014) 147–54.

[14] M.R. Filgueira, Y. Huang, K. Witt, C. Castells, P.W. Carr, Improving peak capacity in fast online comprehensive two-dimensional liquid chromatography with post-first-dimension flow splitting., Anal. Chem. 83 (2011) 9531–9.

[15] M. Verstraeten, M. Pursch, P. Eckerle, J. Luong, G. Desmet, Thermal modulation for multidimensional liquid chromatography separations using low-thermal-mass liquid chromatography (LC), Anal. Chem. 83 (2011) 7053–7060.

[16] M.E. Creese, M.J. Creese, J.P. Foley, H.J. Cortes, E.F. Hilder, R.A. Shellie, M.C. Breadmore, Longitudinal On-Column Thermal Modulation for Comprehensive Two-Dimensional Liquid Chromatography, Anal. Chem. 89 (2017) 1123–1130.

[17] H. Eghbali, K. Sandra, B. Tienpont, S. Eeltink, P. Sandra, G. Desmet, Exploring the Possibilities of Cryogenic Cooling in Liquid Chromatography for Biological Applications: A Proof of Principle, Anal. Chem. 84 (2012) 2031–2037.

[18] S.R. Groskreutz, S.G. Weber, Temperature-assisted solute focusing with sequential trap/release zones in isocratic and gradient capillary liquid chromatography: Simulation and experiment, J. Chromatogr. A. 1474 (2016) 95–108.

[19] H.C. van de Ven, A.F.G. Gargano, S. van der Wal, P.J. Schoenmakers, Switching solvent and enhancing analyte concentrations in small effluent fractions using in-column focusing, J. Chromatogr. A. 1427 (2016) 90–95.

[20] H. Tian, J. Xu, Y. Xu, Y. Guan, Multidimensional liquid chromatography system with an innovative solvent evaporation interface, J. Chromatogr. A. 1137 (2006) 42–48.

[21] K. Ding, Y. Xu, H. Wang, C. Duan, Y. Guan, A vacuum assisted dynamic evaporation interface for two-dimensional normal phase/reverse phase liquid chromatography., J. Chromatogr. A. 1217 (2010) 5477–83.

[22] H. Tian, J. Xu, Y. Guan, Comprehensive two-dimensional liquid chromatography (NPLC×RPLC) with vacuum-evaporation interface, J. Sep. Sci. 31 (2008) 1677–1685.

[23] J.-F. Li, X. Yan, Y.-L. Wu, M.-J. Fang, Z. Wu, Y.-K. Qiu, Comprehensive two-dimensional normal-phase liquid chromatography × reversed-phase

liquid chromatography for analysis of toad skin, Anal. Chim. Acta. 962 (2017) 114–120.

[24] H. Zhang, R.M. Tiggelaar, S. Schlautmann, J. Bart, H. Gardeniers, In-line sample concentration by evaporation through porous hollow fibers and micromachined membranes embedded in microfluidic devices, Electrophoresis. 37 (2016) 463–471.

[25] B.H. Timmer, K.M. van Delft, W. Olthuis, P. Bergveld, A. van den Berg, Micro-evaporation electrolyte concentrator, Sensors Actuators B. 91 (2003) 342–346.

[26] S. Nii, Membrane evaporators, J. Memb. Sci. 201 (2002) 149–159.

[27] M. Takeuchi, P.K. Dasgupta, J. V. Dyke, K. Srinivasan, Postcolumn Concentration in Liquid Chromatography. On-Line Eluent Evaporation and Analyte Postconcentration in Ion Chromatography, Anal. Chem. 79 (2007) 5690–5697.

[28] K. Gethard, S. Mitra, Membrane distillation as an online concentration technique: application to the determination of pharmaceutical residues in natural waters., Anal. Bioanal. Chem. 400 (2011) 571–5.

[29] P. Wang, T. Chung, Recent advances in membrane distillation processes : Membrane development , con fi guration design and application exploring, J. Memb. Sci. 474 (2015) 39–56.

[30] J.Y. Zhang, J. Do, W.R. Premasiri, L.D. Ziegler, C.M. Klapperich, Rapid point-of-care concentration of bacteria in a disposable microfluidic device using meniscus dragging effect., Lab Chip. 10 (2010) 3265–3270.

[31] A. Visioli, Practical PID Control, *Springer London*, 2006.

[32] F. Cacciola, P. Jandera, Z. Hajdú, P. Česla, L. Mondello, Comprehensive two-dimensional liquid chromatography with parallel gradients for

separation of phenolic and flavone antioxidants, J. Chromatogr. A. 1149 (2007) 73–87.

[33] E. Fornells, B. Barnett, M. Bailey, R.A. Shellie, E.F. Hilder, M.C. Breadmore, Membrane assisted and temperature controlled on-line evaporative concentration for microfluidics, J. Chromatogr. A. 1486 (2017) 110–116.

[34] J.T.W. Kuo, L. Yu, E. Meng, Micromachined Thermal Flow Sensors—A Review, Micromachines. 3 (2012) 550–573.

[35] Y. Huang, H. Gu, M. Filgueira, P.W. Carr, An experimental study of sampling time effects on the resolving power of on-line two-dimensional high performance liquid chromatography, J. Chromatogr. A. 1218 (2011) 2984–2994.

[36] J.M. Davis, D.R. Stoll, P.W. Carr, Dependence of effective peak capacity in comprehensive two-dimensional separations on the distribution of peak capacity between the two dimensions, Anal. Chem. 80 (2008) 8122–8134.

[37] P. Dugo, F. Cacciola, T. Kumm, G. Dugo, L. Mondello, Comprehensive multidimensional liquid chromatography: Theory and applications, J. Chromatogr. A. 1184 (2008) 353–368.

[38] S.C. Rutan, J.M. Davis, P.W. Carr, Fractional coverage metrics based on ecological home range for calculation of the effective peak capacity in comprehensive two-dimensional separations, J. Chromatogr. A. 1255 (2012) 267–276.

[39] M. Gilar, J. Fridrich, M.R. Schure, A. Jaworski, Comparison of orthogonality estimation methods for the two-dimensional separations of peptides, Anal. Chem. 84 (2012) 8722–8732.

# IV. On-line solvent exchange system: Automation from extraction to analysis

This chapter has been submitted to a peer reviewed journal as a research article except for the appendix. All efforts were made to keep the original features of this article except for minor changes. Layout, numbering, font size and style were modified in order to maintain a consistent formatting style of this thesis.

## Graphical abstract

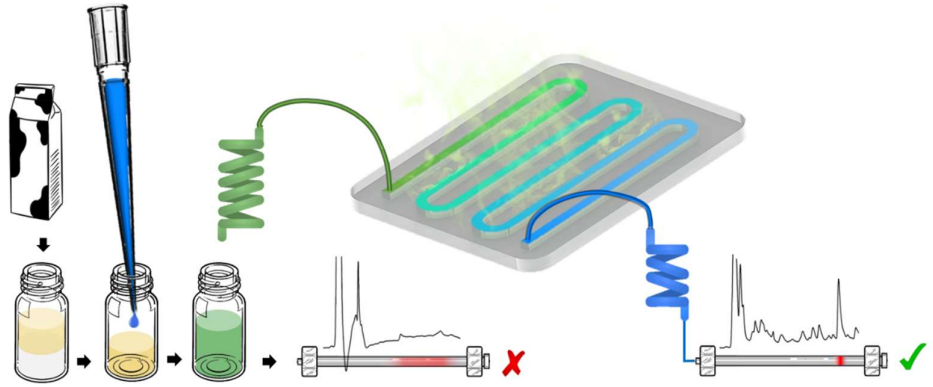

## Abstract

Removal of organic solvent from sample extracts is required before analysis by reversed phase HPLC to preserve chromatographic performance and allow for bigger injection volumes, boosting sensitivity. Herein, an automated on-line extraction evaporation procedure is integrated with HPLC analysis. The evaporation occurs inside a 200 µm microfluidic channel confined by a vapor permeable membrane. A feedback control algorithm regulates evaporation rate keeping the output flow rate constant. The evaporation process across this membrane was firstly characterized with water/solvent mixtures showing

organic solvent removal capabilities. This system allowed continuous methanol, ethanol and acetonitrile removal from samples containing up to 80% organic solvent. An evaporative injection procedure was developed demonstrating the use of the device for fully integrated extract reconstitution coupled to HPLC analysis, applied to analysis of the antibiotic chloramphenicol in milk samples. Sample reconstitution and collection was performed in less than 10 min and can be executed simultaneously to HPLC analysis of the previous sample in a routine workflow, thus having minimal impact on the total sample analysis time when run in a sequence.

## 1. INTRODUCTION

Analytical processes comprise a number of steps, usually including sample treatment such as clean up or preconcentration, separation of components via a suitable technique and analyte detection. The first step, sample preparation, is frequently the most time-consuming and laborious procedure during the whole analytical process as it normally comprises multiple steps [1]. Complete automation or integration is preferable, such that the entire analysis is performed under controlled conditions minimizing human and systematic errors, making it a more cost and time effective process.

Liquid-liquid extraction (LLE) and solid phase extraction (SPE) are the most widely used approaches to extract target compounds from a sample while leaving interfering matrix components behind. In SPE, the stationary phase plays an important part in the optimization process and on the overall analysis cost. In LLE, solvent(s) must be chosen carefully to avoid detrimental issues such as emulsion formation or miscibility. However, when chromatographic techniques are subsequently used, solvents also have a critical impact on chromatographic parameters such as retention, band spreading and peak symmetry [2,3]. On some occasions, the organic solvent extract can be directly

used for the chromatographic analysis [4], but it is rare for reversed phase liquid chromatography (RPLC). If the solvent is too strong it leads to poor peak shapes or elution with the void. In such cases the solvent must be dried down completely or evaporated partially to be later reconstituted to a desired volume in a more compatible solvent.

The automation of LLE and SPE has been previously reported, including extract evaporation, using an autosampler [5,6] or the 96-well format [7]. However, most steps of LLE are performed manually, especially the evaporation under nitrogen current which is usually the longest and more time consuming step [8]. Online SPE goes beyond automation to integration, allowing for fast, simple, and reproducible sample preparation minimizing human error [9]. Such integration has not been reported when extract dry down is required for either SPE or LLE. Issues rising from solvent incompatibilities in LLE-HPLC analysis have been addressed in a case-by-case basis, generally involving time-consuming offline steps.

Here, we present an automated on-line extract evaporation procedure coupled to HPLC analysis. The online evaporation occurs inside a microfluidic channel confined with a hydrophobic gas-permeable membrane. Pervaporation, or gas and vapor transport across the membrane, leads to reduction of the volume but preservation of analytes [10–16]. This type of device has been used for preconcentration purposes [17–20] and more recently for instrument coupling [21]. However, the effects on solvent composition have never been explored or exploited beyond distillation [22,23]. We present its use for on-line reconstitution of LLE extracts in an automated extract evaporation procedure. Firstly, the evaporation process in the developed device was characterized with water/solvent mixtures to better understand the solvent removal process. Then, we demonstrated on-line sample reconstitution of chloramphenicol (CAP) extracts in milk samples by HPLC-UV and HPLC-MS/MS using evaporative injection, obtaining a LOD

under 0.3 µg $L^{-1}$ for the latter, which is sufficient for regulatory reporting in areas with the lowest specified limits such as Europe or Canada [24].

## 2. MATERIALS AND METHODS

### *2.1 EVAPORATIVE MODULE AND OPERATION*

The evaporation module and its operation has previously been described [21]. Briefly, the module consists of a polytetrafluoroethylene (PTFE) membrane sandwiched between a liquid and a gas channel. Hydrophobic PTFE membrane filters with 0.2 µm pore size were used (Sterlitech Corp. Kent, WA, USA). A liquid channel (220 ± 12 µm wide and 216 ± 18 µm deep) was machined on a 1.5 mm thick polyetherimide (PEI) disc from Quadrant Plastics (Lenzburg, Switzerland). The total channel length was 741.7 mm. A 250 µm wide air channel was laser cut into stainless steel and diffusion bonded to other parts to construct the gas inlet and outlet. Vapor was removed from the gas channel by a miniature vacuum pump (model 1420VP BLDC, Gardner Denver Thomas; Fürstenfeldbruck, Germany) providing reduced pressure and a sweeping air-flow from a regulated inlet. The module was leak tight when held together with 4 screws. Four infrared LEDs at a wavelength of 3000 nm from Helioworks Inc (Santa Rosa, CA, USA) were used to irradiate the liquid channel through the PEI channel disc providing very fast heating times. Heating was adjusted through a microcontroller, also used for data acquisition from a calorimetric flow meter (Elvesys, Paris, France).

To implement the on-line solvent evaporator, it is necessary to precisely control temperature to ensure constant evaporation rate and therefore maintain constant flow rate despite the changing amounts of organic solvent. This was addressed by monitoring the evaporator outlet flow rate, and adjusting heating accordingly to maintain it as desired. This was controlled using a PID feedback control mechanism. The difference between inlet flow

rate and setpoint define the extent of evaporation, which we refer to in percentage of evaporation. Figure 1 shows A) a schematic representation of the mechanism used, B) a picture of the evaporation regulation system and its parts, and C) the evaporative module.

### *2.2 REAGENTS AND SOLUTIONS*

Analytical grade ≥98% CAP was purchased from Sigma-Aldrich (St Louis MO, USA). Solutions were prepared in Milli-Q water from a Milli-Q Plus Ultrapure Water System (Milli- pore, Bedford, MA, USA). HPLC grade methanol and ethanol (VWS Chemicals, Fontenay-sous-Bois, France) was used for solvent removal studies and HPLC grade acetonitrile (Unichrom, Taren Point, NSW, Australia) was used for solvent removal and mobile phase preparation. For MS analysis, MS grade acetonitrile was used. Acetic acid 100% (Merck KGaA, Darmstad, Germany) (Univar, Seven Hills NSW Australia) was used for mobile phase preparation.

### *2.3 SOLVENT REMOVAL OF BINARY MIXTURES*

The Capacitively Coupled Contactless Conductivity Detector ($C^4D$) used for evaluation of solvent composition was equipped with a slot for 1/32 inch (0.794 mm) outer diameter tubing, while a 500 µm ID PEEK (polyether ketone) tubing was used for on capillary detection. $C^4D$ data acquisition was performed through a TraceDec module (Innovative Sensor Technologies GmbH, Strasshof, Austria) and an Agilent 35900E Dual Channel Interface module operated by OpenLab software. An Agilent 1290 Infinity HPLC pump (Agilent Technologies, Santa Clara, CA, United States) was used to deliver binary mixtures to the evaporation device.

### *2.4 LIQUID-LIQUID EXTRACTION METHODOLOGY*

Six standard solutions of CAP (10, 25, 50,100, 200, 500, 1000 µg $L^{-1}$) were prepared in a water/acetonitrile/ethyl acetate ($H_2O$:ACN:EA) solution (48:44:8). The standards were analyzed after an evaporative injection to obtain a calibration curve. Spiked samples at levels of 89.3, 177.0 and 348.4 µg $L^{-1}$, as well as blank samples, were also prepared using fresh full fat milk. An aliquot of CAP standard was added to the milk sample and mixed before extraction to obtain spiked samples. A fist aliquot of extractant was added to the milk sample and vortex mixed for 1 min. The mixture was centrifuged at 10,000 rpm for 4 min using a Sigma 1-14K centrifuge. Both liquid phases were decanted and the solid residue was subjected to a second extraction by firstly mixing with water aliquot before adding the extractant. After vortex mixing and centrifugation, liquid phases of both extractions were combined and kept in the refrigerator to maximize phase separation. Supernatant was then removed from the Eppendorf vial. Six different extraction procedures were tested including 4 double and 2 single steps shown in the appendix (Table A1). For solvent removal, extracts were reconstituted by mixing 1:4 with a 40% acetonitrile solution prior to evaporative injection. Analyses were performed in triplicate using 2.8 mg $L^{-1}$ spiked and blank samples. Recoveries were calculated using a calibration curve 50-1000 µg $L^{-1}$ and conditions with the highest recoveries were chosen for further tests. Using the better performing extraction procedure, 3 different spiked samples at a lower range of CAP concentrations (89.3, 177.0 and 348.4 µg $L^{-1}$) were tested by evaporative injection HPLC.

### *2.5 SEPARATION CONDITIONS*

An Agilent 1290 Infinity series HPLC with a Poroshell $C_{18}$ column 2.1 × 150 mm 4.7 µm was used for the separation, performing an acetonitrile gradient from 18 to 30% in 5 min, then increasing to 95% acetonitrile before equilibration.

Both aqueous and organic phase contained 0.1% acetic acid and the column was kept at 30°C. Detection was performed with a UV detector at 270 nm. A 10-port valve was used to transfer reconstituted extract into the HPLC system and start the separation gradient controlled by Agilent 2DLC software.

### *2.6 Mass Spectrometry Analysis*

LC-MS/MS analysis was performed by collecting the reconstituted extracts after evaporation. Standards for MS analysis were prepared by extracting spiked milk samples to construct a calibration curve in the range 0.25-2 μg $L^{-1}$. The HPLC instrument was a Waters Acquity® H-class UPLC system (Waters Corporation, Milford, MA). The HPLC was coupled in series to a Waters Photodiode array (PDA) and Xevo® triple quadrupole mass spectrometer (Waters Corporation). Mass spectrometry analyses were undertaken using multiple reaction monitoring (MRM) in negative electrospray ionization mode. Electrospray ionization was performed with a capillary voltage of 2.7 kV, cone voltage of 25 V and collision energies for each MRM transition: (m/z) 321.2 to 152.1 (collision voltage 17 V); (m/z) 321.2 to 257.2 (collision voltage 11 V). The desolvation temperature was 450 °C, nebulizing gas was nitrogen at 950 L/h and cone gas was nitrogen at 50 L/h. MRM transition dwell times were 0.047 s.

## 3. Results and Discussion

### *3.1 Solvent removal of binary mixtures*

We previously developed an on-line solvent evaporator for preconcentration in sample preparation [18] and multidimensional separation fraction transfer [21]. In the latter, a change in solvent composition was hypothesized, bringing additional benefits to the approach as well as raising other potential

instrumental applications were solvent compatibility is an issue. Intuitively, it is anticipated that organic solvents with lower boiling point will be evaporated and removed from a water mixture in a greater extent than water itself. To prove this concept, the composition of binary solvent mixtures was monitored at several evaporation conditions. To determine the extent of solvent removal, a step increase of organic solvent was pumped through the membrane evaporator and changes in eluent conductivity (σ) were monitored using $C^4D$ [25]. The $C^4D$ on capillary detector was placed at the evaporator outlet as shown in Figure 1A, and used in a similar way as it was previously employed to monitor gradient profiles in liquid chromatography [26]. First, the relationship between organic solvent fraction ($\phi_s$) and eluent conductivity was determined and the obtained calibration curve (Figure 2A) was used to calculate organic solvent fraction after membrane evaporation ($\phi_s^f$). The percentage of solvent increase with time is plotted in Figure 2B, as is the measured eluent conductivity in different evaporation conditions.

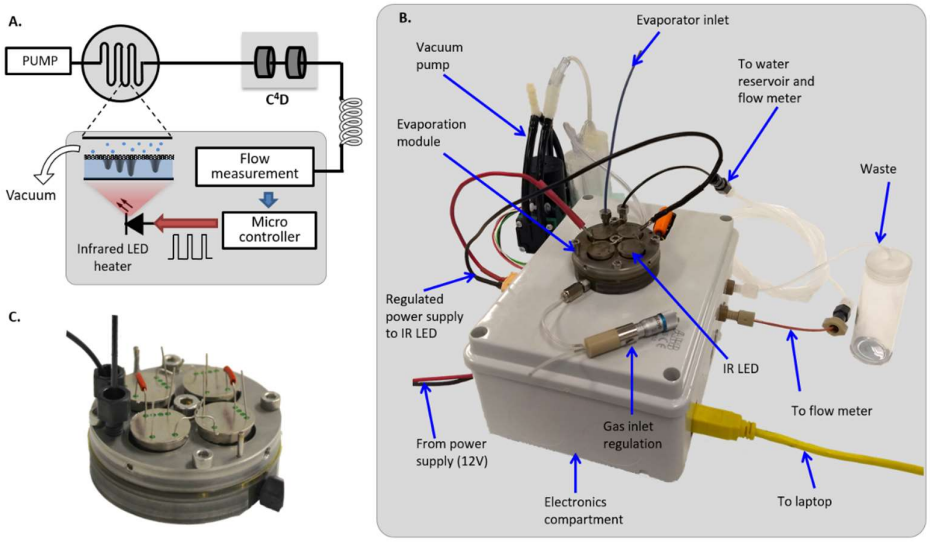


*Figure 1. A. Diagram of the system used to characterize solvent removal by membrane pervaporation using $C^4D$ detection. B. Picture and parts of the*

*evaporation regulation system used for all experiments. C. Assembled evaporation module with inserted LEDs.*

A drop in signal was observed when initial organic solvent fraction ($\phi_s^o$) was increased. The drop, as expected, is smaller the higher the flow evaporation due to the salts being concentrated further.

During evaporation, the flow regulation ($U_{measured}$) and applied voltage ($V_{LED}$) were monitored and an example of a 50% evaporation experiment is shown in Figure 2C. At the start of each step, regulation was compromised for a short period where the IR LED intensity dropped suddenly until excess temperature dissipated and the flow rate stabilized. This is due to a sudden change in solvent composition but such instability does not occur when a gradient is applied. Four replicates of solvent removal studies were carried out using the same membrane in given conditions, which revealed that the first replicate had a slightly lower $\phi_{MeOH}^f$ (methanol content was 3% lower), while the replicates thereafter had an excellent repeatability ($SD(\phi_{MeOH}^f) \leq 0.007$). Therefore, it was concluded that all membranes should be flushed with a high percentage the organic solvent in use before performing any experiments. The solvent removal studies where performed for 3 solvents/water mixtures commonly used in HPLC – methanol, ethanol and acetonitrile. Figure 2D shows $\phi_s^f$ as a function of $\phi_s^o$, where several data series correspond to evaporation conditions where 0%, 50% and 80% of the flow was evaporated. It can be seen that the amount of organic solvent remained the same when evaporation was not performed (0%) following a straight line, while it was reduced when evaporation was higher (50 and 80%). For example, acetonitrile can be selectively removed from a 50% water solvent mixture to obtain eluent with less than 2% organic solvent when 80% of the flow is evaporated. However, when $\phi_s^o$ was increased above a certain limit ($\phi_s^{critical}$) solvent penetrated within the pores wetting the membrane.

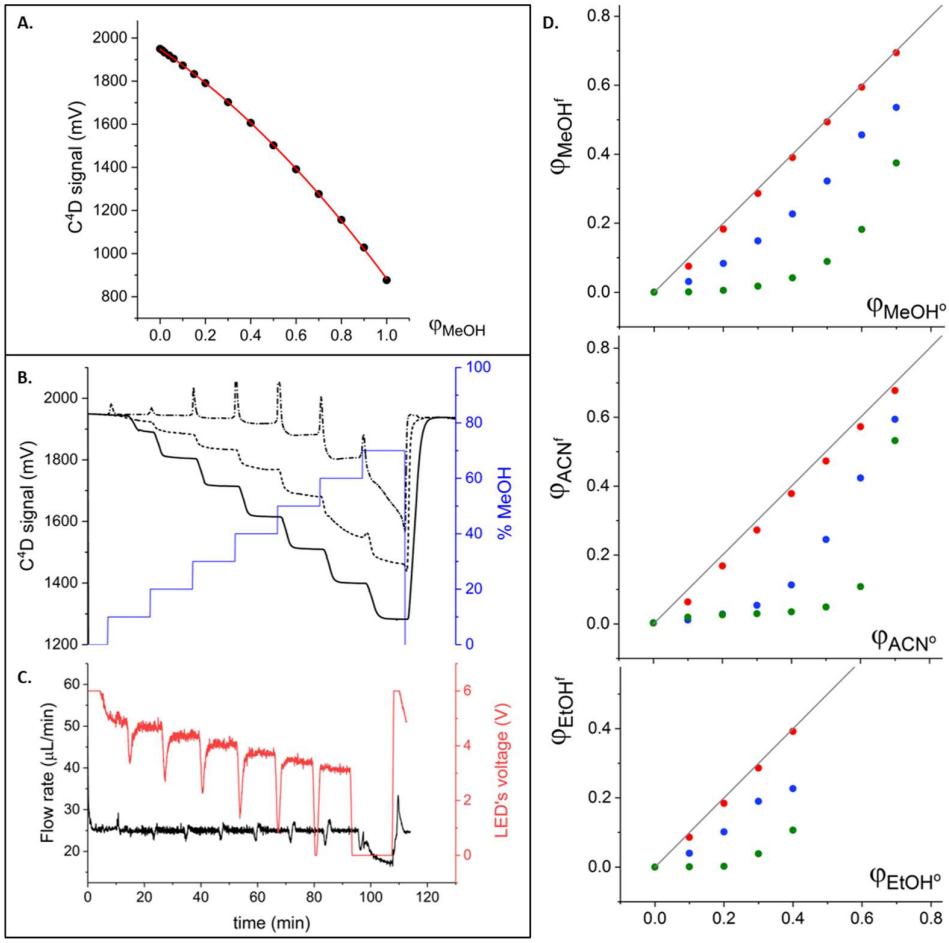


*Figure 2. A. Calibration curve showing the relationship between organic solvent fraction ($\varphi_s$) and eluent conductivity. B. Step gradient performed for acetonitrile (blue) and measured eluent conductivity in different evaporation conditions (0% solid line – 50% dotted line – 80% dashed line). C. Flow regulation showing the monitored flow rate (black) and applied voltage (red). D. $\varphi_s^f$ as a function of $\varphi_s^o$ for 3 common organic solvents at 0% (red), 50% (blue), and 80% (green) evaporation conditions.*

This caused lack of flow rate regulation so evaporation was not possible. The critical solvent limit was solvent dependent: being $\phi_{ACN}^{critical} > 70\%$, $\phi_{MeOH}^{critical} > 70\%$, and $\phi_{EtOH}^{critical} > 40\%$. The membrane solvent removal effect is expected for other organic solvents with a boiling point lower than that of

water. Ethyl acetate, used in the LLE procedure described below, is one of them. It is immiscible with water at over 8.3% (w/w), therefore solvent removal could not be assessed for ethyl acetate. However, acetonitrile and ethyl acetate have similar boiling point (81.6 and 77.1 °C, respectively) and vapor pressure (11.8 and 12.4 KPa at 25°C, respectively), properties that influence their evaporation in the mixture, and they are likely to have a similar behavior.

### *3.2 ONLINE SAMPLE RECONSTITUTION*

Online LLE extract reconstitution was selected to demonstrate the potential of the evaporative module for an integrated workflow, with the detection of CAP in milk used as a case study. CAP is an antibiotic used as a human therapeutic agent but banned from the food production chain due to genotoxicity concerns [27], therefore sensitive and reliable methods for its analysis are needed. Determination of antibiotics in food is not simple since samples of animal origin such as milk, tissue or eggs are generally complex matrices. LLE, either alone or followed by SPE, is widely used for amphenicol analysis although procedures vary for each particular matrix. Ethyl acetate is the most commonly used LLE solvent for the extraction of amphenicols [28].

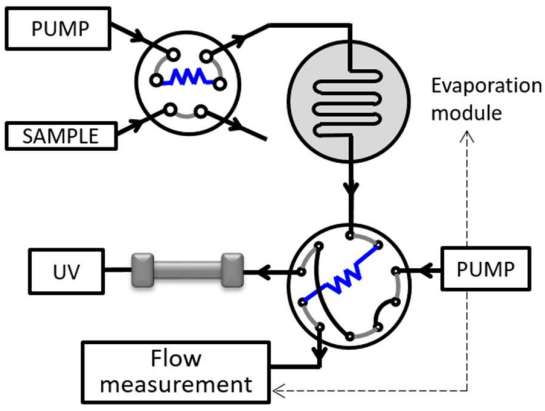


*Figure 3. Diagram of the system used for evaporative injection analysis.*

Regarding separation techniques, the most widely used analytical methods for the analysis of CAP in food are GC and HPLC. However, since it is a polar and non-volatile molecule, derivatization must be performed prior to GC analysis to form a stable volatile compound [29,30]. HPLC-MS does not require derivatization and was therefore the separation technique used here.

To perform dry down and redissolution of the LLE extract, the on-line solvent removal system was coupled with the HPLC injection valve. The sample extract was firstly diluted with solvent mixture containing water before passing through the evaporative solvent remover. This was necessary for two reasons. First, to prevent the membrane from being damaged or wet by pure organic solvent. Second and more importantly, to avoid complete sample dry down. Once the solvent was removed the sample is reconstituted in water or the appropriate solvent/water mixture which is more compatible with the HPLC separation conditions. Using the set up in Figure 3, the injected volume (100 µL) was pumped into the device at a constant flow rate using a HPLC pump, and it left the evaporative unit at a lower, constant flow rate after solvent removal. The sample was injected into a constant flow of carrying solution, which had a composition similar to the sample so that the evaporation process was not disrupted when injection occurred. For the purpose of this study the carrying phase was 55% aqueous acetonitrile at a flow rate of 25 $\mu L.min^{-1}$, and the evaporation setpoint was 10 $\mu L.min^{-1}$ to achieve evaporation of 60% of the flow. After solvent removal, sample was directed to a 60 µL collection loop in a switching valve that automatically switched after 9 min, when all the reconstituted and evaporated extract had filled the loop. Because the evaporation time is lower than the HPLC analysis, they can be done simultaneously for a series of samples in a routine workflow. The contents of the loop were then analyzed by HPLC. Injection and collection loops were 100 and 60 µL in volume, respectively.

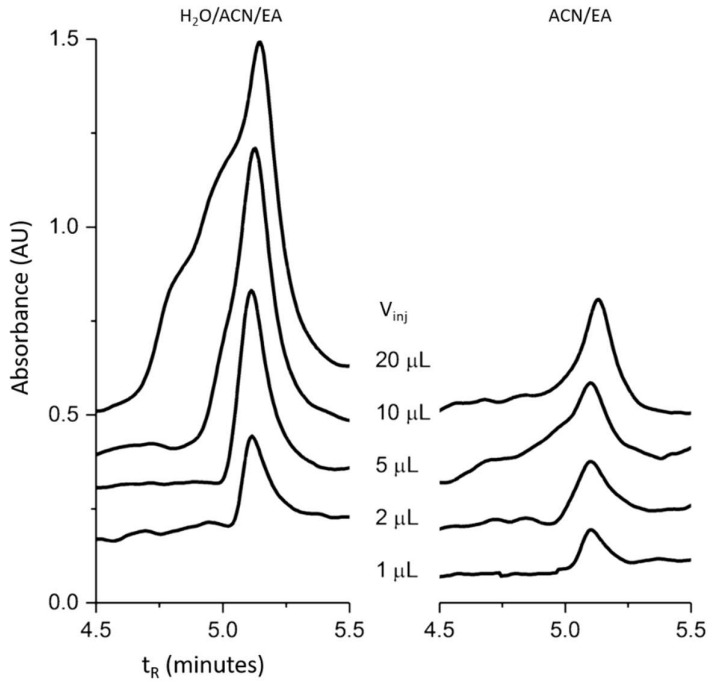


*Figure 4. Effect of injection volume of diluted extracts ($H_2O$/ACN /EA) and extracts (ACN/EA) in chromatographic performance. Chromatographic conditions: $C_{18}$ column, 5 min acetonitrile gradient 18 - 30%.*

It is expected that the injection of samples containing ethyl acetate into the HPLC may cause peak distortion due to strong elution and immiscibility at the start of the gradient and at high pressures. To assess this in the following experiments, standards were prepared mimicking the solvent composition of extracts (ACN/EA) and diluted extract (ACN/$H_2O$/EA). Peak distortion at different injection volumes was monitored to determine the critical volume at which retention was affected by the EA solvent mixture. Based on Figure 4, critical injection volume was 1 and 5 µL for the ACN/EA extract and ACN/$H_2O$/EA diluted extract, respectively. After the evaporation module, a 60 µL injection volume is used. This was also tested with the two solvent mixtures. As presented in the chromatograms in Figure 5, a long split peak eluted between 3.5 and 5.5 min. In contrast, after evaporation, a sharp peak

for CAP was observed at 5.1 min well separated from other components of the matrix, showing the excellent chromatographic performance of evaporative injection in contrast with direct injection. The 60 µL reconstituted extract correspond to 100 µL of diluted extract before solvent removal. Therefore, evaporative injection allowed for a 20-fold increase in sensitivity compared to direct injection of either extracts or diluted extracts. These results show that the dilution performed is not significant since together with evaporative injection it allows for high injection volumes without any loss of separation performance and improved sensitivity.

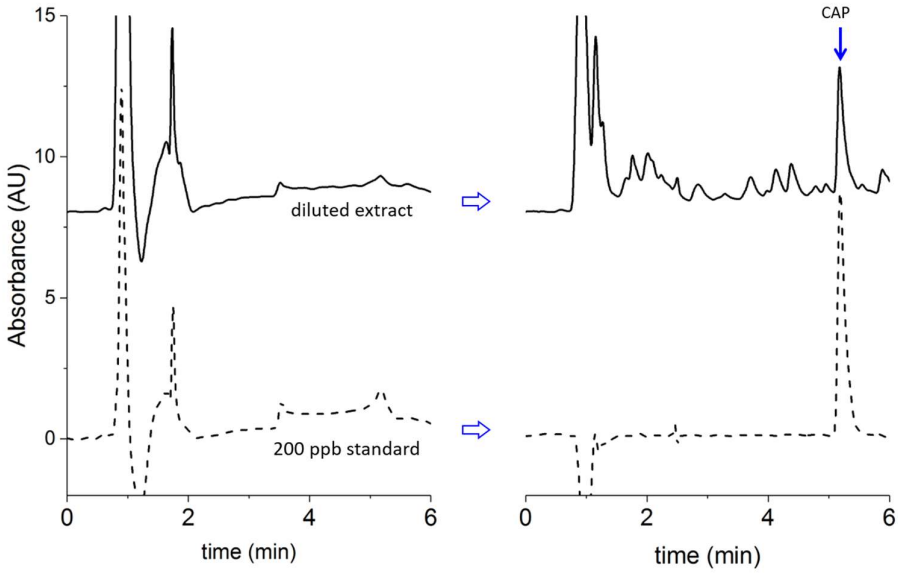


*Figure 5. Direct HPLC analysis (left) and evaporative injection-HPLC (right) using set up in Figure 3. Diluted extracts (solid line) and standards (dotted line) mimicking the solvent composition of diluted extracts are shown, where CAP sharp peak at 5.3 min can only be observed in evaporative injection conditions.*

### *3.4 EXTRACTION AND RECONSTITUTION*

Both acetonitrile and ethyl acetate have been reportedly used to extract CAP from milk. When using acetonitrile, samples should be frozen and/or vortexed

at low temperatures to allow low temperature partitioning [31], which complicates the procedure. While pure ethyl acetate can be used for extraction, the mixture would not be miscible prior to on-line evaporative reconstitution. Since water needs to be added to the extract to provide the final sample media, using only ethyl acetate would make it difficult to obtain a single-phase solution. Therefore, to obtain two separate phases in all studied extraction conditions but also a miscible diluted extract, phase diagrams of a ternary mixture containing water, acetonitrile and ethyl acetate ($H_2O$/ACN/EA) were examined [32]. The composition of organic phase for extraction was chosen to be ACN/EA (60:40). The extract was then diluted 1:4 dilution with water/acetonitrile (60:40), in order to obtain a miscible tertiary mixture of 48:44:8 $H_2O$/ACN/EA with minimum dilution factor. To ensure that the evaporated sample was a single-phase solution, the contents of the 60 µL loop were visually examined before evaporative injection. Evaporative injection was then performed with samples and standards as described previously. Recoveries were calculated at 4 different concentrations from approximately 0.1 to 3 mg $L^{-1}$. As shown in Table 1, recoveries were in all cases around 85%. However, recovery for the lowest spiked sample was significantly greater since UV is not a suitable detection method for this analysis. Complete separation from matrix components cannot be ensured and therefore peak integration becomes difficult and erratic. UV detection has been reported [33,34] for CAP determination, but it was not sensitive enough to provide limits of detection competitive with MS detection at low part-per-billion levels (ppb or µg $L^{-1}$). LC-MS/MS was therefore employed to increase the methods sensitivity. Collected reconstituted extracts were analyzed to determine an indicative limit of detection (LOD) and limit of quantification (LOQ) of the described method. The standard deviation of the calibration curve residuals (σ) as well as the slope (S) were used for this purpose in the following equations: LOD=3*σ/S and LOD=10*σ/S. The determined LOD of 0.088 µg $L^{-1}$ and LOQ of 0.294 µg $L^{-1}$ are below the minimum required performance limit (MRPL) of 0.3 and 0.5 µg $L^{-1}$ in Europe and China, respectively, thus

demonstrating the applicability of the approach for implementation in an analytical laboratory.

Table 1. CAP recoveries.

| $c_{CAP}$ - milk (µg $L^{-1}$) | $c_{CAP}$ - diluted extract (µg $L^{-1}$) | Recovery (%) ± SD (n=3) | |
|---|---|---|---|
| 89.3 | 30 | 95.1 | ± 4.0 |
| 177.0 | 60 | 85.8 | ± 1.6 |
| 348.4 | 120 | 85.3 | ± 3.2 |
| 2805.2 | 960 | 89.0 | ± 1.6 |

Extraction conditions:
Step 1 - 600:400 µL (sample:extractant) followed by decantation
Step 2 - 300:200 µL (water:extractant) followed by decantation
Step 3 - Supernatant removal

## 4. CONCLUSIONS

An on-line evaporative reconstitution system integrated into HPLC analysis was developed and demonstrated for the determination of chloramphenicol in milk samples. Based on membrane pervaporation, the device was proved to selectively remove organic solvent from samples in water/solvent mixtures. Further work regarding membrane material and wettability is crucial to broaden conditions of use and make evaporative injection a more universal dry down method. Also, a decrease of the necessary extract dilution would be possible using more solvent resistant membrane materials. Nevertheless, the evaporative injection approach provides a simple and easy to automate tool. The benefits are clear in terms of labor reduction, time management and ease of use, but it also allows for high injection volumes without any loss of chromatographic performance. This work indicates that implementation of fully integrated solvent extraction coupled to analysis techniques is therefore feasible regardless of solvent incompatibilities.

## ACKNOWLEDGMENTS

This research was conducted by the ARC Training Centre for Portable Analytical Separation Technologies (IC140100022). MCB is the recipient of an ARC Future Fellowship. E. Fornells is the recipient of an ARC CHDR scholarship and a University of Tasmania tuition fee scholarship. The authors thank Dr. David Nichols, Research Fellow in Organic Mass Spectroscopy at the Central Science Laboratory (CSL), University of Tasmania for performing LC-MS studies.

## APPENDIX: ADDITIONAL INFORMATION

Table A1. Tested extraction conditions.

| Conditions | Extract. step | V sample 348.4 µg $L^{-1}$ / V water (µL) | Vorg (µL) ACN/EA (6:4) | Recovery (%) ± SD (n=3) | |
|---|---|---|---|---|---|
| 1 | 1<br>2 | 200 sample<br>100 water | 400<br>200 | 74.8 | ± 0.37 |
| 2 | 1<br>2 | 400 sample<br>200 water | 400<br>200 | 79.5 | ± 1.20 |
| 3 | 1<br>2 | 500 sample<br>250 water | 400<br>200 | 78.1 | ± 4.27 |
| 4 | 1<br>2 | 600 sample<br>300 water | 400<br>200 | 89.0 | ± 1.63 |
| 5 | 1 | 600 sample | 400 | 73.4 | ± 3.35 |
| 6 | 1 | 800 sample | 400 | 79.6 | ± 2.49 |

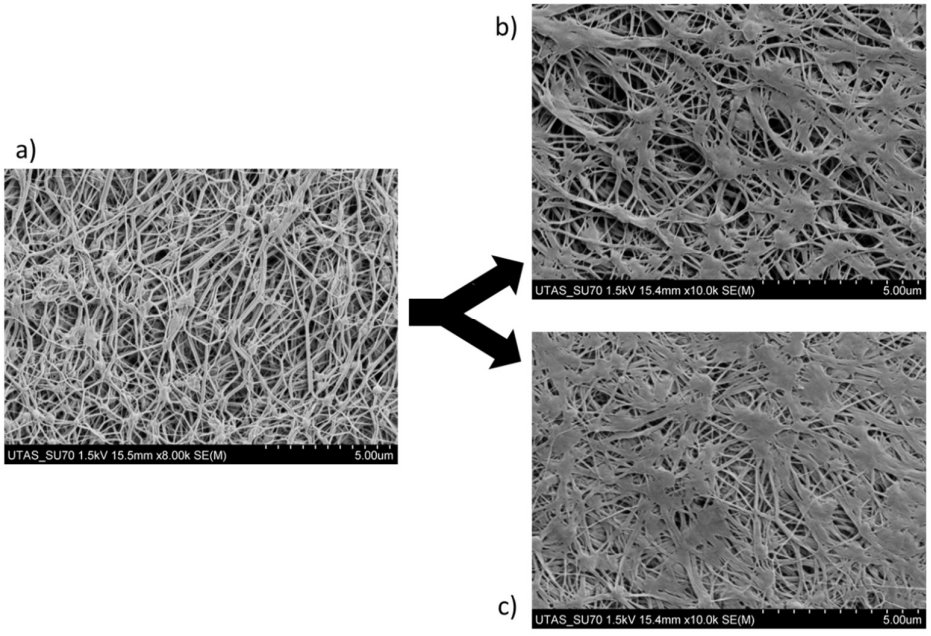


*Figure 6. Scanning Electron Microscopy (SEM) captions of a PTFE membrane before and after a methanol removal study from a water/methanol mixture. a) before use, b) after use at a channel section, c) after use at an inter-channel section.*

## REFERENCES


[1] J. Pan, C. Zhang, Z. Zhang, G. Li, Review of online coupling of sample preparation techniques with liquid chromatography, Anal. Chim. Acta. 815 (2014) 1–15.

[2] L.N. Jeong, R. Sajulga, S.G. Forte, D.R. Stoll, S.C. Rutan, Erratum to "Simulation of elution profiles in liquid chromatography—I: Gradient elution conditions, and with mismatched injection and mobile phases solvents'' (Journal of Chromatography A (2016) 1457 (41–49) (S0021967316307609) (10.1016/j.chroma.2016.06.0, J. Chromatogr. A. 1478 (2016) 84.

[3] B.J. VanMiddlesworth, J.G. Dorsey, Quantifying injection solvent effects in reversed-phase liquid chromatography, J. Chromatogr. A. 1236 (2012) 77–89.

[4] V. David, T. Galaon, H.Y. Aboul-Enein, Effects of large volume injection of aliphatic alcohols as sample diluents on the retention of low hydrophobic solutes in reversed-phase liquid chromatography, J. Chromatogr. A. 1323 (2014) 115–122.

[5] O. Lerch, O. Temme, T. Daldrup, Comprehensive automation of the solid phase extraction gas chromatographic mass spectrometric analysis (SPE-GC/MS) of opioids, cocaine, and metabolites from serum and other matrices, Anal. Bioanal. Chem. 406 (2014) 4443–4451.

[6] K. Purschke, S. Heinl, O. Lerch, F. Erdmann, F. Veit, Development and validation of an automated liquid-liquid extraction GC/MS method for the determination of THC, 11-OH-THC, and free THC-carboxylic acid (THC-COOH) from blood serum, Anal. Bioanal. Chem. 408 (2016) 4379–4388.

[7] Y. Dotsikas, C. Kousoulos, G. Tsatsou, Y.L. Loukas, Development of a

rapid method for the determination of glimepiride in human plasma using liquid-liquid extraction based on 96-well format micro-tubes and liquid chromatography/tandem mass spectrometry., Rapid Commun. Mass Spectrom. 19 (2005) 2055–2061.

[8] S. Moldoveanu, V. David, Solvent Extraction, in: Mod. Sample Prep. Chromatogr., *Elsevier*, 2015: pp. 131–189.

[9] M. Rogeberg, H. Malerod, H. Roberg-Larsen, C. Aass, S.R. Wilson, On-line solid phase extraction-liquid chromatography, with emphasis on modern bioanalysis and miniaturized systems, J. Pharm. Biomed. Anal. 87 (2014) 120–129.

[10] H. Zhang, R.M. Tiggelaar, S. Schlautmann, J. Bart, H. Gardeniers, In-line sample concentration by evaporation through porous hollow fibers and micromachined membranes embedded in microfluidic devices, Electrophoresis. 37 (2016) 463–471.

[11] B.H. Timmer, K.M. van Delft, W. Olthuis, P. Bergveld, A. van den Berg, Micro-evaporation electrolyte concentrator, Sensors Actuators B. 91 (2003) 342–346.

[12] S. Nii, Membrane evaporators, J. Memb. Sci. 201 (2002) 149–159.

[13] M. Takeuchi, P.K. Dasgupta, J. V. Dyke, K. Srinivasan, Postcolumn Concentration in Liquid Chromatography. On-Line Eluent Evaporation and Analyte Postconcentration in Ion Chromatography, Anal. Chem. 79 (2007) 5690–5697.

[14] K. Gethard, S. Mitra, Membrane distillation as an online concentration technique: application to the determination of pharmaceutical residues in natural waters., Anal. Bioanal. Chem. 400 (2011) 571–5.

[15] P. Wang, T. Chung, Recent advances in membrane distillation processes : Membrane development , con fi guration design and

application exploring, J. Memb. Sci. 474 (2015) 39–56.

[16] J.Y. Zhang, J. Do, W.R. Premasiri, L.D. Ziegler, C.M. Klapperich, Rapid point-of-care concentration of bacteria in a disposable microfluidic device using meniscus dragging effect., Lab Chip. 10 (2010) 3265–3270.

[17] J.M. Jani, M. Wessling, R.G.H. Lammertink, A microgrooved membrane based gas-liquid contactor, Microfluid. Nanofluidics. 13 (2012) 499–509.

[18] E. Fornells, B. Barnett, M. Bailey, R.A. Shellie, E.F. Hilder, M.C. Breadmore, Membrane assisted and temperature controlled on-line evaporative concentration for microfluidics, J. Chromatogr. A. 1486 (2017) 110–116.

[19] M. Yu, Y. Hou, H. Zhou, S. Yao, An on-demand nanofluidic concentrator, Lab Chip. 15 (2015) 1524–1532.

[20] P.H. Chao, J. Collins, J.P. Argus, W.-Y. Tseng, J.T. Lee, R. Michael van Dam, Automatic concentration and reformulation of PET tracers via microfluidic membrane distillation, Lab Chip. 17 (2017) 1802–1816.

[21] E. Fornells, B. Barnett, M. Bailey, E.F. Hilder, R.A. Shellie, M.C. Breadmore, Evaporative membrane modulation for comprehensive two-dimensional liquid chromatography, Anal. Chim. Acta. 1000 (2018) 303–309.

[22] Y. Zhang, S. Kato, T. Anazawa, Vacuum membrane distillation by microchip with temperature gradient., Lab Chip. 10 (2010) 899–908.

[23] E. Drioli, A. Ali, F. Macedonio, Membrane distillation: Recent developments and perspectives, Desalination. 356 (2015) 56–84.

[24] Scientific Opinion on Chloramphenicol in food and feed, EFSA J. 12 (2014).

[25] A.J. Zemann, E. Schnell, D. Volgger, G.K. Bonn, Contactless Conductivity

Detection for Capillary Electrophoresis, Anal. Chem. 70 (1998) 563–567.

[26] M. Zhang, A. Chen, J.J. Lu, C. Cao, S. Liu, Monitoring gradient profile on-line in micro- and nano-high performance liquid chromatography using conductivity detection, J. Chromatogr. A. 1460 (2016) 68–73.

[27] J.C. Hanekamp, A. Bast, Antibiotics exposure and health risks: Chloramphenicol, Environ. Toxicol. Pharmacol. 39 (2015) 213–220.

[28] L.R. Guidi, P.A.S. Tette, C. Fernandes, L.H.M. Silva, M.B.A. Gloria, Advances on the chromatographic determination of amphenicols in food, Talanta. 162 (2017) 324–338.

[29] T. Sniegocki, M. Gbylik-Sikorska, A. Posyniak, Transfer of chloramphenicol from milk to commercial dairy products - Experimental proof, Food Control. 57 (2015) 411–418.

[30] J. Shen, X. Xia, H. Jiang, C. Li, J. Li, X. Li, S. Ding, Determination of chloramphenicol, thiamphenicol, florfenicol, and florfenicol amine in poultry and porcine muscle and liver by gas chromatography-negative chemical ionization mass spectrometry, J. Chromatogr. B Anal. Technol. Biomed. Life Sci. 877 (2009) 1523–1529.

[31] E.C.P. do Rego, E. de F. Guimarães, A.L.M. dos Santos, E. de S.M. Mothé, J.M. Rodrigues, A.D. Pereira Netto, The validation of a new high throughput method for determination of chloramphenicol in milk using liquid–liquid extraction with low temperature partitioning (LLE-LTP) and isotope-dilution liquid chromatography tandem mass spectrometry (ID-LC-MS/MS), Anal. Methods. 7 (2015) 4699–4707.

[32] S. Fujinaga, K. Unesaki, S. Negi, M. Hashimoto, K. Tsukagoshi, Specific microfluidic behavior of ternary mixed carrier solvents of water–acetonitrile–ethyl acetate in open-tubular capillary chromatography and the chromatograms, Anal. Methods. 4 (2012) 3884.

[33] J. Han, Y. Wang, C. Yu, C. Li, Y. Yan, Y. Liu, L. Wang, Separation, concentration and determination of chloramphenicol in environment and food using an ionic liquid/salt aqueous two-phase flotation system coupled with high-performance liquid chromatography, Anal. Chim. Acta. 685 (2011) 138–145.

[34] H. Chen, H. Chen, J. Ying, J. Huang, L. Liao, Dispersive liquid-liquid microextraction followed by high-performance liquid chromatography as an efficient and sensitive technique for simultaneous determination of chloramphenicol and thiamphenicol in honey, Anal. Chim. Acta. 632 (2009) 80–85.

# V. CONCLUSIONS AND FUTURE PERSPECTIVES

## CONCLUSIONS

A solvent removal or exchange device was developed in this thesis, and its use explored in different stages of the analytical process. The device is based in membrane evaporation where a vapor permeable membrane acts as an evaporation interface to remove solvent from a flowing liquid.

Initially, the device was used for preconcentration purposes by adjusting the module temperature. A predictive model was also developed to calculate the required conditions to achieve a particular concentration factor. The model also revealed precise temperature control was required for repeatable performance, which lead to the development of a self-regulated temperature control system. The feedback system aimed to keep outlet flow rate constant by adjusting the heating. Because this system showed successful evaporation control regardless of the matrix or solvent composition, it could be used after solvent gradient separations.

Volume reduction after elution is ideal to interface two-dimensional liquid chromatography, and therefore reduce the fraction volume transferred to the second dimension separation. Evaporative Membrane Modulation was implemented in a LC×LC system, eliminating the interference of $^{1}$D solvent in the $^{2}$D separation system and therefore improving reproducibility along the sequential $^{2}$D injections and peak identification. However, unwanted band broadening was observed after evaporation. Despite this loss of peak capacity, it provides a wider choice of chromatographic conditions and stationary phases that would otherwise be unsuitable, and more independent

optimization of subsequent separation systems, easing method development of high orthogonality LC×LC.

Attempting to address the abovementioned band broadening, a study on fluid dynamics at different channel geometries was carried out. The experimental results agreed with simulations when using the current design demonstrating reliable models. However, no remarkable decline was observed on band broadening when alternative geometries were studied. Nevertheless, the observed concentration gradients within the channels are relevant information to proceed with channel geometry studies.

Finally, the device was proved to selectively remove organic solvent from samples in water/solvent mixtures. Taking advantage of this feature, traditionally manual dry-down of sample extracts was integrated in an automated HPLC workflow. Evaporative reconstitution was demonstrated for the determination of chloramphenicol in milk samples. The benefits are clear in terms of labor reduction, time management and ease of use, but it also allows for high injection volumes without any loss of chromatographic performance. This work indicates that implementation of fully integrated solvent extraction coupled to analysis techniques is therefore feasible regardless of solvent incompatibilities.

## FUTURE PERSPECTIVES

The main limitation of using membranes in the gas-liquid interface is the material resistance and wettability. Although membranes provide stability in the interface, they may degrade or get wet when in contact with strong organic solvents. Therefore, a wide screening of different membrane

materials or technologies is essential to widen the conditions of use, thus for successful implementation of membrane evaporation in chemical analysis. Alternatively, other approaches used in gas-liquid microreactors, such as silicon nanowire gas channels, could be adapted as an evaporation interface.

A second relevant limitation that needs to be overcome is the observed band broadening along the microfluidic channel. This limitation is especially important for the use of such devices in separation science, where broadening interferes with the analysis performance. Since the studied channel geometry attributes do not seem to be the main cause of broadening, further tests need to be taken to identify and correct it. Possible causes may be velocity and concentration gradients across the channel. The use of small tubular membranes could overcome this limitation since evaporation would occur in all directions and the gradient would be minimized.

Also, strong temperature gradients along the channel because of focused optical heating must be considered as a potential cause of broadening. Despite infrared radiation being the key to very fast evaporation regulation, in the current set up radiation is focused – it is very strong at the center of the LED and decreases at larger radius from the center. A dispersed infrared source or other types of heating might have benefits in terms of lower band broadening.

Overall, the implementation of flow-through evaporative solvent removal eradicate solvent issues in chromatographic applications was demonstrated. As such, it has potential to find application in other types of interfacing system and is a significant contribution to the development of strategies addressing automation issues in analytical chemistry.